Tidal stream energy integration with green hydrogen production : energy management and system optimisation

Ansu Alex

Normandie Université

THÈSE

Pour obtenir le diplôme de doctorat

Spécialité MECANIQUE DES FLUIDES, ENERGETIQUE, THERMIQUE, COMBUSTION, ACOUSTIQUE

Préparée au sein de l'Université de Caen Normandie

Tidal stream energy integration with green hydrogen production: energy management and system optimisation

Présentée et soutenue par
ANSU ALEX

Thèse soutenue le 24/06/2022
devant le jury composé de

M. SAMIR JEMEI	Professeur des universités, Université de Franche-Comté	Rapporteur du jury
M. AHMED RACHID	Professeur des universités, UNIVERSITE AMIENS PICARDIE JULES VERNE	Rapporteur du jury
M. MAMADOU BAILO CAMARA	Professeur des universités, Université Le Havre Normandie	Membre du jury
M. RAFFAELE PETRONE	Maître de conférences, Université de Caen Normandie	Membre du jury
MME MELIKA HINAJE	Professeur des universités, Université de Lorraine	Président du jury

Thèse dirigée par HAMID GUALOUS (Laboratoire universitaire des sciences appliquées de cherbourg (Caen)) et LIEVEN VANDEVELDE (The Electrical Energy Laboratory)

UNIVERSITÉ CAEN NORMANDIE

ED 591 PSIME

LUSAC

Abstract

The overarching aim of this thesis is to design, implement and compare different energy management strategies and optimisation approaches for a hybrid system involving floating tidal stream energy integration with green hydrogen production. Towards reaching the objectives, the individual system components are modelled initially. The annual system performance capabilities of the tidal stream energy plant are then obtained using frequently occurring daily profiles at the Fall of Warness berth in the Orkney Islands, Scotland. The transitionary operating modes of two polymer electrolyte membrane electrolyser units, when subjected to the energy from the tidal stream plant are analysed based on a rule-based approach energy management strategy. Later, a preliminary evaluation of the hydrogen production cost is assessed based on different daily hydrogen demand and daily tidal profile conditions. Further, an optimisation approach with the objective to maximise the system operating profit ensuring optimal and sufficient operations of both the electrolyser units under real system constraints, is formulated with priority for tidal energy powered hydrogen production. The optimisation problem is solved using a genetic algorithm based on the mixed integer non-linear problem. A comprehensive cost-benefit analysis based on fixed-variable costs and levelised costs factors is performed to analyse the optimal techno-enviro-economic operation of a hybrid grid connected tidal-wind-hydrogen energy system. The outcomes are compared against the rule-based approach results. The annualised profits in the optimisation approach are estimated to be 41.5% higher compared to the rule-based approach. Further, from an environmental view, the best optimisation results are approximately 47% higher than the rule-based approach results in terms of carbon emission reductions. A dynamic electrolyser capable of working at twice of its nominal power rating for limited duration, resulted particularly advantageous when coupled with tidal energy which is cyclic in nature with predictable periods of high and low power generation. Finally, it was determined that the fixed cost (FC) optimisation approach is relatively simple in terms of cost estimation. On the contrary, while the levelised cost (LC) approach yields slightly better results, it necessitates a greater prior knowledge of system operations to reasonably estimate the cost factors. The proposed method can be used as a generic tool for electrolytic hydrogen production analysis under different contexts, with preferable application in high green energy potential sites with constrained grid facilities.

Keywords: Energy management, green hydrogen, optimal power dispatch, tidal energy, PEM electrolyser

Résumé

L'objectif principal de cette thèse est de concevoir, mettre en œuvre et comparer différentes stratégies de gestion de l'énergie et approches d'optimisation pour un système hybride impliquant l'intégration de l'énergie marémotrice flottante avec la production de l'hydrogène vert. Pour atteindre les objectifs, les composants individuels du système sont d'abord modélisés. Les capacités annuelles de performance du système de la centrale d'énergie marémotrice ont ensuite été obtenues à l'aide des profils quotidiens fréquents au poste d'amarrage de Fall of Warness dans les îles Orcades. Les modes de fonctionnement transitoires des électrolyseurs à membrane échangeuse de protons, lorsqu'elles sont soumises à l'énergie de la centrale hydrolienne, ont été analysés sur la base d'une (RBA) stratégie de gestion de l'énergie basée sur des règles. Plus tard, une évaluation préliminaire du coût de production d'hydrogène est effectuée sur la base de différentes conditions de demande quotidienne d'hydrogène et de profils de marée quotidiens. En outre, une approche d'optimisation dans le but de maximiser le profit d'exploitation du système tout en assurant un fonctionnement optimal et suffisant des deux électrolyseurs sous des contraintes réelles du système, est formulée en donnant la priorité à la production d'hydrogène par l'énergie marémotrice. Le problème d'optimisation est résolu à l'aide d'un algorithme génétique basé sur un problème non linéaire à entiers mixtes. Une analyse coûts-avantages complète basée à la fois sur les coûts fixes-variables et sur les facteurs de coûts actualisés est réalisée pour analyser le fonctionnement technico-environnemento-économique optimal d'un système hybride d'énergie marémotrice-éolienne-hydrogène connecté au réseau. Les résultats ont été comparés aux résultats de l'approche basée sur des règles. Les bénéfices annualisés dans l'approche d'optimisation ont été estimés supérieurs de 41,5 % à ceux de la RBA. De plus, d'un point de vue environnemental, les meilleurs résultats d'optimisation étaient environ 47 % supérieurs aux résultats de la RBA en termes de réduction des émissions de carbone. Un électrolyseur dynamique capable de fonctionner à deux fois sa puissance nominale pendant une durée limitée s'avère particulièrement avantageux lorsqu'il est couplé à l'énergie marémotrice qui est de nature cyclique avec des périodes prévisibles de production d'énergie élevée et faible. Enfin, il est conclu que l'approche d'optimisation des coûts fixes-variables est relativement simple dans l'estimation des coûts. Au contraire, bien que des résultats légèrement meilleurs soient obtenus dans le cas de l'approche par coût actualisé, il est nécessaire d'avoir une meilleure connaissance préalable du fonctionnement du système pour estimer finement les facteurs de coût actualisé. Le modèle proposé peut être utilisé comme un outil générique pour l'analyse de la production d'hydrogène dans différents contextes et il est particulièrement applicable dans les sites à fort potentiel d'énergie verte avec des installations de réseau limitées.

Mots-clés : Gestion de l'énergie, hydrogène vert, répartition optimale de la puissance, énergie marémotrice, électrolyseur PEM

Acknowledgements

Firstly, I would like to extend my gratitude to my supervisor, Prof. Hamid Gualous for all the guidance received right from the beginning of this work. Thanks for all the valuable discussions and feedbacks received at each step of the process. Particularly, thanks for making sure that I integrated well in the LUSAC Lab. I would like to extend my thanks to my co-supervisor, Prof. Lieven Vandevelde, for all the valuable advices, critical suggestions and especially for the patient listening in the regular fortnightly meetings held during the last eight months of this work.

A special thanks to Dr. Raffaele Petrone, for always being approachable, for all the critical reviews that has significantly contributed to this work. Thanks, in particular for the support in formulating the structure for this thesis. I would like to thank Dr. Tala-Ighil Boubekeur for the multiple feedbacks and critical suggestions on the work, Dr. Dimitar Bozalakov for all the valuable feedbacks and the much-needed timely motivation. I would also like to express my gratitude to my former lab colleagues, Dr. Mahmoud Barakat and Dr. Huan Li, who had greatly supported me at the beginning of this work.

I thank Prof. Ahmed Rachid and Prof. Samir Jemei for agreeing to review this thesis. I would like to thank Prof. Melika Hinaje, and Prof. Mamadou Bailo Camara, for examining the work.

I would like to thank the ITEG project partners for the funding received for my thesis. The opportunities for participating in the steering meetings and project related platforms have indeed expanded my knowledge on the practical aspects of the system applications.

Thanks to Ms. Adeline Ozenne for all the quick responses in the administrative works. Thanks to all the respective staff of LUSAC lab, IUT Saint Lo, University of Caen and University of Ghent for the timely support rendered.

A warm thanks to my fellow lab mates both former and current for the fun times and thoughtful discussions that we had. Kaoutar, Zahra, Khalid, Ahmed, Rafik, Yassine, Abdel, Rania and many more…I cherish the friendship we have. It definitely made sure that I had a comfortable time in the lab.

My heartfelt gratitude to my family, without whose unconditional love, support and sacrifice, I would not have reached till here. My father, who always let me do what I want without any apprehensions. My mother, my constant positivity booster. Thanks to my siblings, Noel and Sunaina and their families, my husband's siblings and family, for all your loving support and warm encouragement. My heart goes out to my late grandmother, whose zeal for knowledge always awed and inspired me. Thanks to my parents in law for all

the prayer support. I would like to thank the Shout to the Lord community in Belgium for all the spiritual support during the COVID and post covid times.

Last, but not the least, my dear husband, Jomon. Getting married to you during this research journey was indeed the best decision I ever made and I am ever grateful to God for it. Thanks a ton for supporting me in these trying times, even at the cost of keeping your thriving career on the backburner.

I would like to dedicate this thesis to my family.

Above all, thanking my Lord Jesus Christ for all his loving kindness. Great is His faithfulness!

Ansu Alex

May 06, 2022

Saint Lo.

Table of contents

List of figures

List of tables

Nomenclature

Acronyms

AC	Alternating Current
AEL	Alkaline Electrolyser
AEP	Annual Energy Production
BoP	Balance of Plant
BPC	Balance of Plant Cost
CapEx	Capital Expenditure
CC	Compression Cost
CCF	CapEx Cost Factor
CfD	Contract for Difference
CL	Catalyst Layer
CO_2e	Carbon dioxide emissions equivalent
CTV	Crew Transport Vessel
DC	Direct Current
DSOP	Daily System Operating Profit
EC	Electrolyser units Cost
ED	Economic Dispatch
eLCOE	Enhanced Levelised Cost of Energy
EMR	Energetic Macroscopic Representation
EMS	Energy Management System
ETC	Electrolyser Transition Cost
EU	European Union
EWC	Electrolyser Water Consumption Cost
FC	Fixed Costs
GA	Genetic Algorithm
GDL	Gas Diffusion Layer
GER	Grid energy Export Revenue
GIC	Grid energy Import Cost
H_2S	Hydrogen Storage
HCP	Hydrogen Carbon savings Price
HCS	Hydrogen Carbon Savings
HHV	Higher Heating Value
HSC	Hydrogen Storage Cost
HSP	Hydrogen Selling Price
HSR	Hydrogen Selling Revenue
IEA	International Energy Agency
IPCC	Intergovernmental Panel on Climate Change
ITEG	Integrating Tidal Energy into the European Grid
LBOP	Levelised Balance of Plant cost factor
LC	Levelised Costs
LCOE	Levelised Cost of Energy
LCOH	Levelised Cost of Hydrogen
LCOMP	Levelised Compression cost factor
LH_2S	Levelised Hydrogen Storage cost factor
LHV	Lower Heating Value
MAS	Multi Agent System
MCF	Maintenance Cost Factor

MEA	Membrane Electrode Assembly
MG	Microgrid
MMT	Million Metric Tonnes
NDC	Nationally Determined Contributions
NZE	Net Zero Emission
O&M	Operation and Maintenance
OCV	Open Circuit Voltage
OpEx	Operating Expenditure
OPF	Optimal Power Flow
OSV	Offshore Supply Vessel
PEM	Polymer Electrolyte Membrane/ Proton Exchange Membrane
PPA	Power Purchase Agreement
PTC	Payment by Tidal generator to intermediate Company
PtG	Power to Gas
RAM	Reliability, Availability, Maintainability
RBA	Rule Based Approach
RES	Renewable Energy System/ Sources
SC	Storage Cost
SCIG	Squirrel Cage Induction Generator
SET	Strategic Energy Technology
SMR	Steam Methane Reforming
SOEL	Solid oxide Electrolyser
SOP	System Operating Profit
TCS	Tidal energy export Carbon Savings
TEC	Tidal Energy Cost
TSES	Tidal Stream Energy System
UC	Unit Commitment
WC	Water Consumption
WEC	Wind Energy Consumption Cost
WES	Wind Energy System

Symbols

A	Rotor swept area (m^2)
A	Area of reaction (m^2)
c	Electricity cost (€/kWh)
C_p	Power coefficient
C	Concentration (mol/m^3)
E	Energy/ electricity dispatch (kWh)
F	Faraday constant (96485 C/mol)
H_2	Hydrogen
H_p	Hydrogen production (kg)
H_t	Hydrogen production target (kg)
j	Current density (A/cm^2)
N	System life time
O_2	Oxygen
P	Generated power (kW)
pf	Penalty function
P_{t1}	Shaft power at full operations (kW)
P_{t2}	Maximum shaft power before cut-off (kW)
R	Resistance (Ω)

R	Gas constant (8.3145 J/molK)
r	Discount rate (%)
sp	Strike price (€/kWh)
T	Temperature (K)
tcf	Transition cost factor (€/h)
te	Transmission efficiency
v	Instantaneous velocity (m/s)
V	Voltage (V)
X	Decision variable
z	number of electrons transferred per reaction

Greek symbols

α	Activity species/charge transfer coefficient
β	Blade pitch angle (degrees)
λ	Tip speed ratio
ρ	Density (kg/m^3)
Ω	Rotor angular speed (radians/second)

Subscripts

0	reference value
a	anode
act	actuation
c	cathode
ci	cut-in
co	cut-off
diff	diffusion
e	electrolyser
e1	electrolyser unit 1
e2	electrolyser unit 2
elc	electrode
ex	export
g	grid
i	time in hours
im	import
in	interface
m	number of generating units
max	maximum
me	membrane
min	minimum
n	number of electrolyser units
ohm	ohmic
p	plates
r	rated
s	source
start	start operating mode
stb	standby operating mode
stop	stop operating mode
t	tidal turbine

tr	operating mode transition
tx	transformer
w	wind turbine

Chapter I

Introduction

I. Introduction

As per the emissions gap report of 2021, the newly announced nationally determined contributions (NDCs) to reduce global emissions will reduce emissions by about 7.5% by the year 2030, compared to the previously decided unbounded NDCs. However, at least 30% of emission reduction is needed to limit global warming to 2°C and about 55% is needed to limit to 1.5°C [4]. Therefore, prompt actions are necessary to limit the global emissions in line with Paris Agreement. Further, towards achieving the European Green Deal of turning Europe carbon neutral by 2050, increased implementation of renewable energy systems (RES) is essential. Increased utilisation of offshore RES is assessed as a key aspect among other prominent technologies to achieve net zero emission (NZE) targets [5]. The European Union (EU) commission estimates the requirement of 1 GW of ocean energy by 2030 and at least 40 GW of installed capacity by 2050 [6]. Additionally, to achieve the Paris Agreement target, the installed capacity of ocean energy globally is to be increased to 70 GW by 2030 and 350 GW by 2050 [6]. The intermittent nature and reduced reliability due to the forecasting uncertainties are issues often associated with RES like solar and wind energy. Among the different RES, the main advantage of tidal energy is its highly predictable nature [7].

Additionally, the EU hydrogen strategy aims to have 40 GW of renewable linked electrolysis capacity by 2030 [8]. Hydrogen, recognized as a significant energy vector for the future, is already used in a wide range of applications ranging from industrial, power generation, transportation, long term energy storage and heating applications [9].

Most of the islands and remote locations around the world depends on diesel as the main source of energy primarily due to the transmission grid constraints at such locations. Highly volatile crude oil market and the associated pollutant emissions are a cause of concern in this context [10]. Hybrid systems involving two or more RES along with energy storage system (ESS) could be a solution for increased reliability, energy security and reduced emissions in such a scenario. Further, implementing these solutions could even provide sustainable economic development in the region.

The predictable nature of tidal energy will be an important factor to solve the reliability concern, in addition to providing diversification of RES. As an example, a hydrogen based micro-grid can be integrated with the grid energy import/export exchanges and other RES sources to store and provide energy, when tidal power is insufficient. In order to manage the energy flows efficiently, an optimised energy management system (EMS) is required.

The overarching aim of this thesis is to design, implement and compare different energy management strategies and optimisation approaches for a hybrid system involving floating tidal stream energy integration

with green hydrogen production. This chapter will introduce the thesis by first discussing the context and the purpose of the thesis, followed by a literature review. The research gaps are then identified and the thesis objectives are formulated. Subsequently, the overview of the thesis structure is provided.

II. Context and generalities

The proposed thesis is performed under the framework of the Interreg European project 'Integrating Tidal energy into the European Grid' (ITEG) [1]. ITEG project initiated in 2017, comprises of actors from different part of North Western Europe, both industrial and academic partners led by the European Marine Energy Centre (EMEC). The aim of the project is to combine three low carbon technologies, namely the tidal stream energy, green hydrogen production and an efficient energy management system (EMS). The Orkney Islands in Scotland is selected as the test site for the project. The region is rich in tidal and wind energy potential with constrained grid. It is estimated that UK has 32 GW of tidal stream resource with 11 GW in Scotland, out of which 6 GW is in the Orkney Islands [11]. The graphical representation of the current system configuration of the ITEG project is highlighted in Figure I-1 [1]. As illustrated in the figure, the configuration includes a floating tidal stream energy system of 2 MW by Orbital Marine power, a 500-kW proton exchange membrane (PEM) electrolyser by ELOGEN (formerly AREVA), an electrical grid connection through a substation along with an embedded energy management system.

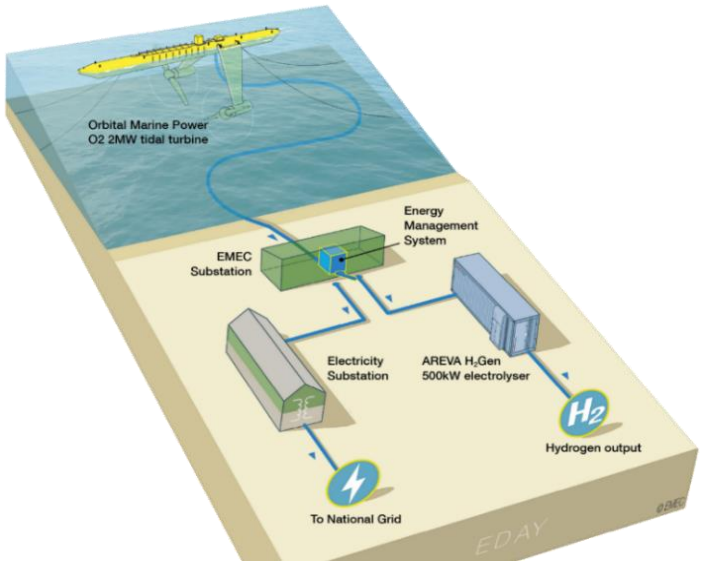

Figure I-1. Graphical representation of the current system configuration of the ITEG project. Courtesy- European Marine Energy Centre (EMEC) [1].

The tidal plant is deployed at the Fall of Warness in the Orkney Islands, which is a highly energetic tidal site with tidal currents as high as about 4 m/s.

The layout of the existing hydrogen plant at the EMEC site at the Eday in the Orkney Islands is shown in Figure I-2 [2]. A substation, power supply unit (PSU), electrolyser, compressor, associated heat exchangers, buffer tank for hydrogen storage, tube trailer and the static store for hydrogen are marked in the picture [2]. The electricity input from tidal stream plant/grid is delivered through the substation. The PSU houses the power converter devices like transformer, AC – AC converters and the rectifier. The water from the water/O_2 separator tank is fed to the electrolyser stacks through the heat exchanger. The electrolyser unit converts water and electricity to hydrogen and oxygen at 30 bar. A buffer tank is used in between the electrolyser output and the compressor to ensure a steady flow rate of hydrogen to the compressor. The compressor pressurises the hydrogen gas up to 200 bar. There are two main storage for hydrogen, called the static store and the mobile tube trailers [2]. The static store consists of pressurised hydrogen tanks. The compressed hydrogen could be filled in the storage units and transported through tube trailers. The objective of the proposed system is to generate compressed green hydrogen efficiently from the tidal stream plant to transport it to the main island through tube trailers to be used in suitable applications.

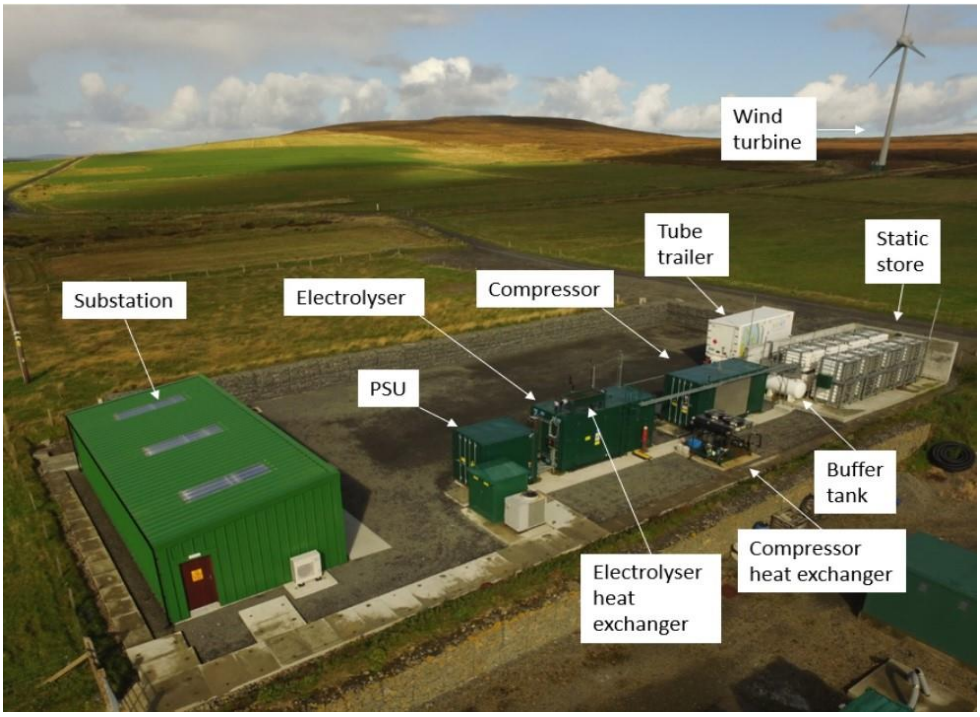

Figure I-2. Hydrogen plant layout at the EMEC site. Reproduced with permission from Fergusson and EMEC (credit- Orkney Sky Cam). Technoeconomic modelling of renewable hydrogen supply chains on islands with constrained grids, (PhD thesis, 2021). Copyright 2021, University of Edinburgh, IDCORE and EMEC [2].

Currently, a rule-based energy management approach is used to manage the power flow to the electrolyser. The large potential of RES in the site like tidal energy and wind energy could be harnessed effectively through green hydrogen production as there is a constrained electrical grid facility at the site. A community wind turbine rated at 900 kW is situated nearby to the site (refer to Figure I-2) and it has the potential to integrate with this overall system to increase its productivity. In addition, the site hosts a PEM electrolyser rated at 500kW by ITM Power.

The overall purpose of this thesis is to design an effective EMS for the proposed system configuration. Towards reaching this goal, initially the system configuration in Figure I-1 is integrated with the ITM electrolyser. Later, the current rule-based EMS approach followed is investigated by designing appropriate set point functionalities for the electrolyser units based on its different operating modes. The cost benefit analysis using the RBA is initially explored. Subsequently, an optimisation approach is proposed in this thesis, with an objective to maximise the operating profit and to maximise the hydrogen production with a priority for hydrogen production from tidal stream energy; while making sure all the system constraints are satisfied. Here, wind energy system, in addition to grid connectivity is also integrated to the system to effectively produce 'green' hydrogen and to ensure that minimum power requirement of the electrolyser units is maintained thereby aiding in optimal system operation. The optimisation approach results are then compared with the RBA approach to assess its effectiveness.

III. Literature review

An overview on the available literature on the marine energy systems, green hydrogen and energy management system domain is reported in the following. Results of this preliminary examination composes the state-of-the-art, defining the thesis context and objectives. A number of relevant scientific papers including both review and research articles were specifically referred as part of the literature review process apart from other sources like white paper reports, new articles, web pages etc. Mostly studies done in the past six years (2017-2022) have been selected; however, studies prior to 2017 have also been checked for learning on the fundamental concepts. As the topic is interdisciplinary in nature, a domain based systematic review is presented initially. A detailed review on the specified case studies undertaken is proposed in the chapters, where the case studies are conducted (chapter III and IV).

This review mainly focuses on three axes as mentioned below:

1. Electrical energy extraction from marine renewable energy focusing on tidal stream energy systems (TSES).
2. Green hydrogen production by polymer electrolyte membrane/proton exchange membrane (PEM) electrolysers.
3. Energy management system (EMS) and optimisation approaches of integrated renewable energy systems (RES).

Fundamental aspects of the above fields are presented for introducing the concepts initially, along with state-of-the-art technological advancement in each field. The perspectives on the current implementation of the technologies in a global context is mentioned. It is been particularly noticed that most of the research work in the given field especially for the tidal stream energy systems and green hydrogen system is in the European Union (EU27) and the UK and for the EMS, the implementations are mainly in the North America. As the following chapters, refer to the EMS strategies and operational synergies of a grid-connected hybrid tidal-wind energy system for electrolytic hydrogen production with a focus on economic and environmental aspects, the research gaps in existing literature is discussed in this context.

The scope of this sub-section is as described below:

Section 1 presents a general selection of the scientific articles covering fundamental concepts of marine energy especially tidal energy and research progress in the tidal stream energy systems (TSES). Studies from both categories of academic publishing and industrial projects covering different regions of the world have been sorted for reference to get an overview of the field. A brief note on main ideas of each article and its relevance to the thesis is presented. Section 2 presents the hydrogen consumption details, the green hydrogen state-of-the-art technologies, and the water electrolysis technologies focusing on polymer electrolyte membrane electrolysers. Section 3 presents the energy management system (EMS) design in micro-grids and discusses on different levels of EMS strategies. All these aspects are summarised in the Figure I-3.

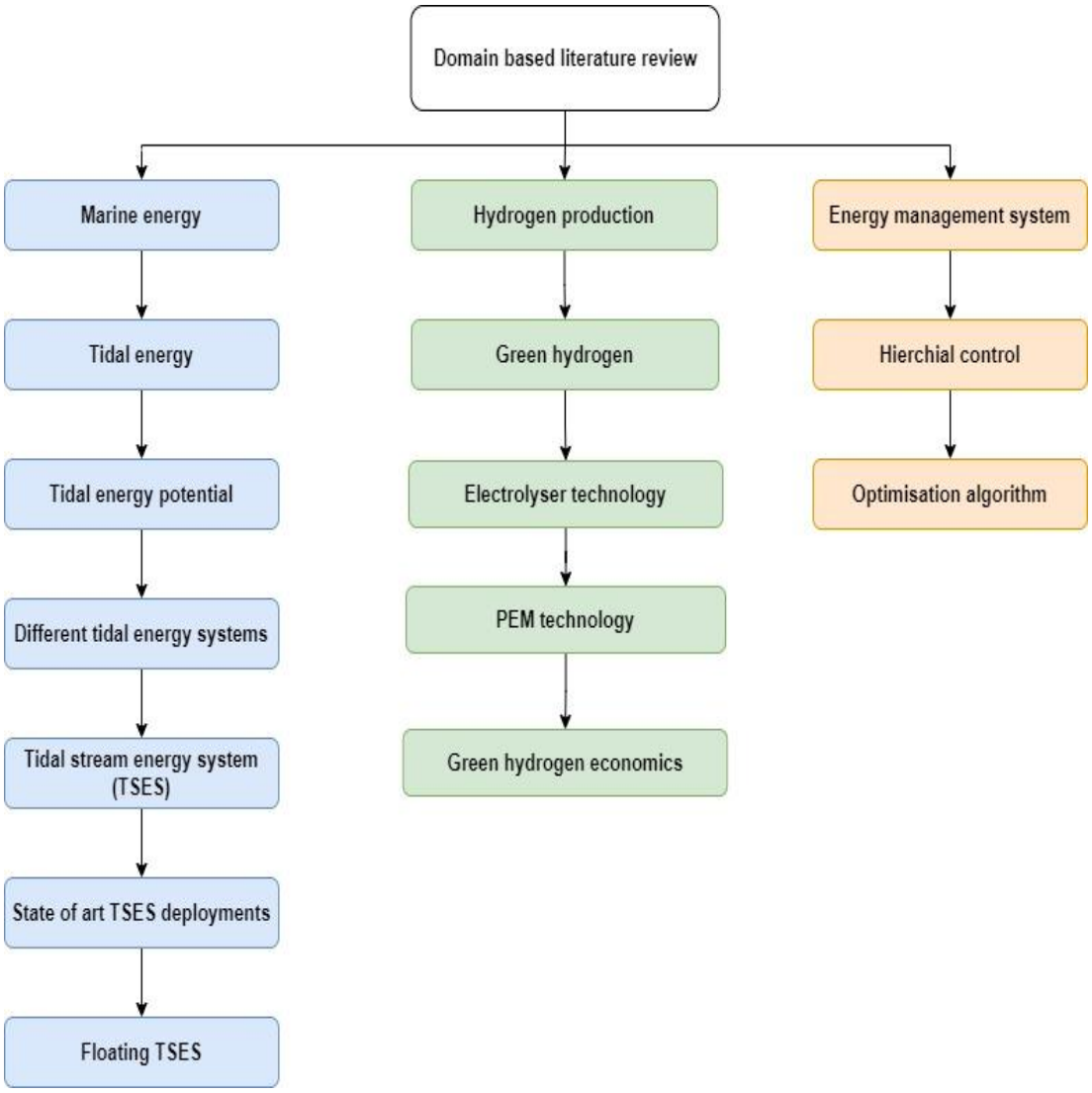

Figure I-3. General framework of the proposed literature review.

1. Electrical energy extraction from marine renewable energy focusing on tidal stream energy systems.

Marine energy systems also referred as ocean energy is a part of offshore RES. The main marine energy technologies are wave, tidal and ocean thermal energy conversion (OTEC) technologies. It is estimated that there is a global marine energy potential of 337 GW available that could produce over 885 TWh/year [12]. The main perceived benefit of ocean RES implementation is the diesel displacement, especially in the remote islands that are highly dependent on the fossil fuel for energy related applications. Apart from it, increased interest in including ocean energy technologies as part of a global energy system is also pursued. However, marine energy technologies are largely under prototype stage currently, with quite a number of

financial, environmental and technical risks to be addressed. The International energy agency (IEA) report, prepared for the pathways to achieve net zero emissions (NZE) by 2050 [13] estimates that the share of RES in total electricity generation globally should increase from 29% in 2020 to over 60% in 2030 and to nearly 90% in 2050. Among this, electricity generation from marine RES should be 1TWh in 2020 to 27 TWh by 2030 and 132 TWh by 2050, about 2% increase in the duration 2020-2030 and 14% increase in the duration 2030-2050. Marine electricity system capacity being 1 GW in 2020 is to be increased to 11 GW in 2030 to 55GW in 2050. This is about 34% increase projected for the duration in 2020-2030 and 16% increase from 2020-2050. As highlighted earlier, under the regional European scale, towards reaching the European Green Deal which was initiated in the late 2019, utilisation of offshore RES is essential [5].

Among the different marine energy solutions, particular interest is devoted to the tidal stream energy in the last decade. Tides are nothing but the rise and fall of the sea level due to the gravitational interactions between the sun, moon and the earth [14]. The underlying character of tidal energy is universal i.e. they are cyclic; that are either diurnal, semidiurnal or mixed tides with specified periods of high and low tides also called as flood and ebb tides respectively. In most places with tidal resource availability, a semi-diurnal tidal cycle is observed i.e., both flood tide and ebb tides occur twice a day with duration of approximately 12 hours 24 minutes along with slack tide period. This pattern and its amplitude can be predicted with up to 98% accuracy well in advance [1]. Coles et al. [3], have demonstrated the tidal current pattern and the capacity factor of the tidal power generation capabilities over different durations. Following the cyclic daily tidal current availability, there is a variation in resultant tidal power over a day. The tidal power capacity is high on spring tides, when there is direct alignment between sun, moon and the earth. On the contrary, the tidal power availability is low during neap tide periods, when there is misalignment with sun, moon and starts and this cyclic repeats about twice a month. It is observed that the monthly capacity factor does not vary significantly as the tidal current pattern over all the months is almost the same. Subsequently, there is a slight variation in tidal current pattern over a course of 18.6 years, called as the lunar nodal cycle, when there is variation in orbital path inclination of the moon relative to the plane of the earth. As a result, there is a ±10% yearly variation in resultant tidal power over the course of 18.6 years. The cyclic, predictable nature of the tidal current over the courses of a day, month, year and 18.6 years respectively with semidiurnal tidal cycle is presented in the Figure I-4 [3]. The deterministic predictable nature of tidal energy along with its high energy density are the key factors which makes it stand apart from other conventional RES like solar, wind etc. that ultimately depend on stochastically varying solar energy [15][16]. Tidal stream energy system (TSES) is an energy technology that harnesses power from the tidal current. Its operating principle is analogous to wind energy system. An interesting observation by Lewis et al. [17], states that in places having three TSES placed at 120 degree in phase with each other. It can generate constant power which could cater to a fixed base load of electricity continuously.

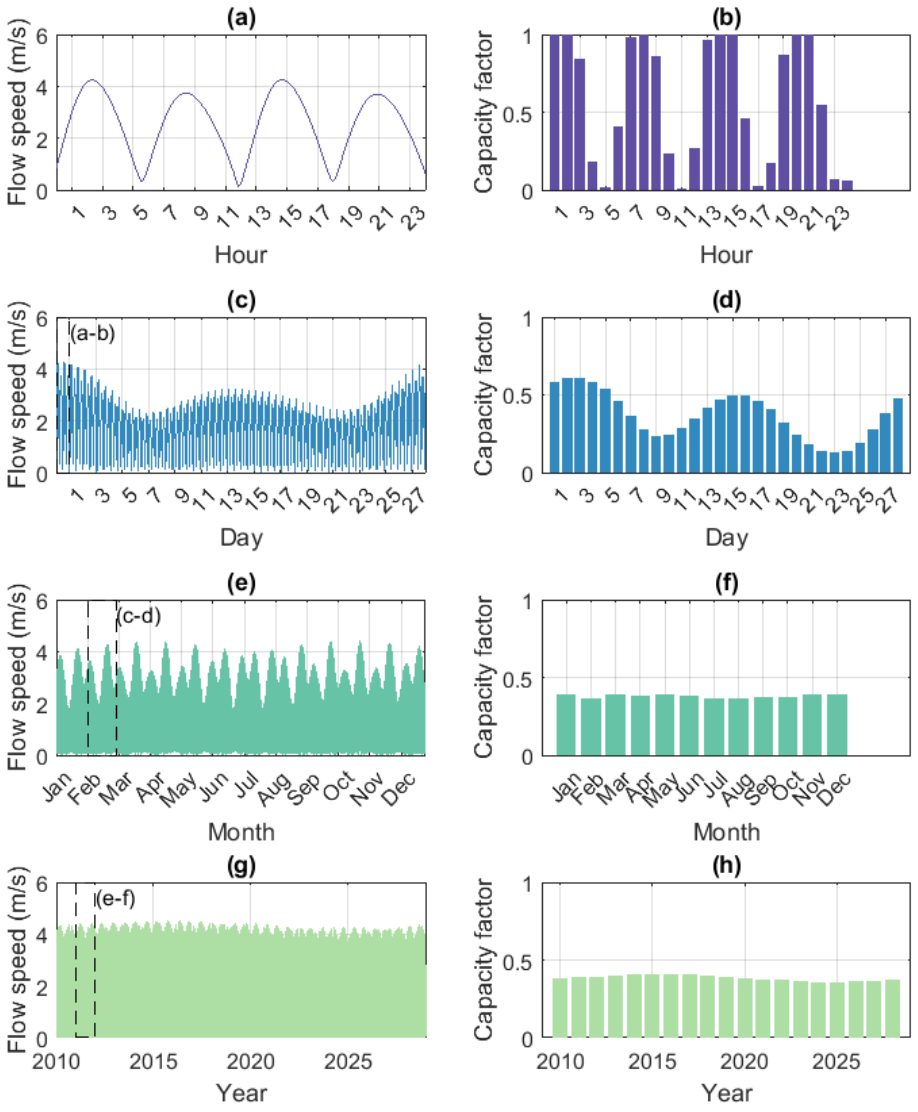

Figure I-4. Demonstration of predictability and cyclic nature of tidal energy and its associated power generation capabilities over a day(a,b), a month (c,d), a year (e,f), a span of 19 years (g,h). Reproduced with permission from Coles. A review of the UK and British Channel Islands practical tidal stream energy resource (The Royal Society publishing, 2021). Copyright 2021 The Royal Society publishing [3].

Lewis et al. [18], classified the first generation tidal stream technologies as the ones designed for rated speed of about 2.5 m/s, with second and third generation having lower rated speeds. Its observed that the first generation tidal stream system could be used in grid connection applications, while the second and third

generations can be used in 'high value markets' like islands or remote places to displace diesel use [18]. Another advantage with respect to second and third generation technologies is the possible reduction in whole system energy cost as the storage solutions capacity will be less due to the lower down time for no power output. This duration is higher for first generation tidal turbines.

Levelised cost of energy (LCOE) is a measure typically used to compare energy costs of different technologies. It is calculated as the ratio of net present values of total costs with respect to the total energy generation [19]. Considering the above aspects, the LCOE is relatively low for first generation turbines, due to its high annual energy production [18]. Further, it is estimated that compared to a similarly rated wind energy system, the size of the tidal stream energy device is smaller due to the higher density of seawater (seawater is 800 times denser than air) [2].

As per Neill et al. [20], the global tidal dissipation is about 2.4 TW, with 1.7 TW concentrated in narrow channels called as shelf sea conditions. The authors further observed that considering that the annual mean global electricity consumption is about 3 TW, a 10% extraction from the available tidal energy at about 170 GW could provide a significant contribution to the energy mix [20]. Additionally, a global tidal energy potential in the range of 64-120 GW is estimated in different assessments [15][21]. Figure I-5 highlights the global high tidal energy potential sites [22]. Europe and Americas have some of the highly energetic tidal sites in the world with flow speeds up to 4m/s and wave height 6m or even greater during storms [16][23]. Further, the UK has the highest tidal energy technology attractiveness index as per the PESTLE (political, economic, social, technical, legal and environmental) analysis done by Andres et al. [12], followed by France, Canada, the USA, Spain and Chile. It is almost an entirely unharnessed resource as per the estimates available. The only limitation in the UK for the tidal stream technology development is the constrained grid infrastructure as the tidal energy potential sites are near islands with relatively smaller grid facilities [12]. South East Asian countries like Malaysia and Philippines are estimated to have lower energetic tidal flow with maximum flow range at about 1.4 m/s and the gulf of California, where tidal current is estimated in the range of about 1-2.4m/s [18].

In the European regional level, it is estimated that 48-50% tidal resource is in the UK, followed by 40-42% in France and 8% in Ireland [24]. Carbon Trust in 2011 assessed that there is a UK wide tidal stream potential of about 21-31 TWh/year with a uncertainty bounds of -50% to +20% [25]. The various levels of uncertainty in the assessment of tidal energy potential is mainly due to the lack of updated standard over the definition of practical constraints for resource assessment [25]. As highlighted by Coles et al. [3], the large variation in resource assessment is due to the different parameters selected to estimate tidal energy potential like the hydrodynamic modelling used, use of mean tidal speeds, depth of water and high sensitivity of economic and environmental constraints. The Carbon Trust report re-estimated that the UK tidal energy potential to

be about 34 TWh/year, which according to [3], constitute 11.5 GW of tidal energy potential and if realised completely, it could provide about 11% of the current electricity demand of the UK.

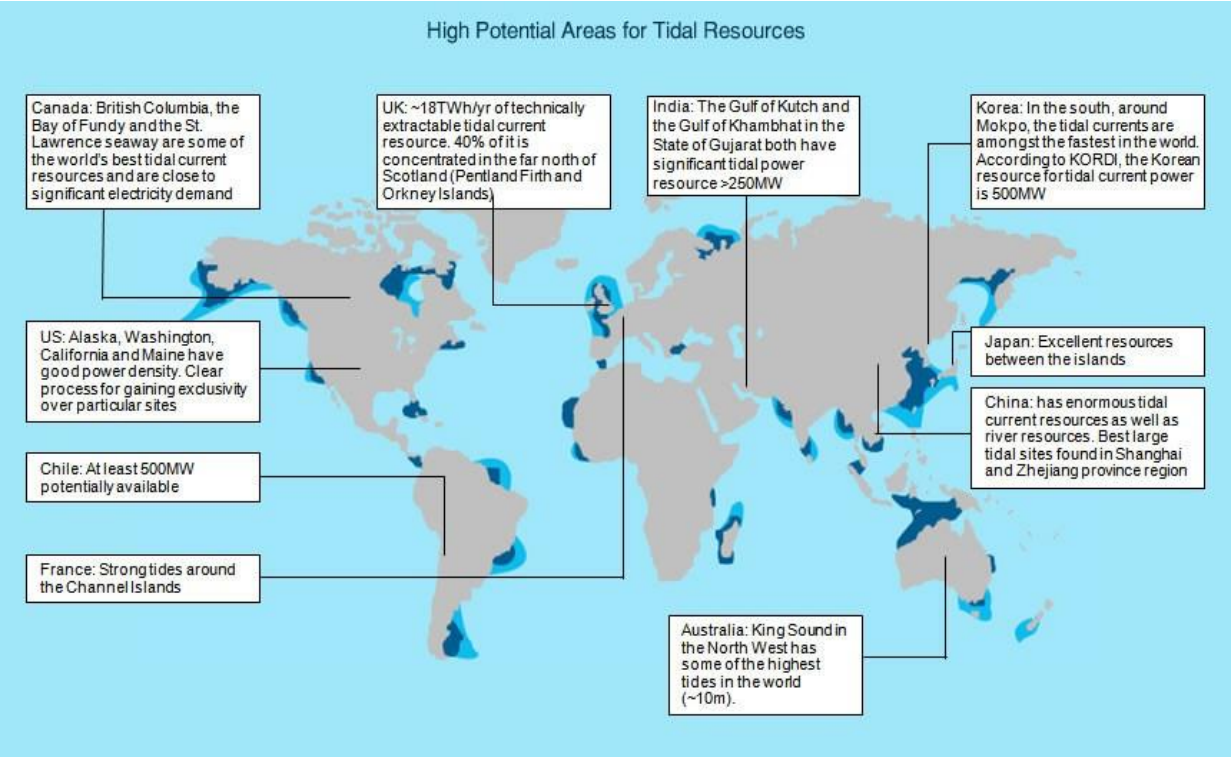

Figure I-5. Global high energetic potential sites for tidal energy. Courtesy- opportunityenergy.

Three technologies are mainly utilised to extract energy from the tides. They are the tidal barrage, the tidal stream energy systems (TSES) and the tidal fence [4]. Tidal barrages are dam like structure built on seabed to harness the potential energy of water. The earlier tidal energy harnessing projects were tidal barrages. Tidal barrages are commonly constructed across the tidal regions. The main disadvantages of this solution are its high capital cost and relatively larger ecological effects on marine life. On the contrary, TSES technologies, as mentioned earlier harness the kinetic energy of tidal currents by mechanical rotors fitted with rotating blades to convert it into electricity using a generator. Tidal stream turbine has been increasingly reproduced of- late due to its similarity to the wind turbine technology and reduced environmental effects [3][26]. A number of TSES demonstration projects are under operation in many parts of the world currently. Finally, another relatively sparingly used technology, is the tidal fence, where typically vertical axis turbines are mounted on a fence or row placed on seabed and utilises the tidal current for energy production. Particularly this solution is perceived to cause lower ecological damage compared to the tidal barrage in a long run. Concluding, tidal energy is still largely unexploited. In this context, an increasing number of devices is currently under testing or demonstration phase, with the exception of tidal barrage technologies.

In literature, TSES are also termed as tidal current turbines, tidal in-stream generators, tidal energy converters and marine current turbines [14]. The typical components of TSES, in analogy with wind energy systems (WES) include a turbine with blades, rotor, gearbox, generators, power converters etc.

Expertise from the wind turbine and Oil & Gas industries are extensively being reproduced to the design, installation and operation of TSES [3]. As it is in the early stages of research, development and operation, a large variety of concept designs for tidal energy conversion have been explored in the last few years [27]. Similar to the developments in the wind energy and offshore energy industries, different types of TSES designs are being explored. The broader difference is in the choice of axis, mounting of turbines, foundation type and the other different characteristics of the associated electrical and mechanical equipments [21][14]. Each design differs based on the choice of axis types, i.e., horizontal or vertical axis, the mounting type being fixed or floating type, the foundation type to be moored using an anchor, gravity based or piled structure. Other design considerations include the type of generator configuration, number of blades, fixed pitch or variable pitched yaw control, sealed and flooded generator, location of converters etc. Currently, horizontal axis fixed bottom devices with fixed pitch constitute the major share in the deployments. A comprehensive view on the different TSES system configurations classified primarily based on the ducting, extractor type, mounting type and foundation type is illustrated by Walker et al. [15], and it is given in Figure I-6 for reference.

The following sub section focuses on the state-of-the-art deployment of TSES. As of 2019, the global installed capacity of tidal stream energy devices is at 35.5 MW which approximates to 0.06% of the lowest resource estimate [15]. A number of prototypes and early commercial technologies are currently under study. As per the literature estimates from 2006 to 2013, more than 40 novel systems in TSES are identified with major ones being 6 different technologies. There are about 75 designers worldwide with 15 in USA and 29 in UK being the major players. Among the 75 projects, 34 are at TRL 7-8, i.e., prototype scale testing being performed at sea; 8 are at TRL 9 i.e., experimentation of a demonstrator system at sea for longer periods [14]. Till date, 58 deployments of tidal stream devices are identified in the review by Walker et al. [15] from the year 2003 to 2020. The majority being in Scotland (20) understandably having some high energetic tidal potential in the world followed by France (10) and Canada (7). Deployments were also recorded in the USA, Netherlands, China, Northern Ireland, England, Wales, Australia, Denmark, Belgium and Norway [15]. It is estimated that the tidal stream energy technologies have completed 1.4 million operating hours globally by 2020. As suggested by the assessment in [15], comparing it with the learning rates of wind energy technology it can be stated that the sector is currently at the same learning rate as that of the onshore wind energy technology in the year 1985-1990 with a learning rate of about 15-17% [15].

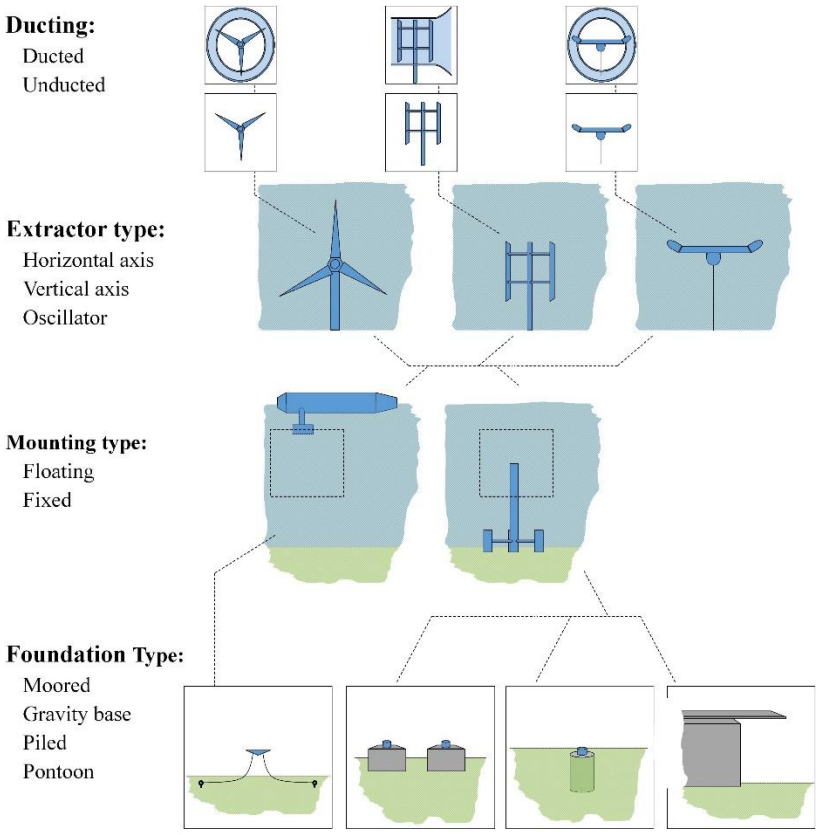

Figure I-6. Different types of TSES. Reproduced with permission from Walker. A review of component and system reliability in tidal turbines deployments (Renewable and Sustainable Energy Reviews, 2021). Copyright 2021, Renewable and Sustainable Energy Reviews.

The updated TSES installed capacity for the UK and the British Channel Islands was examined by Coles et al. [3] and it is illustrated in the Figure I-7. The projects which are already planned and the trajectory required to reach the practical resource potential of 11.5 GW was also highlighted. The updated global tidal stream installed capacity by 2020, excluding the UK was also included. The offshore fixed bed wind energy systems deployment in the UK was also included for an effective comparison. The economic support schemes for TSES are also referred here. The renewable obligation certificate (ROC) was the support scheme for RES generators practiced in the UK till 2015, using which the electricity providers were required to ensure certain renewable energy composition in their electricity mix. The RES generators were then paid for each unit of electricity supplied. Later, the scheme called contract for difference (CfD) was applied for RES generators. The advantage of the CfD scheme is that it protects the RES generators from the volatile electricity market prices by providing a flat rate for electricity called the strike price, typically for a duration of 15 years [3]. The difference in cost is met by the CfD supplier obligation, a levy on the electricity suppliers.

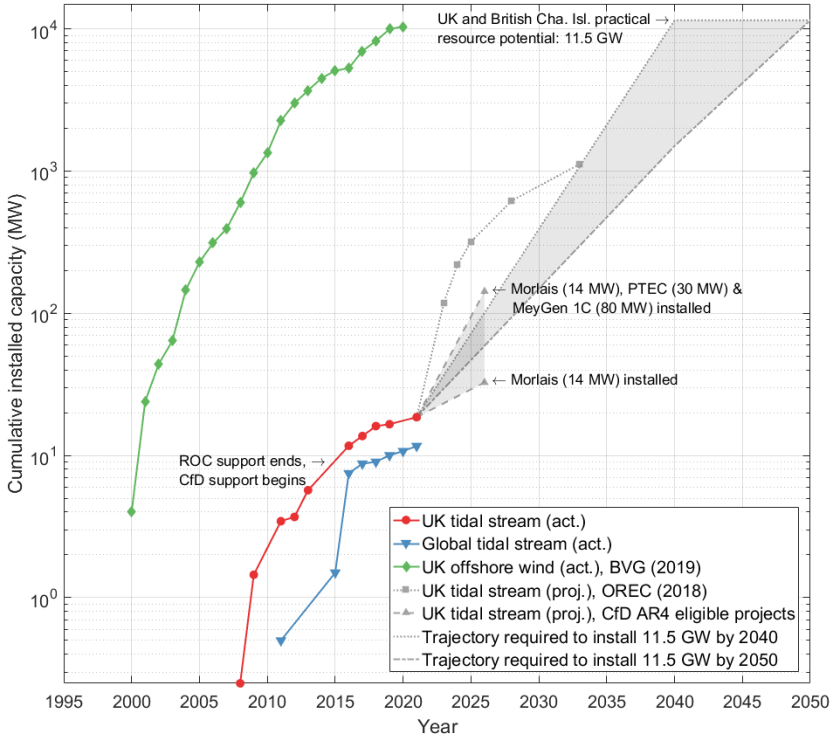

Figure I-7. Actual and projected TSES capacity in the UK and on a global scale. Reproduced with permission from Coles. A review of the UK and British Channel Islands practical tidal stream energy resource (The Royal Society publishing, 2021). Copyright 2021, The Royal Society publishing.

The test site of EMEC at the Orkney Islands in Scotland has been a major test site for a number of tidal stream energy technologies with prominent ones being O2 by Orbital Marine Power, Open hydro, HS1000 and Voith Hydro Turbine technology. Both Open hydro and Voith Hydro Turbine technology uses fixed pitched blades and permanent magnet synchronous generator to achieve a compact size. The Seaflow turbine owned by Siemens (originally Marine Current Turbine), has been a pioneer in horizontal axis TSES fixed on to the seabed [24]. Another well-known tidal stream turbine is the Sea Gen S, which is a variable pitch bottom fixed turbine. It is a 1.2 MW system, that is installed and it is in operation in Northern Ireland, since 2008. Sea Gen S was the world's first grid-connected tidal stream energy plant and it had generated close to 6 GWh of electricity as of 2015 which was the highest cumulative energy export from a TSES till then. The commercial success of the Sea Gen has then ignited further interest in the field. SR200 device by Orbital Marine Power with a floating TSES technology is currently decommissioned and it had exported 3 GWh of electricity in its first year of operation [14]. O2 device, the latest version of SR200 has commenced its grid – connected operation at the Fall of Warness in the Orkney Islands since 2021.

In this review, for the purpose of comparison, two main TSES classified based on the mounting types are chosen for further discussion. They are,

a. Fixed bed devices - TSES mounted on the seabed
b. Floating devices - TSES floating on the sea surface that are anchored to the seabed.

The typical illustrations of a sea-bottom fixed device (a) and a floating device (b) are presented in Figure I-8 (a-b).

Operation & Maintenance (O&M) is a major factor for tidal energy cost reduction and reliability improvement. It is estimated that O&M in floating energy devices and fixed bed devices are at 17-20% and 43% of the total cost respectively [15]. The floating TSES requires smaller vessels and barges for its installation and maintenance operation, significantly reducing the associated costs. Further, floating devices can be towed easily to the shore for any repairs, if needed. The towing capability allows for changing the location of the energy harnessing compared to the sea bed mounted device, where the device is fixed. Installation costs are lower for floating devices due to the requirement of smaller vessels for installation and lower material requirements compared to bottom fixed TSES. In a laboratory scale comparative analysis done on both a fixed and a floating TSES device, it is observed that the floating devices generated more power and experienced lower force on the support structure than the fixed bed devices for operation under same flow velocities and wave conditions [16].

(a) (b)

Figure I-8. (a). Artistic impression of sea-bottom fixed tidal stream energy system. Courtesy – Energybc. (b). Floating tidal stream energy system. Courtesy – Orbital marine power.

In the event of waves, turbines with floating structures performed better at around 40% than the turbine mounted on the fixed structure [16]. Additionally, the LCOE of fixed bed TSES is estimated to be 300 £/MWh (351€/kWh) in 2020 with a potential to reduce to 150 £/MWh (175 €/kWh) at 100MW of deployment [15]. As per the updates from industrial representatives, LCOEs of 255 £/MWh (298 €/kWh) have been reported for some floating devices currently [12].

As per Walker et al. [15], floating TSES were less likely to fail than fixed TSES and more likely to be curtailed comparing all major TSES deployments in the recent years, the authors further observes the cause of lower failure rate, being the easier access for curtailment and maintenance before the occurrence of a complete failure. Further, the most critical components of a floating TSES that are typically prone to cause disruption in its operation was identified by Le Diagon et al. [26]. The components in the decreasing order of their criticality assessed through a reliability, availability and maintainability (RAM) analysis method were the pitch systems with a likely failure rate of 43%, blades (20%), gearbox (10%) followed by high speed shaft, power converters, control system, low speed shaft bearings. On the contrary, for the fixed bottom devices, the critical components in the decreasing order of their critically were gearbox/ high speed shaft (19.1%), power electronic converter (17.5%), pitch system (17.5%), yaw system (12.6%), control system (9.5%), blades (8.1%) and generator (4.3%) [26]. Neill et al. [20], observed that the fortnightly variation in tidal stream current is minimised in less energetic tidal sites. However, often less energetic sites are located in deep water in the open sea farther from the shore and grid connections. In such a scenario, floating TSES are the best solution as these are the preferable option for installation at deep sea levels. The floating TSES can be used to power weather buoys, tsunami monitoring devices, communication and defence application [20]. Floating TSES has a disadvantage over fixed bed when it comes to its placement, as it could cause disruption to the shipping transport, especially when array design in considered. However, similar is the case with offshore RES like wind and floating solar. It is observed that, the solution which could have a near competitive edge with respect to offshore wind plant (currently at an LCOE of about 0.194 €/kWh) is floating TSES [12]. Thus, among the different technologies, floating tidal stream energy systems are advantageous over the traditional tidal barrages or fixed sea-bed tidal stream devices in terms of investment cost, ease of maintenance, decreased ecological impact, and increased annual energy output [28][29]. Floating TSES is used in the proposed thesis and the specifications of which are detailed in chapter II. Lastly, another type of variant is the fixed surface piercing model, in which the turbine rotor is placed on a pole that is pierced on to the sea bottom [12], typically having twin rotors placements which are movable vertically aiding easier maintenance and repair works. This design accounts for the benefits of both fixed and floating TSES devices. The commissioning of bottom fixed tidal stream system (a) and floating systems (b and c) are presented in Figures I-9 (a-b-c).

(a)

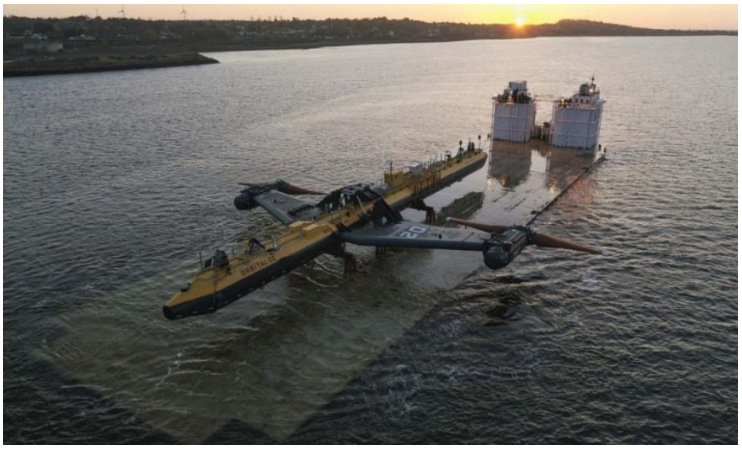

(b)

(c)

Figure I-9. (a). Commissioning of sea-bottom fixed TSES. Courtesy – Maygen.

(b) and (c). Commissioning of a floating TSES. Courtesy – Orbital Marine power.

Understandably, the initial research in the field has been mainly on resource assessments and site identification. Later research phases were to build prototypes and scaled models of TSES developing commercial prototypes and testing. Of late, with the support from the UK government early commercial projects have been deployed with a plan to deploy 124 MW by 2031 [3]. As tidal energy is highly site specific and usually occurs around a narrow range, it is important to harness the complete energy potential and to justify for the economic reasons that tidal farms is a feasible and necessary solution. It is therefore studied and recommended, to use the tidal turbine in array arrangement.

One of the main aspects for tidal stream energy development currently is the intervention of policy makers. Often times, the currently expensive tidal stream energy costs are compared with relatively mature technologies like onshore/offshore wind energy systems which poses disadvantage to the technology development. Also, decreased investor confidence is also a factor that the field is experiencing due to the perceived failures observed in the early development models, which is multifaceted [15]. It is important to analyse and improve the return on investment of this technology to gain investor confidence [10]. Current focus in tidal energy is in cost reduction, as was the case with wind energy two decades back. Financial support instruments such as CfD could help to reduce the current cost gap and it is explored in the proposed thesis. Further, future revenue streams are a cause of concern for investing in ocean energy technology that is where the integration of the technology with other RES technology could benefit the overall system. Observations by [15][26], suggests that as the TSES devices cover a large design topology, there is lack of extensive learning and understanding for a single technology to help in assessing the overall picture of the technology. Bahaj et al. [28][30], observed that even though tidal energy is costly in the current context due to high capital costs, if the associated high load factors in a suitable site is exploited effectively, it can compensate the higher costs. Also, the relatively high reliability of the tidal stream energy may be undervalued in the current energy mix [17]. The long-term reliability of tidal energy solely in terms of forecast accuracy is quite high when compared with wind or solar energy technologies.

The whole system energy costs accounts for the overall cost of a system, when two or more systems are integrated together. Enhanced LCOE (eLCOE) is a metric that includes whole system energy costs in its calculation for an improved representation of cost of energy. According to a study conducted by Department of Business, Energy and Industrial Strategy (BEIS) [3], the eLCOE of offshore wind energy systems is 50-100% higher than its projected LCOE for the year 2035. This is largely due to the additional costs on back up capacity. A preliminary analysis has explored that the tidal stream energy has the potential for cost savings under eLCOE context [3]. Another analysis have highlighted that when comparing a TSES integrated with short term energy storage (ESS) and a backup diesel generator configuration to a wind energy system integrated with a backup diesel generator configuration and ESS, the corresponding annual

use of diesel is reduced by about 50% when TSES-ESS-generator configuration is used [31]. Further, due to the cyclic nature of tidal energy regular charging and discharge periods occur in contrast to WES where long periods of high winds and low winds occur. Finally, the curtailment of energy is also reduced, when TSES-ESS-generator configuration was used [31]. However, more research is needed in this direction. Thus, the proposed advantages of tidal energy as a diverse RES into the current energy mix are numerous. It helps in reduction in energy storage requirements, improved grid integration benefits and possibility for islands or coastal areas to act as a net energy exporter. Additionally, it helps in increased improvement for the design of whole system model and possibly the costs, because of the high degrees of certainty in the tidal power prediction that requires less intervention in the later stages [3].

A brief note on the environmental aspects that the TSES are affected by and the ecological effects of the TSES is given in the following:

Tidal turbines are affected by the environmental factors like wind, waves, turbulence, cavitation, and bio-fouling especially in the case of tidal farms [14]. Tidal turbines are subjected to two types of turbulence, ambient and wake turbulence [20]. Ambient turbulence is the turbulence cause by natural water flow. Wake turbulence is the turbulence caused by the movement of another adjacent turbine. Osalusi et al. [20], has studied on the turbulence effect at the Fall of Warness site. The study was focussed on near sea bed turbulence interactions as most the of TSES currently deployed are sea bottom fixed devices. As per Nachtane et al. [14], biofouling on the turbines could reduce 70% efficiency. A power performance drop as high as 43% is reported on a fouled rotor compared to a ‘clean’ one on a test done on a floating system with the rotor kept stationary under the surface of water for four weeks [32]. Further, ecological impacts of TSES arrays have been under research in recent years. Even though, sea-bottom fixed tidal arrays could cause ecological impacts on marine life, there has been no evidence of considerable impacts [3]. Habitat change and marine life displacement cause due to tidal arrays is relatively small compared to the magnitude of impacts of climate change [3]. Additionally, standalone TSES has shown to cause little to no harm to its environment. Overall floating devices have the benefit of having a lower impact on marine ecosystems. Continued research is in progress in this area as the industry is in early stage development. Finally, social acceptance of TSES technologies is another field that is being investigated with keen interest.

2. Green hydrogen production by PEM electrolysers.

Hydrogen is the most abundant and simplest element on earth; however, it doesn't exist by itself. Hydrogen is typically combined with carbon in hydrocarbons (natural gas, oil) or with oxygen in water. The advantage of hydrogen as an energy carrier is its high energy density (120 MJ/kg) compared to conventional fuels like diesel (45.5 MJ/kg) and petrol (45.8 MJ/kg) [9]. Hydrogen is considered as an important energy carrier vector that can aid in process of decarbonisation of the sectors that are currently difficult to decarbonise such as transportation [33]. Hydrogen has a wide variety of applications, also termed as H_2 to X pathways, as a feedstock in industries, power generation through fuel cells, injection into the gas network, transportation etc. [33][34]. Hydrogen stored in tanks or caverns is also identified as a suitable candidate for long-term energy storage solution to provide seasonal flexibility to the power system compared to the batteries which are most suited for short term storage [35]. Long term storage is especially important in the future with the anticipated increase in excess renewable electricity production for NZE [36]. It is observed that the hydrogen can be the key factor to couple the currently largely decoupled market of transportation and energy markets. Direct injection of hydrogen in the current natural gas network is possible for up to 12% of total composition depending on different country standards in EU [37]. The value could be up to 17% from a technical perspective as observed by J.J. Brey [34].

Electrolysers are devices that convert electricity and water to hydrogen and oxygen. It was discovered in the year 1789 [38]. The electrochemical reaction of reduction at cathode and oxidation at anode enable the production of hydrogen and oxygen [37]. It is estimated that for every 1g of hydrogen, 8g of oxygen is produced in the process. Water electrolysis is a mature and commercially available technology.

Globally, 120Mt of hydrogen was produced in 2020, which represents 4% of global final energy use [33]. The European Union currently uses about 9.7Mt of hydrogen annually, out of which 30% is used in oil refineries [33]. Around 95-96% of the current global hydrogen production is through the carbon intensive steam methane reforming (SMR) process and coal gasification, being responsible for adding up to 1.8% of the global CO_2 emissions [9] [39]. The rest about 4-5% is through water electrolysis technology especially for chlorine production industry typically from carbon intensive electricity sources [33]. As per NZE report [13], hydrogen-based fuels are accounted for 30% of the global final energy demand in 2050. 150 Mt of low carbon hydrogen with a capacity of 850 GW electrolysers by 2030 and 435 Mt of low carbon hydrogen with 3000 GW capacity by 2050 electrolysers are identified as key miles stones in the pathway to NZE. The current global electrolyser capacity is about 0.3 GW. The European Union (EU) hydrogen strategy aims to have 40 GW of renewables linked electrolysis capacity in the EU by 2030 [8]. In the European green deal, clean hydrogen is identified as a priority area for decarbonisation by 2050 [33]. At least 6 GW capacity of

electrolysers powered by renewable energy is to be installed between 2020 and 2024. By 2030, it should be 40 GW, by then the hydrogen demand in UK and EU27 would be 16.9 Mt [33].

Hydrogen is also defined in different color codes based on its production pathways. The hydrogen produced from SMR or fossil-based pathways are termed as grey hydrogen. Grey hydrogen with carbon capture implementation is termed as blue hydrogen. Green hydrogen, also called as type of Power to Gas (PtG) process is the hydrogen produced through water electrolysis by RES powered electricity. The grey hydrogen through SMR process and coal gasification is highly carbon intensive and it is responsible for about 8.9 $kgCO_2/kgH_2$ and 29.66 $kgCO_2/kgH_2$ carbon emissions respectively [37][38]. As it is evident, green hydrogen is the most sustainable solution among the alternatives mentioned. However, it does not contribute into hydrogen production mix currently largely due to its high cost [37].

The three main electrolysers available are alkaline electrolysers (AEL), polymer electrolyte membrane (PEM) electrolysers and solid oxide electrolysers (SOEL). The major differences with the three types of electrolysers are the electrolytes used and the range of temperature at which they operate [38]. AEL is the most commercially used electrolysis technology, typically used in large-scale industries. It is relatively cheaper compared to other technologies. AEL has the drawback of operation at low current densities and low pressure [40]. As AEL is based on liquid electrolyte, its inertia is larger with slower ion transportation making it less suitable for dynamic operations [40]. PEM electrolyser uses solid polymer electrolyte membrane and it is especially useful for integration with RES due to its efficiency with dynamic operation, i.e., very quick responses to current changes in the order of milliseconds [41]. PEM electrolyser are compact. PEM cells can be connected in series to increase the power rating [42]. It is able to operate at lower cell voltages, higher current densities, has lower carbon footprint and has typically less downtime compared to AEL [41][42]. Main disadvantages of the PEM are the high materials cost for the membrane, cross permeation phenomena that increase with pressure and higher degradation rate. PEMs are commercially available. Initially, PEM electrolyser application was focused on small scale systems; however, the trend is changing now. For instance, Cummins (former Hydrogenics) have installed 25MW (5×5MW) in Germany to produce hydrogen for rail applications. SOELs, originally reported in the literature in the 1980s is still under research and development stage [38]. It is considered that if the SOEL technology can be realised successfully, it would make it possible to have high conversion efficiency under higher temperature operation [38]. Direct electrolysis of seawater (DES) is also a possible method using a well-known technology in chemical industry known as chlor-alkali process [41]. In this process, seawater acts both as the electrolyte and the feed. Its investment cost estimation is too high about 6000 US $/kW with operation and maintenance costs about 4-5% of the investment cost per year. This is due to the requirement of desalination of water and hence, there are no commercial plants available yet.

A multi-criteria analysis of different electrolysis technologies by Domenech et al. [41], has shown that PEM electrolyser is the most suited technology for marine environment in the short term by weighing various economic, environment and social factors. In the proposed thesis, the focus is on PEM electrolyser technology and hence it will be discussed in detail in the following.

The first PEM electrolyser was developed by General Electric Company in 1960s [40]. PEM electrolyser is an electrochemical converter that utilises DC electricity to convert water to produce hydrogen and oxygen. The cross section of a PEM electrolyser cell is given in Figure I-10 [43]. The structure of the PEM electrolyser consists of two electrodes at the sides of a thin proton conduction membrane with catalyst layer (CL) at either side. This entire assembly is called the membrane electrode assembly (MEA) on sides of which, there is the gas diffusion layer (GDL).

The simplified working principle of a PEM electrolyser is as follows, the water enters through the flow channel to diffuse at the GDL at the anode. At the CL, water is dissociated to electrons, protons and oxygen. Oxygen leaves the system freely or could be valorised based on specific applications. Protons pass through the PEM to combine with electrons which passes externally in the circuit to form hydrogen at the cathode side [43]. The bipolar plate is the structure that holds entire assembly together which contains pathways for products and reactants to flow accordingly and separate one cell from the other in a stack [42]. The bipolar plate material should have high mechanical strength and corrosion resistance like titanium [40]. For the GDL at the anode side, titanium is preferred as it requires high corrosion resistance, works under high potential, and suitable to work in acidic conditions [40]. The MEA should conduct the proton transportation, make sure that electrons are deviated to the sides, and should prevent gas crossover. Currently, fluro-polymer Nafion membranes are used for this purpose [40]. Nafion based membranes are effective due to their desirable properties for proton conductivity however, they are expensive and also disposal at the end of the system lifetime is a cause of concern due to the fluorine component [38]. Research is under way to find substitutes for the MEA materials like hydrocarbons for possible improvement in the system performances like low cost, good proton conductivity, low gas permeation, and the capability to work under relatively low humidity [40]. The various physical components of a PEM stack are illustrated in Figure I-11 [44].

The decomposition of water in water electrolysis occurs when the applied potential is greater than the thermodynamic reversible potential. Thermodynamic reversible potential is the potential difference between anode and cathode under reversible conditions; a value of 1.229V is usually considered.

Considering no heat source, additional energy is to be supplied for the reaction. The potential threshold is called thermo-neutral voltage, which is about 1.481V.

Thus, the potential of a single PEM electrolyser cell is given by (I-1) [43]:

$$V = V_{\text{ocv}} + V_{\text{act}} + V_{\text{diff}} + V_{\text{ohm}} \quad \text{(I-1)}$$

where, V_{ocv} is the open circuit voltage, V_{act} is the activation overpotential, V_{diff} is the diffusion overpotential and V_{ohm} is the ohmic overpotential. Activation overpotential are caused by the potential losses from electrolysis electrochemical reaction. Activation losses are the major cause for lower efficiency, when operating at high voltages and lower current densities. The diffusion overpotential is caused by the mass transport inside of the electrodes. As the electrolysis process occurs, water must be transported to the reaction layer and the gas is to be removed from the reaction site. The electrical resistances of plates, electrodes, membrane and interfacial resistance between the layers are the main causes for ohmic losses.

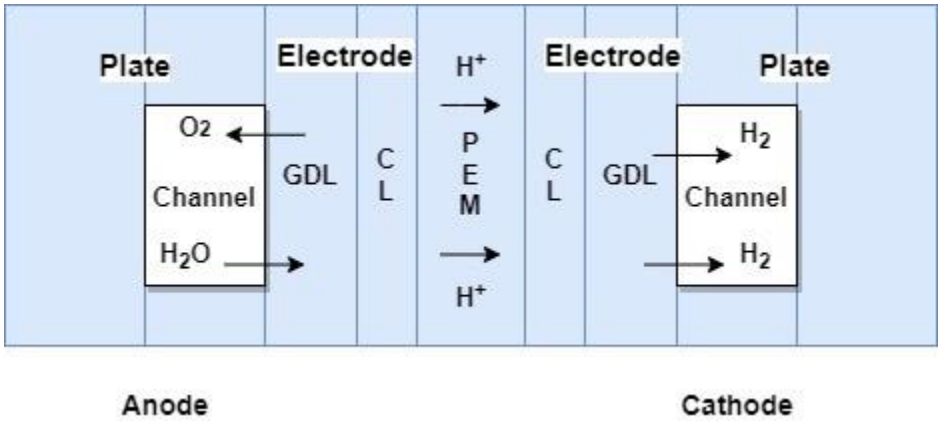

Figure I-10. Cross section of a PEM cell, adapted from [43].

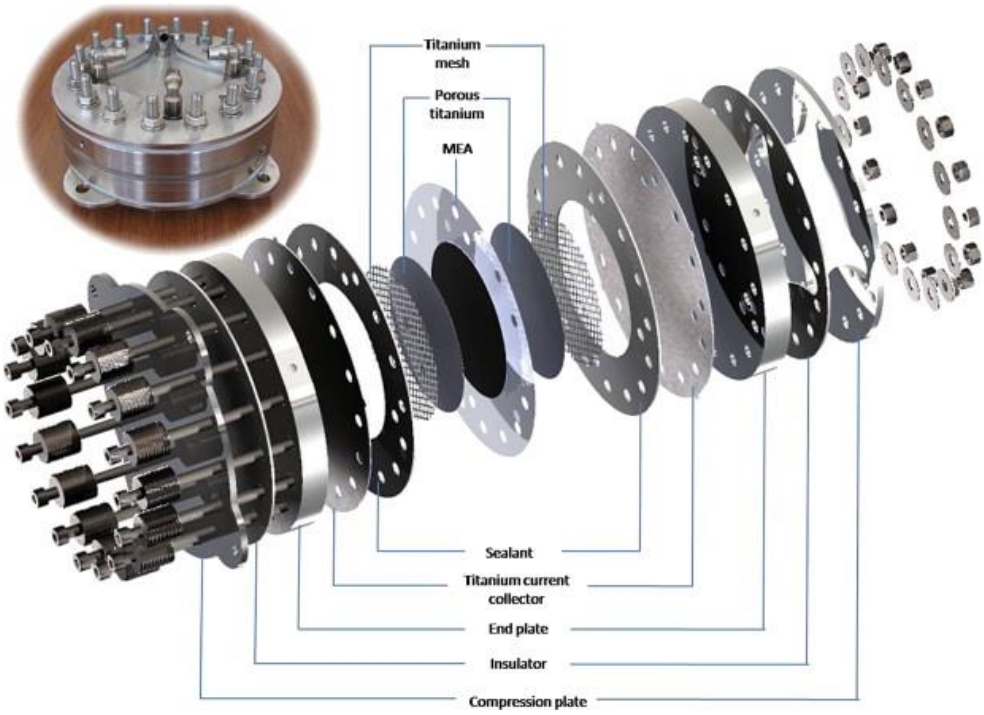

Figure I-11. CAD drawing of a PEM electrolyser. Reproduced with permission from Kaplan, Development and testing of a highly efficient proton exchange membrane electrolyser stack, (International Journal of Hydrogen Energy, 2011). Copyright 2011, International Journal of Hydrogen Energy.

In the middle of the operating range, the predominant trend is mainly characterised by the ohmic overpotential due to the electrolyser cell resistance generated by ionic and electronic conduction. At high current densities, the mass transfer phenomenon is introduced. At this stage, the gas bubbles block the active area and damages the contact between the electrode and the electrolyte; thereby, decreases the catalyst utilisation. Mass transport over potential is not usually seen until moderate current densities. The conductivity of electrolyser cell is higher for increased temperature and low pressure operation [42].

The selection of the membrane thickness results in a trade-off between the expected operating pressures across the membrane, mechanical resistance, low gas crossover and ohmic resistance. It has been observed that very thin membranes allow reducing ohmic losses and operating the membrane in high pressure due to its high mechanical resistance. In contrast, higher the operating pressure, the higher is the hydrogen crossover rate. As a result, activation loses due to hydrogen and oxygen crossover increase. As activation losses are related to faradic efficiencies, it leads to decrease in PEM electrolyser energy efficiency [40]. In case of low current densities and high pressures, the mobility and solubility in the membrane also increases which is hazardous for the system [38]. Hence, it is important to define the minimum stack operating current to restrict hydrogen crossover rate and ultimately guarantee the operational safety [45]. Increasing the outlet pressure causes the system to operate safely only in a narrow range [45]. Hence, it is also important to reduce

the operating pressure to have wider control range as the area of safe operation increases. Typically, manufacturers specify the safe operating range and it is desirable especially when coupled to intermittent RES [45]. Membrane thickness and operating pressures are key issues to enhance the performance of PEM electrolyser [40]. It is possible to reach values more than 100% of the nominal rated power density, which is obtained from fixed current density as the hydrogen permeability is low through the Nafion membrane [38]. Newly designed PEM electrolyser can reach operating pressures as high as 350 bars. Operating PEM electrolyser at higher pressure is desirable in the view to avoid compression stage [38]. Understandably, high temperature has a positive influence on water electrolysis and high pressure has negative influence. The efficiency drops in electrolysis due to increased pressure operation overrides the energy requirement to compress the hydrogen, hence it is more preferred in some cases [37].

As observed in Figure I-12, PEM electrolyser unit includes several ancillary devices like power supply unit, water purification system, heat exchanger, hydrogen processing system like compressor if necessary and buffer storage tanks, and cooling system with associated pipes, valves, etc. [40]. A picture on PEM electrolyser container enclosing the auxiliary equipments are given in Figure I-12. Towards this purpose, an ISO certified container is generally used enclosing the integrated electrolyser system with stacks, piping, airflow system, and the cooling system.

Figure I-12. A PEM electrolyser unit container. Courtesy - Elogen.

Operation of PEM electrolyser leads to the degradation of the catalyst in a slow pace [38]. Impure feed water can contribute to MEA poisoning leading to degradation, which affects the system efficiency [38][41]. As PEM electrolyser is a sensitive technology, the presence of impurities like calcium and magnesium ions in feed water could cause blister development in the cathodic side of the MEA [41]. Operation of longer hours can lead to material deposit at the anode and cathode resulting in reduction of active catalyst area ultimately reducing the current density [38]. When electrolysers are operated beyond 1000 hours, the chance for mechanical stress on the membrane like crack, tear due to the pressure of the reactants are high [38]. The texture of GDL could also be a cause of concern. Researchers believe that the holes created in the membrane due to the surface of GDL being rough are the reason for high permeability of hydrogen crossover, once pressure is increased [38]. The chances of mechanical failure are quite high on operation at high pressure. Degradation caused by thermal operation and chemical factors are also a cause of concern and is detailed in the studies in [38][46]. State of the art in PEM water electrolysis has been reported to have a voltage degradation of 14 µV/h [45]. Integration of RES with PEM electrolyser causes recurrent variation in operating modes due to the inherent intermittent characteristics of the RES. Even though, this is operationally possible, it is not advisable due to the possibility of gradual electrolyser degradation such as likely corrosion of stack components and reduced durability due to voltage fluctuations [35][47]. Weiß et al. [46], conducted an accelerated stress test on a PEM electrolyser under different current densities operations alternating with idle periods during which no power is supplied. The test concluded that a significant decrease in performance during prolonged open circuit voltage (OCV) cycling is obtained due to an increase in high frequency resistance. Authors in [46] also conclude that the analysis showed that operating the electrolyser at a small current density during idle periods in combination with a recombination catalyst is a promising operating strategy to avoid OCV periods and associated performance degradation due to hydrogen permeation. Finally, the reliability of PEM electrolyser has already been reported for close to 60000 hours of operation showing only a marginal loss of performance [46][48].

As electrolyser works on DC, it is important to have it connected to power electronic converters to make it suitable for integration with electric grid or typical RES systems. Generally, if a PEM electrolyser is to be integrated to a TSES or wind energy system, a AC-DC converter also called as the rectifiers and DC-DC (buck) converters are used in suitable topologies [40]. The PEM electrolyser works on low voltage DC, hence in order to adjust the voltage ratio multiple stacks of PEM electrolyser can be connected in series to increase to the required voltage level. It was stated that the power converters decrease the overall efficiency slightly and they could affect the system power quality, if not controlled properly [49]. In fact, power converter devices typically have an efficiency of 92-95% reducing the overall system efficiency (including the ancillaries) by 2-6% [40].

The green hydrogen production is currently expensive largely due to the high capital cost of electrolysers and electricity cost. Additionally, a lack of sufficient operating hours of the electrolyser caused especially when coupled with intermittent RES utilising the otherwise curtailed electricity leads to increase in unit cost of hydrogen production. As for the operating hours, it is estimated that for low full load hours operation capital expenditure (CapEx) is dominant, while for high full load operation, operating expenditure (OpEx) cost factor is dominant. An estimate of Maggio et al. [50], projects a significant reduction in the capital cost of electrolysers and an extension of their lifetime by 2020 and then to 2030, which should reflect in a decrease of hydrogen cost. It is expected that the cost of green hydrogen will reduce by 70% in the coming decade [51]. Clearly, to realise this, policy makers should lend critical support for economic viability.

In fact, the higher costs are particularly seen for onsite green hydrogen production in small scale rather than centralised large scale production [50]. The largest green hydrogen plant in the world has been planned to build to operate with a capacity of 650 tonnes/day of hydrogen production. For this purpose, several renewable energy solutions, such as solar and wind plants will be integrated to storage systems to rise 4 GW of available power for electrolysis in 2025 [51].

It is anticipated that the implementation of Paris agreement, other regional NZE and climate emergency targets would create excess RES production which could be used for power to gas (PtG) strategies [37]. Hydrogen council foresees that by 2030, about 250 to 300TWh of excess renewable electricity could be stored in the form of hydrogen for use in other segments [50]. Regions in the EU have sufficiently high technical potential to be self-reliant for green hydrogen production [33]. At the European regional level, there would be 50% surplus of RES providing an option to produce hydrogen required for current consumption [33]. Belgium and Luxembourg could lack enough excess RES for green hydrogen to replace current H_2 production but there is an option to import.

As per Götz et al. [37], even though methane production from electrolytic hydrogen (PtG process) is not profitable in comparison with common natural gas synthesising process at a micro economic scale. It has been estimated that the PtG strategy contributes to minimise the expansion of grid infrastructure and increase the share of renewables in heating and transportation from a macroeconomic perspective. Generally, the efficiencies of hydrogen technologies are lower compared to advanced lead acid batteries on a DC to DC basis, but the cost of hydrogen storage is competitive with batteries and could be competitive with compressed air energy storage (CAES) and pumped hydro in locations where they are not favorable [50]. Green hydrogen benefits reduced pollution and increased safety of energy supply. Green hydrogen profits could also be increased through the sale of carbon credits [33].

Hydrogen council highlights that to build the hydrogen economy, investments amounting to 280 billon must be realised by 2030 involving whole value chain for hydrogen from production to distribution to retail [50]. The potential of valorisation of otherwise curtailed renewable energy is considerable [50]. First market of green hydrogen is estimated as feedstock for industrial application, followed by power generation in stationary applications and then the mobility sector [50]. Among the multiple applications, the use of hydrogen as an alternative fuel in shipping industry is analysed by Atilhan et al. [51], where it has come to the conclusion that the liquified hydrogen could be used for smaller vessels operating on fixed routes initially in the short term and then can be expanded to larger vessels due to lack of required infrastructure for hydrogen use currently. Most of the studies of RES hydrogen production and its techno economic analysis, consider solar or wind integrated green hydrogen production, due to the relative favourable electricity costs. The global average hydrogen production cost from low carbon electricity is estimated in the wide range of 2-20 €/kg depending on different production pathways [36][52]. According to Kakoulaki et al. [33], green hydrogen production cost of about 5.09 €/kg was estimated for 2020 with the costs projected to be about 2.12 €/kg by 2030 using the European average wind energy productivity. As per Glenk et al. [53], the breakeven prices of green hydrogen produced from wind are compatible with small and medium scale hydrogen supply in certain niche applications, but not with large scale industrial purposes yet. The conventional hydrogen reference prices of 1.5-2.5 €/kg for large scale, 3-4 €/kg for medium scale and above 4 €/kg for small scale applications were considered for comparison here [53]. The NZE report by IEA [13] suggests that increasing global demand for low carbon hydrogen provides a means for countries to export renewable electricity resources that could not otherwise be exploited. The hydrogen transportation could add to 1-3 $/kg to its price. Based on scenarios of each country, producing hydrogen domestically may be cheaper than importing it, even if domestic production costs from low carbon electricity or natural gas with carbon capture and storage (CCS) are relatively high. Report suggests that GW scaled projects in pipeline for green hydrogen production alone amounts to 250 GW scale globally. These are mainly powered by solar, onshore and offshore wind including goals to bring production costs to €1.50/kg before 2030 [54].

3. Energy management system strategies for optimal system operation

Energy management system is a broad term and it is multidisciplinary in nature including electrical, electronic, environmental, economic and social aspects attached to it based on the specified objectives.

The RES use is increasing its popularity due to its various social and environmentally desirable characteristics. RES integration with the traditional electrical grid or even integration among different RES in a hybrid energy system needs solutions in multiple aspects such as overall system stability, reliability and safety concerns. Hence, it is important to plan the management of energy optimally among the different system components and also to balance the supply with the demand.

It is estimated that around 90% of the power outages and disturbances have their root at the distribution level; hence a trend towards smart grids starts at the distribution levels [55]. Smart grids refer to electrical grids with monitoring and controlling capabilities having micro-grids as its fundamental building block [55]. A micro-grid consists of distributed energy systems typically RES and conventional generation units (dispatchable and non-dispatchable), energy storage systems (ESS), switches, communication interfaces and loads (controllable and non-controllable) which can be either grid-connected or operates in islanded mode under dedicated controllers supervision [56][57][58][59]. The block diagram of a typical micro-grid is presented in Figure I-13 [57].

Generation scheduling and demand side management are two main functions of micro-grids [55]. Micro-grids (MGs) can provide significant advantages such as reliability improvement, operating cost reduction, improved environmentally friendly operations, and power quality improvement [58]. MGs are particularly useful in remote locations, military applications and different industrial sectors. It is often designed based on different objectives, suitable RES availability and the other application requirements [57]. Research on energy management began in 1998-1999 [60]. During the last decade, a large number of studies were done in this field [56][58]. Total installed capacity of MG in world is greater than 4GW as of 2016 with north America being the world leader with a share of 67%. The global deployment is expected to increase by 8.8 GW by 2024 [57]. Some companies that are deploying EMS technologies are Advantech, Siemens, Schneider Electric, and Alstom [60]. A broad and effective categorisation of EMS is given in the review by L. Meng et al. [56] where the EMS control has been divided into hierarchical control structures initially, further describing that the functions of the EMS can be implemented by centralised or decentralised control modes.

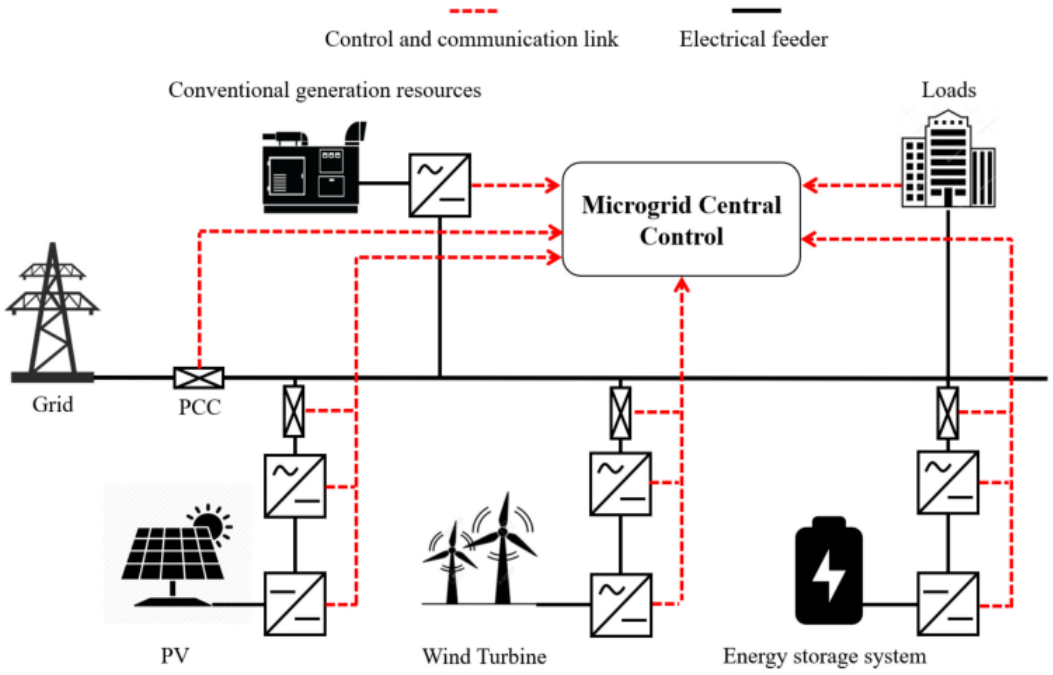

Figure I-13. General block diagram of a micro-grid. Reproduced with permission from Mekhilef. Energy management system in microgrids: A comprehensive review (Sustainability MDPI journal, 2021). Copyright 2021, Sustainability.

In convention of its use in the traditional power systems, EMS can be carried out for two main goals, unit commitment and economic dispatch. Unit commitment (UC) has larger time horizon and it is generally termed as day ahead scheduler in which the optimal operation of the system is analysed a day ahead based on the input and load demand prediction [56]. Unit commitment problem can be defined as a preliminary calculation of power set points over a given time period [55]. An interesting review of UC problems evolution over time is given by Abdou et al. [61]. A database of research papers on formulation, solution of UC from 1940s is given here [61]. Recent approaches of UC problem in the presence of intermittent RES started from the 2010s [61]. UC problem is described as among the tough problems in the electricity market [61]. Economic dispatch (ED) is more of a real time scheduler where more accurate details of the system are executed on a real time basis for the system optimisation.

The multi-layer hierarchical control of a micro grid is divided into primary level, secondary level and tertiary level [56]. The bottom control level i.e., the primary level includes the control of power, voltage and current of the individual local units. The secondary level typically consists of power quality control, such as voltage or frequency restoration, voltage unbalance and harmonic compensation. It also deals with the external grid for synchronisation and management [56]. Tertiary level control is to introduce control on the whole system,

mostly based on the efficiency and economics. Some reviews suggest multiple MG coordination is also performed at this level [56]. Similarly, secondary level is termed as *EMS* level in the review by Y. Zahraoui et al. [57], as it deals mostly with the intra MG system components behaviours and control. Tertiary control is mainly for the grid integration and economic evaluations [57]. Either way, it is understood that the stability, demand response and enviro-economic optimal operations of an integrated hybrid system is a multi-objective and multivariable complex computation that requires systematic approach with the specific objectives clearly defined for the system operation. From an execution time point of view, it is considered that the duration of execution time increases from primary level to tertiary level with tertiary level typically contributing to larger execution time due to complexity in dealing with the communication of multiple components [56]. The standard time of execution for primary is milliseconds, with few seconds for secondary control and ranging from seconds to hours in tertiary level decision making process [56].

The centralised control is used in which the control configuration is centralised by acquiring data from different MG components and external grid. The centralised scheme has advantages as its implementation is relatively easy compared to decentralised control, it is more suited to integrated systems covering a small area and on systems where privacy is important. On the other hand, decentralised control is typically done through multi agent systems (MAS), has the advantages being reliable, scalable and requires less communication infrastructure compared to centralised control. It is specifically useful for large scale MGS where the individual systems are far away from each other and also when they belong to different third parties [56].

A comprehensive review of micro grid elements, the different DERs, that comprises a hybrid system and the various types of control, operating strategies and goals in an EMS is given in the review by Zahraoui et al. [57]. The classic EMS objectives are minimising operational cost, minimising pollutant emission, ensuring power quality, increasing the system reliability and minimising outage duration [57]. To achieve the objectives, the various EMS approaches are aimed to control the output power of DERs, capacitor control for reactive power management, energy storage system (ESS) control, and demand response [60]. Generally, the EMS goals are realised through various optimisation algorithms. Significant amount of research is done in this field for different system configurations based on different optimisation objectives, approaches and solution algorithms [57].

Optimal power flow (OPF) is a nonlinear programming problem and is used to determine optimal output of generators, bus voltages and transformer tap setting in power system with an objective typically to minimise the production cost [62]. OPF was observed to be introduced in literature in 1968 [62]. Several optimisation techniques have been proposed to reach to the optimal solution with respect to the optimisation time range and accuracy of the solution. Optimisation techniques can be broadly classified as deterministic and meta-

heuristics approaches [61]. Several methods like linear programming method and gradient based method are used to solve OPF. However, all these methods assume continuity and differentiability of the objective function, which is not actually allowed in a practical system for which discrete variable consideration is also needed such as transformer tap setting [62]. In recent years, meta- heuristics method have been widely used for UC problems, because of their capability to handle large scale problems [61]. Heuristics optimisation algorithms is one of the best optimisation techniques available that performs trade-off between time and computational efforts [63]. Heuristics algorithms are powerful optimisation tools based on artificial intelligence that have attracted considerable interest as solvers for complex optimisation problems [64]. It is worth noting that, many optimisation algorithms like Genetic Algorithm (GA), Particle Swarm Optimisation (PSO), Grey Wolf Optimiser (GWO), Ant bee colony optimisation etc., are available in the literature extensively apart from the classical optimisation methods, but they are not examined as it is out of scope of this thesis except for GA. However, interested readers can refer to [56][57][60] for details. Additionally, models including comprehensive analysis on weather forecasting, grid energy market participation, and uncertainty consideration in RES data are highly useful in evaluating the technical and economic reliability of the system.

As discussed in the previous sections, a significant amount of research has been carried out in the individual and collective fields of the EMS design and optimisation, such as for tidal and wind energy technologies, and electrolytic hydrogen production [7][37][53][60]. As highlighted by Falcão et al. [42], synergy between RES, electricity and hydrogen is very attractive from a sustainability perspective. Models to simulate electrolyser performance in an annual context are also very useful owing to the lack of research papers in the field [42]. Offshore renewable energy, especially offshore wind energy systems and marine energy systems integration with hydrogen production, is a field that is been explored with great interest of late [65]. As understood from the literature review, most of the TSES deployed as of now are considered for standalone operation, testing and/or integration with the grid. There is a scarcity of available literature in particular for floating tidal energy integration for hydrogen production.

In this scenario, a set of studies and projects particularly focused on this domain is detailed in the following.

Barakat et al. [7], presented a rule-based energy management strategy for a grid connected - tidal stream energy system for hydrogen production with a megawatt scale PEM electrolyser. The paper focuses on power loss minimisation strategy for the tidal stream generator by varying the control modes to analyse its effect on the hydrogen production. Here, the authors [7] adopted a strategy to run the electrolyser at the rated nominal power for the entire duration of the day for maximum hydrogen production. Power is fed to electrolyser from the tidal energy system or the electrical grid as per the availability. A 3.33% of total losses reduction of the tidal energy system is obtained which is translated to a 100kg increase in annual hydrogen

production. Another work by the same authors [66], presented the detailed modelling of a hybrid fixed pitch permanent magnet based marine current-hydrogen power generation system including the fuel cell system to facilitate active power generation. Here, the concept of excess RES power is used for hydrogen production after meeting the electricity grid demand and whenever, the consumption is higher, fuel cell is activated to provide the required energy [67]. All the system components and control strategies are modelled using Energetic Macroscopic Representation (EMR). EMR is a graphical representation of system components using physical and causality principles [66]. Optimisation and system economics were not accounted in the scope of above two studies.

Kartalidis et al. [68], have studied a demand side management-based EMS strategy in the Orkney Islands ; considering the current and proposed future scenarios on an island level, including grid connected wind-tidal and electrolyser systems. The detailed grid models were built using Modelica language in Power systems library. Rule based EMS was employed here. Electrolyser were modelled as constant load here and it was operated only using the otherwise curtailed power in the study.

Ferguson et al. [69], conducted a hydrogen demand driven analysis to find the optimal unit cost of hydrogen produced in a predominantly wind farm system with tidal stream energy and grid electricity, connected as the backup energy sources. The scope of this paper was high level cost analysis, and hence fixed costs was used [69]. Further, a constant specific energy consumption of the electrolyser was used by the authors. However, this was justified in other work of the first author [2], in which, it was concluded that the difference between the use of a constant specific energy consumption in comparison with variable value is about 1.6% and hence, its suitable for higher scope-low detail studies. Different combination of scenarios was performed by the authors and they concluded that even though tidal energy is costly for hydrogen production when compared to wind energy; when tidal energy used in place of the grid electricity, the unit cost of hydrogen can be reduced as the electrolyser loading is increased. A similar system configuration used in the proposed thesis, is used by Ferguson [2], with the exception of an additional electrolyser unit with peak power switching capabilities. The system configuration included analysis of hydrogen supply chain with logistics and end use. A rule-based EMS was employed here. Additionally, environmental analysis was not under the scope.

Laazar et al. [70], have analysed the modelling and control of a hydrogen based green data centre in which tidal stream and solar energy are used as main energy sources along with a MW scaled PEM electrolyser, fuel cell and lithium ion battery. EMR based modelling is used in the work by the authors along with a rule-based energy management approach. A simulation based on annual tidal current data at the Alderney race in France is used here. Additionally, the authors have performed an optimal sizing for a similar configuration using genetic algorithm [71].

A recent analysis conducted by Rinaldi et al. [27] presents a hydrogen production integrated system with tidal stream energy plant on a floating platform with an onboard electrolyser unit. In this case, the authors analyse the fixed operating and maintenance costs. The practical considerations of operations and maintenance of a floating tidal energy system array like crew vessel for onsite repairing of the system, and mobilisation cost are considered here, concluding that the O&M cost are dominated by repairs and replacement costs. The analysis highlights the importance of integration with hydrogen for economic purposes as the current market value of green hydrogen is higher than sale of electricity. However, the optimal electrolyser operation and grid connection dynamics are not under the scope of this analysis. As per Rinaldi et al. [27], the proposed future work aims to analyse the commercial viability of the planned project including the capital cost data and more refined inputs to calculate the generated income and the support needed for technology development.

Apart from the ITEG project, the recently launched Forward 2030 project (initiated in September, 2021) aims to combine floating TSES with onshore wind for green hydrogen production with storage facilities in the context of a grid-connected island [72]. Furthermore, a newly announced memorandum of understanding (MoU) in March, 2022 by RINA [73], includes the design of a offshore floating green hydrogen vessel in which readymade tidal stream and wind energy systems are combined with off the shelf electrolysers to produce green hydrogen.

IV. Objectives and expected contributions of the research

Despite the multiple investigations on hybrid-hydrogen based renewable energy systems, a comprehensive analysis on the optimal technical, economic and environmental operation of a grid-connected hybrid tidal-wind-PEM electrolyser system is not available and therefore, it is proposed in this thesis. The main objective of the thesis is to design, implement and compare different energy management strategies and optimisation approaches for a hybrid system involving floating tidal stream energy integration for dedicated green hydrogen production; in addition to tidal energy export to the grid capabilities. The thesis focuses on the optimal energy management within the context of centralised tertiary control of a micro-grid operating in a grid connected mode. The strategy aims to combine both the energy management and system economics aspects. The Fall of Warness in the Orkney Islands is selected as the case study for the thesis.

Towards reaching the objectives, the individual system components are initially modelled. The annual floating tidal stream energy performance indicators are then assessed. Investigation on PEM electrolyser units loading and transitionary operation of its different operating modes based on the yearly tidal energy availability is analysed later. For these purposes, the energy management strategies for hydrogen production are analysed from a rule-based approach (RBA) and then treated with an optimisation approach. Further,

the thesis aims to ensure optimal electrolyser utilisation and maximises the daily operating profit ensuring priority to green hydrogen production from tidal energy as far as possible to reduce the overall system emissions. The RBA implementation and dynamic optimisation of an electrolyser unit capable of working up to twice of its nominal capacity for a limited duration is also considered. The system optimal operation is ensured by using a mixed integer genetic algorithm. Furthermore, the proposed case study attempts to evaluate the comprehensive cost analysis of the system based on fixed-variable costs and levelised costs optimisation approaches. Carbon emission savings and the associated economic benefits are also discussed. Towards the end, a comparison between RBA and optimised approach is undertaken. To validate the methods implemented, scientific papers related to the optimal operation of electrolysers connected to RES are referred. In short, the main novelty of this thesis is that, it addresses the techno-enviro-economic operational synergies of a grid connected floating tidal stream-onshore wind energy systems integration with hydrogen production; with a focus on optimal electrolyser operation and maximised operating profit using a mixed integer metaheuristic optimisation algorithm. Parts of the contents presented in this thesis are referred to the research article submitted to the International Journal of Hydrogen Energy (currently under review) [74] and the research article published in the proceedings of the 14th European Wave and Tidal Energy Conference, 2021 [75].

V. Dissertation overview

This thesis is structured as follows:

Chapter II presents the models of the individual components in the hybrid system i.e., the floating tidal stream energy system, the onshore wind energy system and polymer electrolyte membrane (PEM) electrolysers, respectively. The electrolyser working based on three operating modes-stop, standby and running mode is modelled. The important aspects about the compressor, hydrogen storage and the balance of plant component models for the analysis are mentioned. The renewable energy profiles to the system, such as the tidal current and the wind velocity profiles from the available data set are analysed towards the later part of this chapter. Further, analysis of the most occurring daily tidal profiles data set are presented.

Chapter III presents the different parameters like tidal energy production, associated carbon emission savings, capacity factor, availability factor, production hours, zero production hours and peak power production hours in an annual context for the selected floating tidal stream energy system. It is analysed by using the most concurrent daily tidal profiles presented in Chapter II. The LCOE evaluation of the TSES and its sensitivity with respect to different parameters are then presented. A preliminary economic analysis of tidal energy export to grid is presented later. Tidal stream energy integration with green hydrogen production is then introduced with the application of rule-based approach (RBA). The associated hydrogen

production, carbon emission savings, energy consumption during transitionary and standby operating modes, utilisation factor, load factor and specific energy consumption are analysed in an annual context. The number of zero hydrogen production hours, standby operating hours and stop hours of two different electrolyser units based on the available input tidal energy are determined. The corresponding number of cold and warm starts based on electrolyser units loading is analysed. The RBA EMS strategy is then extended to tidal-wind/grid energy system to present the possibilities for EMS design and improved electrolyser utilisation.

In addition, a preliminary assessment of the hydrogen production cost based on daily tidal energy availability and hydrogen demand in the context of standalone tidal-hydrogen system configuration and tidal-grid-hydrogen system configuration is explored in Chapter III.

Chapter IV presents the optimal techno-enviro-economic aspects of hydrogen production using PEM electrolysers powered by a hybrid grid-connected tidal-wind energy system. The methodology including RBA and optimisation approach is initially presented. The cost function formulation under both the approaches is then detailed. The fixed cost factor method and levelised cost factor method for the cost benefit analysis is described. The input data considerations to the system are detailed later. GA algorithm working and application to the optimisation problem is then included. Results of the two optimisation approaches are evaluated and compared. In addition, overall system performance indicators are compared against the results of RBA.

Finally, the overall conclusions, key findings, contributions of the thesis and the future work recommendations are presented in Chapter V.

Chapter II

Components modelling and renewable energy profiles

The characterisation of the hybrid system requires the different components know-how and modelling. The main sub-models used for system components are detailed in this chapter. Particularly, the models of the below three systems are described:

1. Floating tidal stream energy system.

2. Onshore wind energy system.

3. Polymer electrolyte membrane electrolyser.

Further, the tidal power conversion and transmission aspects are included. The electrolyser units modelling, primarily focusing on operating modes are presented. All the models are realised in MATLAB R2019a software. The renewable energy profile data characterisations especially the tidal current profiles in terms of daily, monthly and annual operations are extracted and analysed using harmonic mean method. For a comprehensive analysis and to reduce the computational burden, the most occurrent daily tidal current profiles are used to analyse the tidal stream plant performance in an annual context. Similarly, harmonic mean analysis is used to extract the average daily wind velocity reference profiles.

I. System components modelling

The models of the individual components in the hybrid system is described in the following.

1. Floating tidal stream energy system

As mentioned in Chapter I, the tidal stream energy system (TSES) design under consideration for this study is a floating horizontal axis tidal stream system called the O2 turbine by Orbital Marine Power. O2 is a twin rotor TSES with 1 MW rating mounted on each side and it is electrically rated at 2 MW at the onshore end. O2 is termed as the most powerful TSES in the world currently and it is the first to include variable pitched functioning in floating TSES. O2 is mounted to the sea bed through anchors. The O2 TSES with its associated system components at maintenance mode is illustrated in Figure II-1. During the maintenance mode, the hydraulic legs of the TSES can be retracted and brought to sea surface for easier access for repairs and maintenance. During the operation mode, the hydraulic legs move under the sea surface and operate. The graphical representation of the system under operation is given in Figure II-2. The proposed system is currently at a technology readiness level (TRL) 9, which means it is at the stage of commercial demonstrator experimentation at sea for a prolonged period [14].

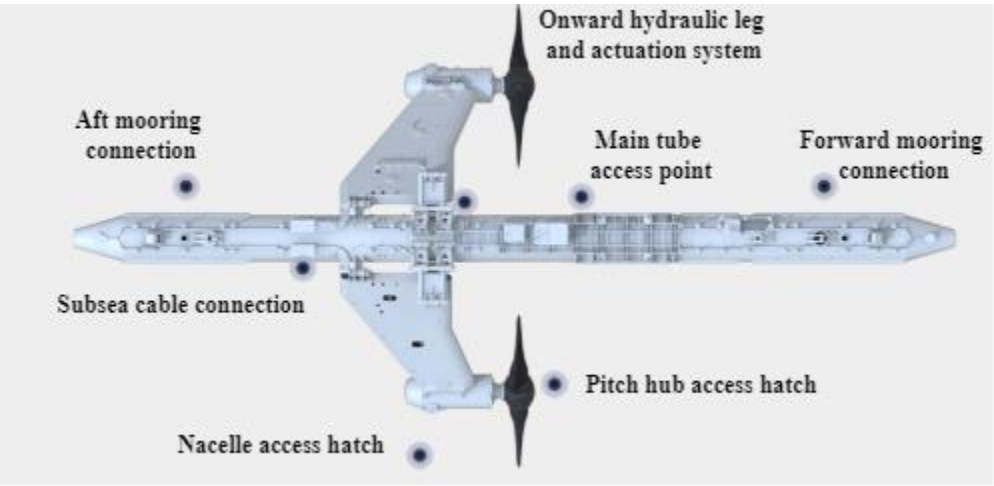

Figure II-1. Birds eye view of the floating tidal stream energy system. Courtesy- Orbital Marine Power.

Analogous to the wind energy system (WES), the tidal system rotors are directly coupled to a gearbox. The gearbox is connected to a squirrel cage induction generator (SCIG) for electric power generation. Induction generators are used in the system configuration, as this turbine is required to work at variable speeds. Both the rotors are integrated with a pitching system to control the turbine output with respect to the tidal flow in both directions using the blade angle control method. The blades can rotate over 180 degrees to respond to the change in tidal current direction. The blades has the ability to feather on its on axis too, to lessen the resistance of incoming seawater [76]. Similar to a wind energy system control, the generator control applies a controlled torque and speed on the rotor shaft to extract maximum power from the tidal current for tidal current speeds below the rated speed. Pitch control is applied for current speeds above the rated current speed to maintain a stable output power. Basically, the tidal turbine control is a function of tidal current.

Figure II-2. Graphical representation of the tidal stream system in operation. Courtesy- Orbital Marine Power.

The standard tidal energy system model in literature, which is analogous to a wind energy system is used to deduce the power generated by the TSES [30]. The power extracted by the tidal turbine is given by equation (II-1) [30]:

$$P = 1/2 C_p \rho A v^3 \quad \text{(II-1)}$$

where, C_p is the power coefficient (a dimensionless quantity) ρ is the sea water density (kg/m^3), A is the cross-sectional area of turbine (m/s) and v is the tidal current velocity (m/s).

Power coefficient is technically the percentage of power that can be extracted by the turbine after accounting the hydrodynamic losses. The typical value range of *Cp* for TSES is 0.16-0.5 [20][24].

C_p is generally modelled as a function of the tip speed ratio (λ) and the blade pitch angle (β).

where, $\lambda = R\Omega/v$ (II-2)

with, R as the rotor radius (m) and Ω as the rotor angular speed (radians/second).

According to the Betz limit, the maximum C_p that a turbine can have in 'open-sea' is about 0.59. However, in cases of tidal turbines, where the water flow is constrained in narrow channels, it has been theoretically suggested that the Betz limit can be exceeded [20][77]. A detailed explanation of it is given in the study by Vennell [77].

The main specifications of the tidal stream system under consideration are given in Table II-1.

In order to model the given floating TSES, a first indicative tidal turbine characteristic curve, i.e., the *shaft* power with respect to the tidal current velocity was generated in consultation with the manufacturer cf. to Figure II-3. The tidal model parameters were then identified and the results were validated against the power curves. The simplified models in [30] were then integrated by using the equation (II-1) representing the shaft power of the tidal energy system in order to match the specifications given in Table II-1.

Table II-1. Main specifications of the selected tidal turbine.

Parameter	Value
Cut in current speed (m/s)	1
Rated velocity (m/s)	2.5
Cut off current speed (m/s)	5
Swept area (m^2)	2×314
Rotor diameter (m)	20
Name plate rating (MW)	2

The shaft power produced by a single rotor of the tidal stream system, P_t is obtained in equation (II-3) [74]:

$$P_t = \begin{cases} 0 \text{ for } v_t < v_{t_{\text{ci}}} \text{ and } v_t > v_{t_{\text{co}}} \\ \frac{1}{2}\rho A {v_t}^3 C_p \text{ for } v_{t_{\text{ci}}} \leq v_t < v_{t_r} \\ P_{\text{t1}} \text{ for } v_t = v_{t_{\text{r}}} \\ P_{\text{t2}} \text{ for } v_{t_r} < v_t \leq v_{t_{\text{co}}} \end{cases} \quad \text{(II-3)}$$

where, v_t is the instantaneous tidal current velocity (m/s), $v_{t_{\text{ci}}}$ is the cut-in current velocity of the TSES (m/s), $v_{t_{\text{co}}}$ is the cut-off current velocity of the TSES (m/s), $v_{t_{\text{r}}}$ is the velocity of the TSES at the rated power (m/s), $P_{\text{t1}}$and P_{t2} are the values of shaft power at full operations and maximum shaft power before cut-off respectively (kW).

Some studies account that C_p includes all the TSES losses including generator, and power converter losses. However, in this thesis they are estimated separately. A C_p value of 0.434 is considered, similar to other literature estimate of similarly rated system [70]. A constant power coefficients value is used for tidal turbine power calculations as it was matching with the available power curve suitably. However, for a detailed understanding variable power coefficient value based on change in tidal current speed can be calculated as mentioned in [20]. A sea water density value of 1023 kg/m^3 is considered.

As observed in the tidal shaft power curve in Figure II-3, the TSES is at zero power production mode or parking mode for velocities before cut-in tidal current velocities and for velocities after cut-off current of TSES. It can be seen that the generators reach rated power at a current velocity of 2.5 m/s with a cut-in current velocity of 1 m/s. This mode is called the generator control mode. The generator power is maintained at constant rates from rated velocity to cut-off velocity and this control mode is called the pitch control. It is also worth noting that the cumulated shaft power at the turbine is slightly above 2 MW.

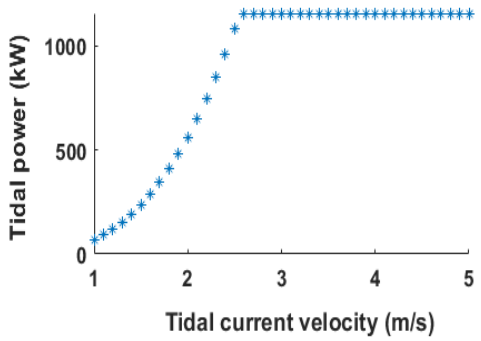

Figure II-3. Tidal shaft power curve of a single rotor rated at 1 MW [75].

The overall schematic diagram of the TSES is given in Figure II-4. The tidal turbine is connected to the associated power conversion devices, to adapt the power generation to suit the electricity transmission and grid integration requirements. At each rotor end, the power is generated and transferred to generator side converters (inverters). It is worth noting that due to the variable nature of RES, the generated power is variable. At the output of the inverter, the DC power is then transferred to a dc bus at 690V. Subsequently, it is converted to from DC to AC for grid connection. A step-up transformer then rises the voltage from 690V to 11 kV. This higher voltage is used for long distance transmission through a subsea power cable. The corresponding schematic diagram of the entire tidal plant is given in Figure II-5. This converter topology is proved to meet the electricity grid power quality standards and the voltage control in acceptable limits [78]. Furthermore, static compensator is used with SCIG to compensate the reactive loads and to ensure stable voltage under dynamic and steady state operation. It ensure active and reactive power controls between the generator, DC link and the loads/grid [78].

A practical efficiency of 97% is considered for the generator. In order to account for the power converter and transmission losses, the conventional transformer efficiency of 99.4% for 1-2 MVA rated devices is considered. The typical conversion efficiencies of 94% are considered for both AC/DC converters and DC/AC converters [40]. The detailed modelling of power converter devices is not presented in this analysis. Study by B. Yodwong et al., is a useful reference for those interested in these aspects [49].

The power loss in the cable is calculated using the joule losses formula (II-4) [79]:

$$\text{Cable power loss} = \left(\frac{P_{\text{tr}}}{V}\right)^2 \text{R} \qquad \text{(II-4)}$$

where, $P_{\text{tr}}$is the power available at the transformer end (kW), V is the transmission voltage (kV), R is the cable resistance (Ω). A subsea cable with resistance 0.52 Ω/km and 600m length is considered for the given system. As resistance is directly proportional to length, the effective cable resistance for 600 m is 0.312 Ω.

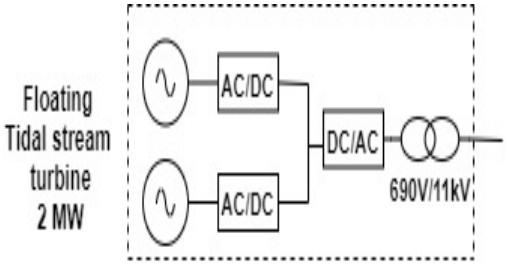

Figure II-4. Overall schematic diagram of the tidal energy system [74].

Since, all other power values are referred to the unit kW, a conversion factor of 0.001 is applied to equation (II-4) to obtain the value in kW. The referred power converter and transmission efficiencies are accounted for to evaluate the electrical power available from the TSES.

It is worth noting that mere adaptation of WES working principle to TSES has a problem in that the working fluid and environmental conditions are different in TSES compared to WES. Nevertheless, the knowledge base in the field has been continuously increasing over the past two decades thanks to the matured learning rate achieved in WES technologies [80]. In contrast to the WES, the TSES operate in hostile marine environment subjected to much disturbances. A study by M. Lewis et al. [17], on the effect of ambient turbulence intensity on tidal system power variability conducted in a highly energetic site with 9-12% of turbulence intensity has found that the turbulence intensity has caused only 1% of reduction in the assessment of annual energy yield; in comparison to the studies, where the estimate was done without considering the turbulence intensity. Wake turbulence effect on the given floating tidal energy plant is not considered as the selected tidal stream system is a standalone system, since these effects are more applicable for tidal farms. Considering these factors, turbulence characterisations can be considered negligible under the given system conditions.

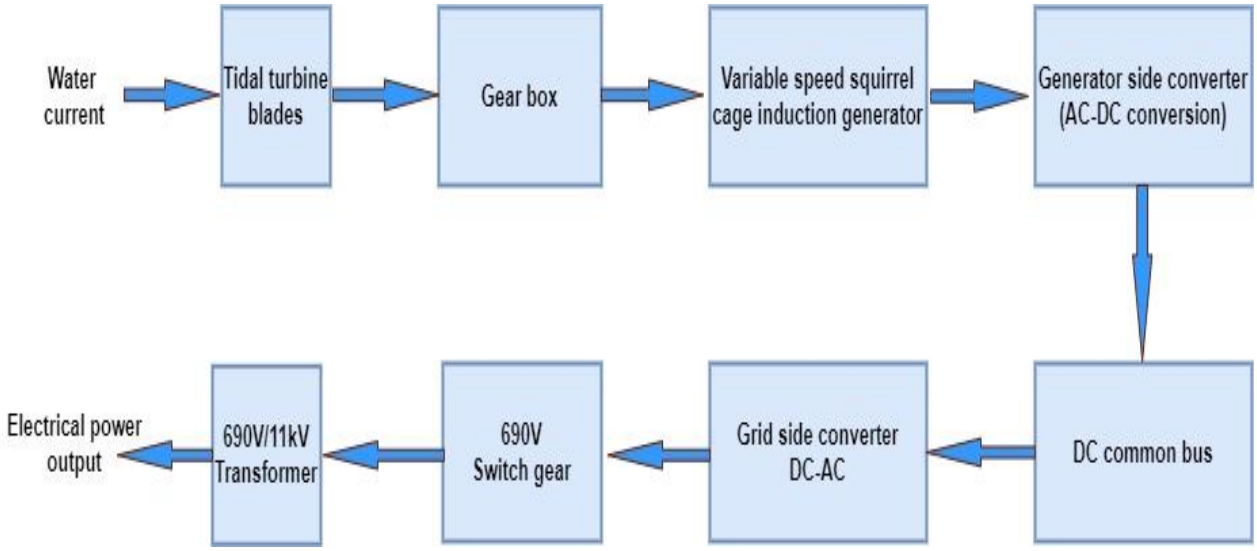

Figure II-5. Detailed schematic diagram of the tidal energy system.

2. Onshore wind energy system

Possible connection to other external RES is also considered in Chapter IV. For this purpose, an onshore WES is also modelled. The standard model of WES available in the literature [78] is used for WES modelling. The specifications of the WES are given in Table II-2. The manufacturer specifications of the onshore wind turbine Enercon E-44 (c.f. to Figure II-6) are used for model parameter finetuning. Similar to TSES, the power conversion devices like AC/DC converter, DC/AC converter and transformers are required for the wind turbine to smoothen its output to be acceptable for the distribution grid standards. The general schematic diagram of the wind energy system is given in Figure II-7. As the wind energy plant is located onsite, it is assumed that the transmission losses are negligible compared to the transmitted power.

The characteristic curve of the wind turbine i.e., the generated power with respect to wind velocity was available from the manufacturer [81]. The wind turbine power equation parameters are then fitted using available power profile. The electrical power of the WES, P_w is given in the equation (II-5) [74][78]:

Figure II-6. Selected Onshore wind energy system. Courtesy- Enercon [81].

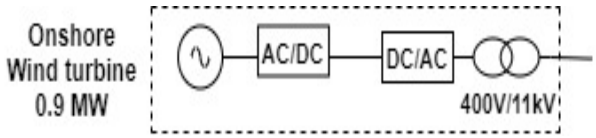

Figure II-7. Overall schematic diagram of wind energy system.

Table II-2. Specifications of the selected wind turbine [81].

Parameter	Value
Cut in velocity (m/s)	3
Rated velocity (m/s)	15
Cut off velocity (m/s)	28
Swept area (m^2)	1521
Name plating rating (kW)	900

$$P_w = \begin{cases} 0 \text{ for } v_w < v_{w\,\mathrm{ci}} \text{ and } v_w > v_{w\,\mathrm{co}} \\ \mathrm{P_{w1}}(v_w) \text{ for } v_{w\,\mathrm{ci}} \leq v_w < v_{w\,\mathrm{co}} \end{cases} \quad \text{(II-5)}$$

where, v_w is the instantaneous wind velocity (m/s), $v_{w\,\mathrm{ci}}$ is the cut in velocity (m/s), $v_{w\,\mathrm{co}}$ is the cut off velocity (m/s), P_{w1} is the power of wind turbine (kW). The calculated power values from the model are given in Figure II-8. It can be observed that similar to TSES, generator control and pitch control are applied to WES.

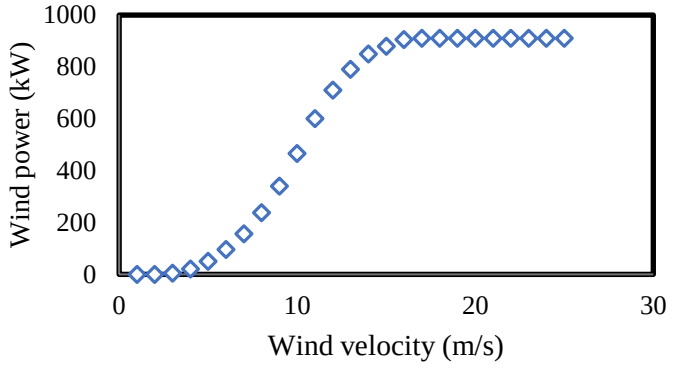

Figure II-8. Resultant wind power model evaluation from the model.

3. Polymer Electrolyte Membrane Electrolyser

Water electrolysis separates the water molecule to hydrogen and oxygen through electric supply. It is observed in the existing literature that the PEM electrolyser modelling studies are few, when compared to PEM fuel cells [42]. However, in the previous five years, there is an increased interest in the PEM electrolyser modelling studies due to their increased applications. This trend is expected to go for the next decade too [42]. Modelling studies of PEM electrolyser have been developed with varying degrees of detailing in literature [40]. As the PEM electrolysers are essentially thermodynamic-electrochemical systems, models based on electrical, chemical and thermal properties are developed. Analytical, empirical/semi-empirical and mechanistic models are used in the literature [42]. Analytical tools are satisfactory tools to learn the simplified behaviour of main variable to obtain a fairly accurate polarisation curve. Empirical models are useful to predict the system behaviour under various operating conditions like different temperatures and pressures. Mechanistic models use detailed equations based on electrochemistry which could accurately predict the system behaviour, but involves large computation time and hence are not suitable for real time applications [42]. Interested readers can refer for detailed modelling steps in the study by O. Ulleberg [82]. Here, an empirical relation between electrolytic cell voltage and current is deduced. In order to apply control strategies on PEM electrolysers, from an electrical perspective, they have also been modelled as resistive load, static load and dynamic load in [40].

PEM electrolyser has a nonlinear behaviour [40]. For this study, the electrolyser working in different operating modes based on the input power is modelled initially. Later, a physical model is developed from the study by Bo Han et al. [43]. This model is then simplified, and adapted to the considered electrolyser units and its operating modes. As this analysis is mainly to assess the different operating modes, hydrogen production and related efficiency of the electrolyser, a detailed model considering the thermodynamics is not under the scope of this thesis.

In the examined system, the electrolyser units intake AC power at 400V. DC power conversion technology is built-in in the electrolyser unit. The power supply unit (PSU) generally consists of a transformer, AC to DC converter (if it is connected to an AC supply unit) and a buck converter. Typically, it has a collective conversion efficiency of 95% [2]. The balance of plant units essentially contains all the associated PSUs and hydrogen gas handling units like heat exchangers, deoxidiser, dryer, pumps, piping etc. De-oxidiser is used to remove traces of oxygen from the electrolyser outlet. Dryer is used to remove water content for the hydrogen at the outlet. Similarly, heat exchangers and pumps are used to transport water efficiently to the electrolyser stacks. An overall schematic diagram of the electrolyser unit with the power supply unit, connected to an external compressor and hydrogen storage is given in Figure II-9.

Two different PEM electrolyser units are modelled in this thesis. Both the electrolyser units are rated at 500kW. Particularly, the electrolyser unit 2 has the ability to operate at 1 MW i.e., twice of its nominal rating for three hours a day. This functionality is termed as peak power operation in this thesis. The configuration of the latter helps the avoidance of oversizing the electrolyser [83].

As stated before, initially, the electrolysers are modelled considering their different operating modes. Mainly, the operating modes running, standby and stop are considered. The main features of the different electrolyser modes are given in Table II-3. The different electrolyser operating modes, related transition times, and associated costs are shown in Figure II-10 [74]. This simplified model has been deduced from the discussions with the electrolyser manufacturer- Elogen (ex AREVA).

Additionally, a minimum power requirement of 10% of the nominal rating of the electrolyser units is required to ensure safe operation. Thus, a minimum power of 50 kW required by the electrolysers to ensure safe hydrogen production operation.

Table II-3. Features of different electrolyser operating modes.

Operating mode	**Features**
Stop	Electrolyser does not produce hydrogen. It does not consume energy at this operating mode.
Running	Electrolyser produces hydrogen based on the input energy consumption.
Standby	Electrolyser does not produce any hydrogen. It consumes relatively smaller amount of energy to remain in this operating mode.

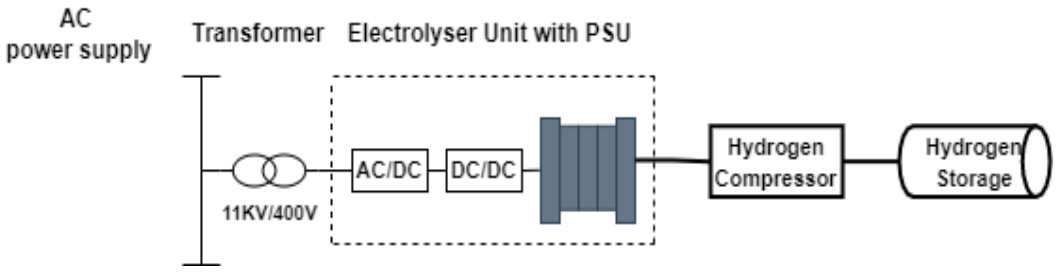

Figure II-9. Schematic diagram of electrolyser unit connection [74].

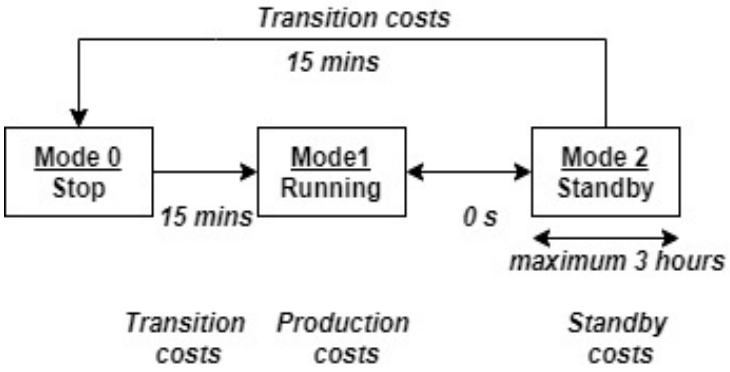

Figure II-10. Different operating modes of the electrolyser unit considered and the associated costs factors [74].

Consequently, a range between 50 and 500 (1000) kW is defined as the running operating mode of the electrolyser units. A power requirement of 5 kW is considered as standby operating mode power consumption [2]. This agrees with the empirical equation in [69], where a value close to 5.9kW and 6.3 kW is the standby power consumption values for an electrolyser capacity of 500kW and 1 MW, respectively. Energy consumption during operational mode transitions is considered as $1/4^{th}$ of standby mode energy consumption in a typical operational cycle based on its time duration. Once running operating mode is initiated the electrolyser unit will then go to standby mode, if the input power is insufficient. The maximum allowed continuous duration of standby operation mode is considered as three hours for both the electrolyser units. It is worth noting that this time duration is an assumption made according to the discussions with the electrolyser manufacturer. However, in reality, standby duration is not a function of time, but rather it is dependent on the pressure leakage in the system. It is assumed that after the specified time duration considered for maximum standby operation, the pressure leakage in the system is significant. So, the electrolyser unit is then automatically switched off to avoid any damage to the membrane.

The electrolyser operating modes transition from stop to running mode also termed as cold start, requires a delay of 15 minutes. In addition to reaching the minimum nominal current, the warm up procedure of electrolyser unit includes the drying of hydrogen unit, circulating de-ionised inlet water for electrolyser, building up sufficient oxygen and hydrogen stack pressures. The electrolyser operating mode transition from standby operating mode to running mode is called the warm start. Once in running operating mode, the time required for the electrolyser unit to reach 100% of its capacity is about 60 seconds and to reach 200% of its capacity is about 90 seconds. The flowchart for electrolyser operating modes modelling, according to the prescribed rules is presented in Figure II-11.

The advantage of referring to this model is that it supports in identifying the number of production hours, standby operating mode hours and non-production hours which further helps in estimating the availability factor and utilisation factor of the electrolysers. The number of warm and cold start and stops can also be

estimated. Degradation aspects are not considered specifically in this thesis. However, the degradation could be integrated in the actual model for further studies, to estimate the possible effects of ageing and scheduled maintenance. For instance as pointed out in [2], a study on trade-off between electrolyser operating hours and stack replacement economics could also be an area for further research in this direction.

Further, the electrolyser standby cost, c_{stb} and electrolyser transition costs, $c_{\mathrm{tr,el}}$ are estimated using the equations (II-6) and (II-7):

$$c_{\mathrm{stb}} = E_{\mathrm{stb}} c \tag{II-6}$$

Where, E_{stb} is the energy consumption during standby operation mode (kWh) and c is the associated electricity cost (€/kWh).

$$c_{\mathrm{tr,el}} = E_{\mathrm{tr}} c \tag{II-7}$$

where, E_{tr} is the energy consumption during transitionary operating modes (kWh).

As mentioned earlier, a reduced physical model is now used to calculate the hydrogen production as a function of the electrolyser input power [43]. As stated in Chapter I, the potential of a single PEM cell is given as the summation of open circuit voltage, activation over potential, diffusion overpotential and ohmic overpotential.

Thus, the open circuit voltage (V_{ocv}) calculated based on Nernst equation is given as [43]:

$$V_{\mathrm{ocv}} = V_0 + \frac{RT}{zF} \mathrm{In}\left(\frac{\propto_{H_2} \propto_{O_2}{}^{0.5}}{\propto_{H_2O}}\right) \tag{II-8}$$

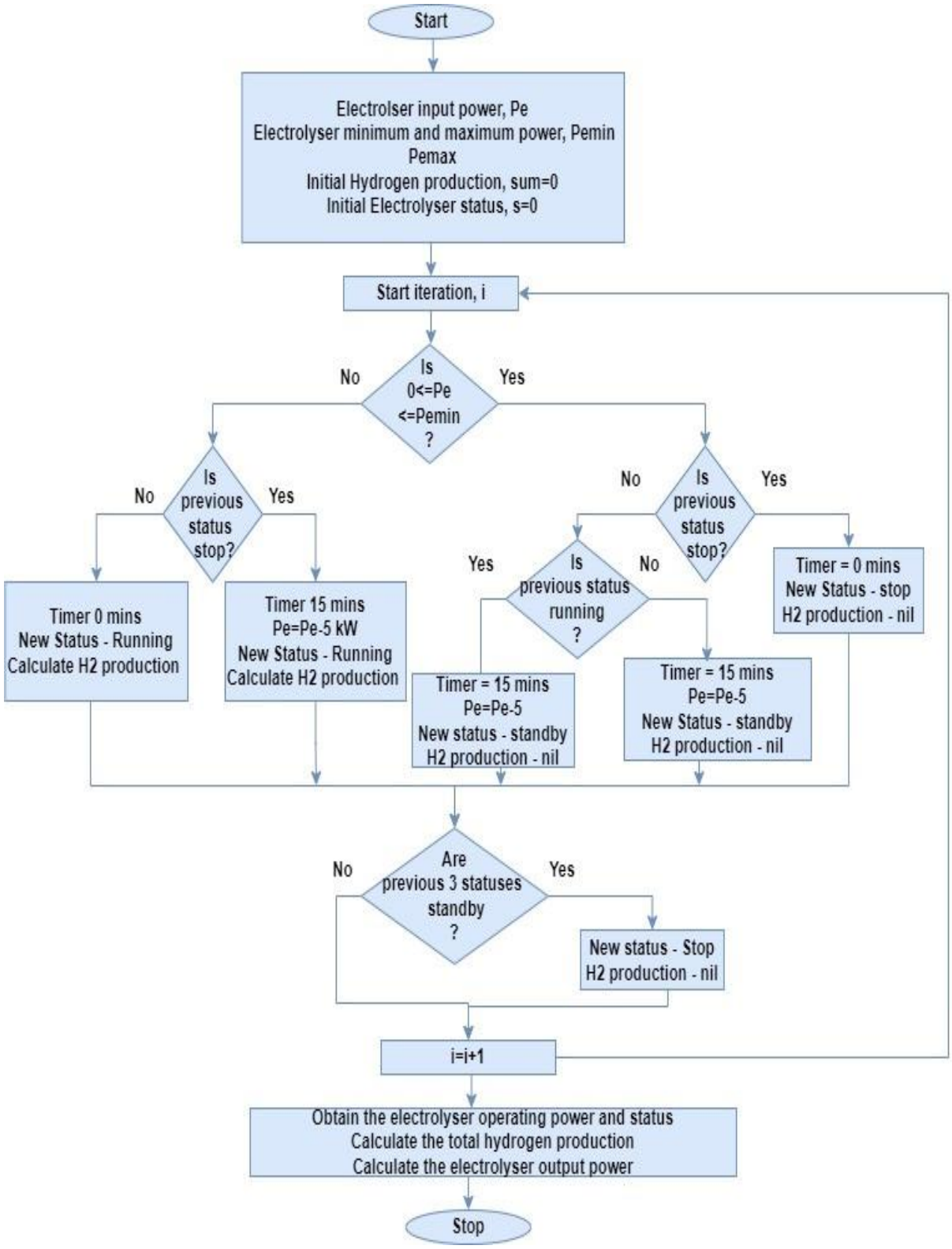

Figure II-11. Flowchart for electrolyser operating modes estimation.

Where, V_0 is the reversible voltage with standard pressure (V), R is the gas constant (8.3145 J/molK), T is the operating temperature of the electrolyser (K), z is the mole numbers of electrons transferred during electrolysis operation, F is the faraday constant (96485 C/mol), $\propto$ is the activity species.

The activation overpotential (V_{act}) derived form Butler-Volmer equation model in [43] is given as :

$$V_{\text{act}} = V_{\text{act},a} + V_{\text{act},c} \quad \text{(II-9)}$$

where, $V_{\text{act},a}$ and $V_{\text{act},c}$, are the activation overpotential at anode and cathode, respectively.

$$V_{\text{act},a} = \frac{RT_a}{\propto_a F} \text{In}\left(\frac{j}{2j_{0,a}} + \sqrt{1 + \left(\frac{j}{2j_{0,a}}\right)^2}\right) \quad \text{(II-10)}$$

$$V_{\text{act},c} = \frac{RT_c}{\propto_c F} \text{In}\left(\frac{j}{2j_{0,c}} + \sqrt{1 + \left(\frac{j}{2j_{0,c}}\right)^2}\right) \quad \text{(II-11)}$$

where, $\propto_a$ and $\propto_c$, are the charge transfer coefficient at the anode and cathode respectively, j is the current density on the electrodes (A/cm^2), $j_{0,a}$ and $j_{0,c}$ are the exchange current density on the anode and cathode electrode (A/cm^2).

The diffusion overpotential can be calculated using the Nernst equation at the anode and cathode [43]:

$$V_{\text{diff}} = V_{\text{diff},a} + V_{\text{diff},c} = \frac{RT_a}{4F} \text{In}\left(\frac{C_{O_2,m}}{C_{O_2,m0}}\right) + \frac{RT_a}{4F} \text{In}\left(\frac{C_{H_2,m}}{C_{H_2,m0}}\right) \quad \text{(II-12)}$$

where, $C_{O_2,m}$ and $C_{H_2,m}$ are the oxygen and hydrogen concentration at the electrode and membrane interface (mol/m^3), $\text{C}_{O_2,m0}$ and $\text{C}_{H_2,m0}$ are the oxygen and hydrogen concentration under a reference operating condition (mol/m^3).

The ohmic overpotential is estimated as follows [43]:

$$V_{\text{ohm}} = V_{\text{ohm},a} + V_{\text{ohm},c} + V_{\text{ohm,me}} = \left(\text{R}_{p,a} + \text{R}_{\text{elc},a} + \text{R}_{\text{in},a}\right)j\text{A} + \left(\text{R}_{p,c} + \text{R}_{\text{elc},c} + \text{R}_{\text{in},c}\right)j\text{A} + \text{R}_{\text{me}}j\text{A} \quad \text{(II-13)}$$

where, R_p is the resistance due to plates (Ω), R_{elc} is the resistance due to electrodes (Ω), R_{in} is the resistance due to the interface between the membrane and the electrode (Ω), $\text{R}_{\text{me}}$is the membrane resistance (Ω) and A is the area of reaction (m^2). The model is assumed to have perfect permeability i.e., no direct mixing of the gases. Electrodes operating at maximum capacity without gases accumulation, perfect separation of the gases from the liquid. The resultant I-V curve of the electrolyser cell is given in Figure II-12. The main

specifications considered for the electrolyser units modelling are given in Table II-4. Rated power scaling is introduced at this step and a simplified scaled model is developed adapting the electrolyser units specifications in Table II-4 and their related operating modes. This part of the model gives the reference specific energy consumption curves for output detection.

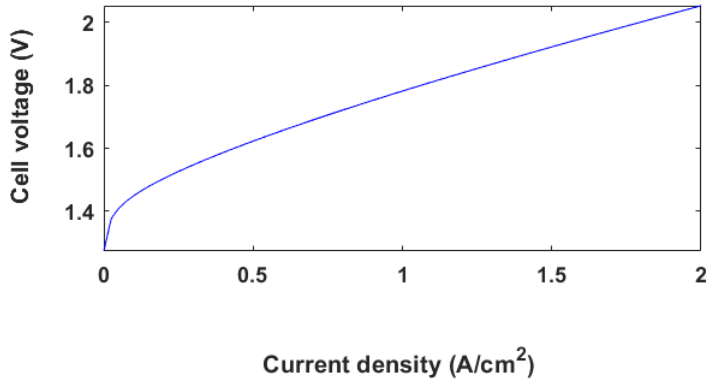

Figure II-12. I-V curve of the electrolyser cell.

The specific energy consumption of the electrolyser unit with respect to the percentage of rated power is presented in Figure II-13. The corresponding cost can also be estimated based on the electricity cost. The usefulness of referring to a model in which hydrogen production is a function of input power is the suitability of the use of model for various technologies, while making sure that the parameters are calibrated properly. The parameters of the electrolyser units were identified as per the manufacturer specifications, similar to the TSES and WES model, to ensure appropriate matching between the hydrogen production and energy consumption.

In parallel, the specific energy consumption of the electrolyser unit with respect to the percentage factor of the rated current, which is analogous to the rated power of a similar PEM electrolyser used in the study [2], is referred for validating the model. The specific energy consumption and thereby the estimated hydrogen production of both the electrolyser unit 1 and 2 are then deduced.

Table II-4. Main specifications of the selected electrolyser units.

Parameters	Electrolyser unit 1	Electrolyser unit 1
Rated power (kW)	500	500
Operating Pressure (bar)	30	30
Operational range (% of rated power)	10-100	10-200
Operating hours	60,000	60,000

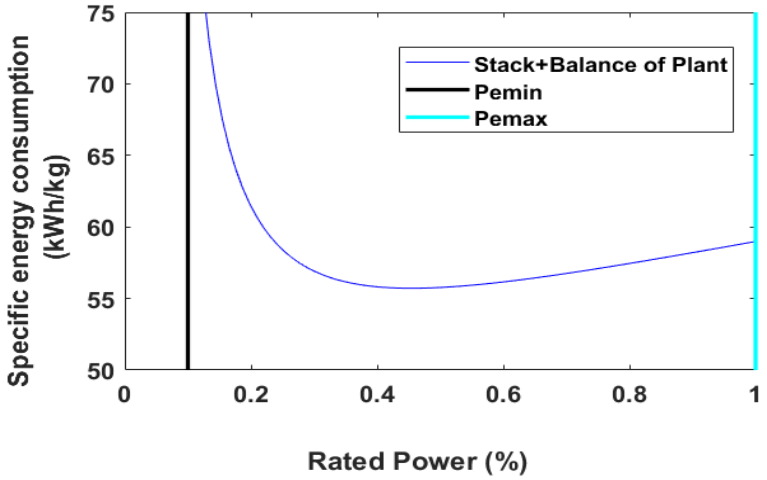

Figure II-13. Specific energy consumption of the electrolyser unit.

The PEM electrolyser in [2] is rated at 600kW, however, the parameters are adjusted to 500kW rated values. The specific energy consumption values, considered includes the energy consumption of hydrogen purification unit as well. The resulting specific energy consumption curves for both electrolysers with the optimal parameter values and the considered data points are given in Figures III-14 and III-15. The measured data are referred to the work of [2]. It can be observed that for the electrolyser unit 2, the capability of working at 200% of nominal power is considered. Generally, hydrogen production increases with increased power input. It is observed that in the running operating mode of the electrolyser, efficiency of hydrogen production is lower at the beginning with the efficiency improving at around 50% of the rated power and then there is a slight decrease in efficiency with high specific energy requirement. The findings correlate with the model and the report [35], where it states that at lower than nominal power operations, efficiency is higher and hence results in lower specific cost of hydrogen production.

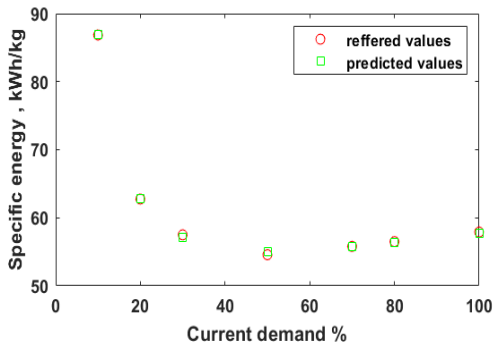

Figure II-14. Specific energy consumption curve of electrolyser unit 1.

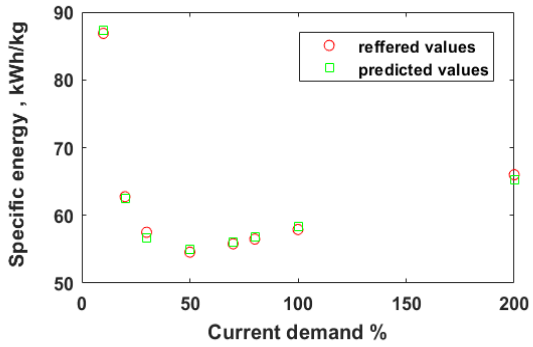

Figure II-15. Specific energy consumption curve of electrolyser unit 2.

In this case, a compromise on hydrogen revenue is to be made due to lower amount of hydrogen production. The resulting equations are especially useful to optimise the operational efficiency of electrolysers based on incoming power. It is to be noted that the parameters change for different electrolysers. Hence, it is necessary to assess separately for each considered PEM electrolyser units. Consequently, the hourly hydrogen production (kg/h) is evaluated as the quotient of electrolyser working power (kW) divided by the specific energy consumption (kWh/kg).

Finally, the electrical efficiency of the electrolyser units is evaluated using the standard equations based on higher heating value (HHV) and lower heating values (LHV) of hydrogen, as per equations (II-15) and (II-16):

$$\mathrm{HHV} = \frac{\text{HHV of hydrogen}}{\text{Input Energy}} \qquad \text{(II-15)}$$

$$\text{LHV} = \frac{\text{LHV of hydrogen}}{\text{Input Energy}} \quad \text{(II-16)}$$

The hydrogen compression is considered at 30 bar at the outlet of the electrolyser units. A compressor unit is then required to raise the pressure from 30 bar to 200 bar. It is estimated that 5% of the energy of hydrogen at its LHV is consumed, when it is compressed at 350 bar which amounts to approximately1.67 kWh/kg [84][85]. Similarly, at the 200 bar compression, an electricity requirement of 1.57 kWh/kg is estimated [86]. A single stage mechanical compressor is considered for the analysis. From a technical perspective, the mechanical compressors generally used in the industries are mature technologies. It favours high hydrogen flow and high discharge pressures. The main drawbacks are said to be its many moving parts, embrittlement phenomena by hydrogen molecules, resulting in the formation of polluted hydrogen as a product, its structural complexity and maintenance. In addition to it, noise and vibrations are also cited as a common drawback. Sdanghi et al. [86], estimates that the compressor represents the 54% of the hydrogen production capital expenditure (CapEx) [84]. Hydrogen has a gravimetric storage density of 6 wt.% and volumetric storage density of 30 g/L [84]. In the following analysis, hydrogen is stored in high pressure storage tanks at 200bar. It is generally the cheapest solution to compress the hydrogen onsite and transport it through truck delivery among the other alternatives [37]. The details on deriving hydrogen compression and storage cost is described in Chapter IV.

II. Input renewable energy profiles

The input data used, particularly the tidal current data and wind velocity data, are characterised in detail in this section. In order to characterise the reference dataset, various tidal current profiles in terms of different duration such as daily, monthly, and annual profiles are analysed. Data analysis considering the frequency of occurrence of specific daily tidal current profiles for a time frame of 10 years at the given site is also presented for a comprehensive analysis. Further, deduction of a reference daily wind velocity profile is detailed.

1. Tidal current profiles

Tidal currents historic velocity data for 10 years from the year 1996 to 2005 were available. Data were sampled at 1 hour for the considered flow berth of the proposed tidal site at the Fall of Warness. The available tidal currents velocity data were in u and v directions and the resultant tidal current speed, v_t was calculated by the equation (II-17) [87]:

$$v_t = \sqrt{u^2 + v^2} \quad \text{(II-17)}$$

Figure II-16 shows the *u* and *v* components of the tidal currents. Figure II-17 shows the measured tidal current velocities in u, v directions and the resultant tidal speed for the tidal profile dated, December 30, 2005. It can be observed that the tidal cycle at the considered site is semidiurnal in nature, i.e., two tidal cycle in a day with two high and two low tides.

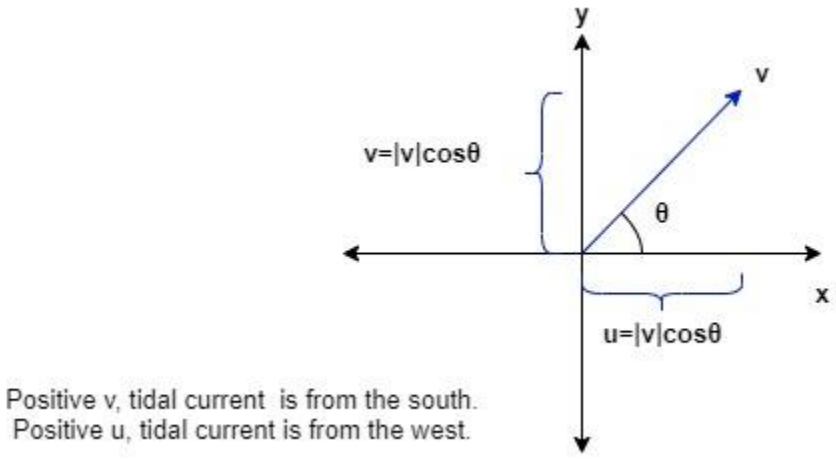

Figure II-16. u and v components of tidal current velocity.

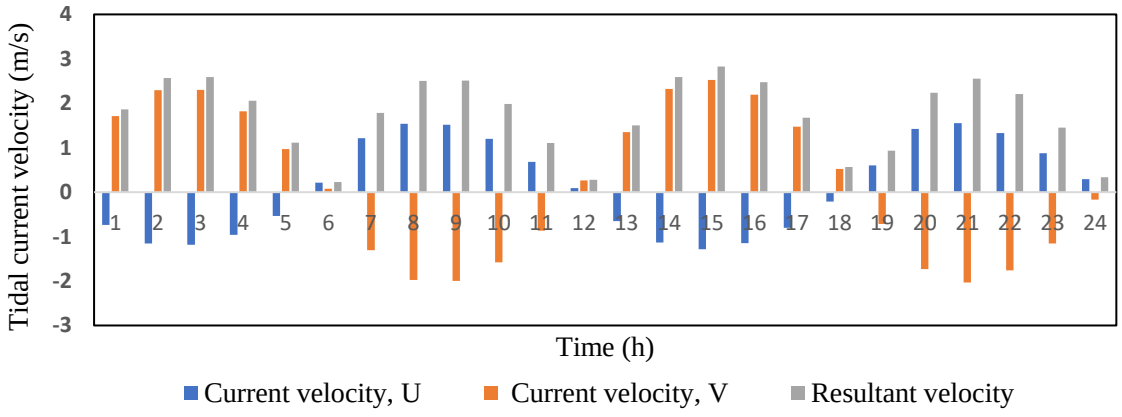

Figure II-17. Resultant tidal current estimation of a daily tidal profile sample.

At first instance, a common set of tidal current daily profiles data is extrapolated at each hour in terms of the highest, lowest, and average conditions by using the harmonic mean analysis. Harmonic mean is used for sampling as they are good at handling large outliers compared to the arithmetic mean, It is considered appropriate especially for situations, when the average of rates is desired. The data is selected as follows,

the year with the highest harmonic mean is extracted first, followed by the highest month and then the highest daily profile. Similar method is used to extract the average and the lowest daily profile samples. This daily data set is selected keeping in mind that, it is useful to analyse the possible highest, average and the lowest tidal profiles and the corresponding green hydrogen production potential at the test site. It is seen that the highest, average, and the lowest daily profile is observed for March 28, 1998, February 25, 2000 and December 24, 2001 respectively. Figure II-18 shows the highest and the average daily tidal profiles for the considered duration.

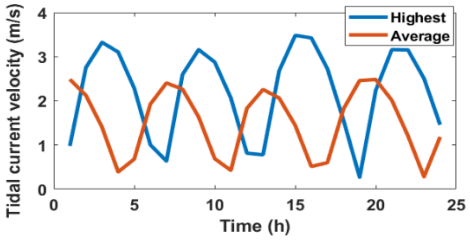

Figure II-18. Highest and the average daily tidal profiles.

It is observed that the year 1998, has the highest daily profile sample. The sample annual tidal profile for the year 1998 is given in Figure II-19. Annual occurrences of specified tidal current speeds are evaluated for the year 1998 in Figure II-20. It is estimated that occurrences of tidal current speed above 1 m/s which is the cut-in velocity of the selected tidal turbine, is 72.5% out of which 18.14% accounts for the speed above the rated speed of 2.5 m/s which makes about 27.5% of occurrences of tidal current below 1 m/s. Annual occurrences of specified tidal current speeds are evaluated for the perceived lowest year, 2001 in the Figure II-21. It can be observed that the occurrences of tidal current speed above 1 m/s which is the cut-in velocity of the tidal turbine is 66.45% out of which 13.89% accounts for the speed above the rated speed of 2.5 m/s which makes about 33.5% of occurrences of tidal current below 1 m/s. Therefore, preliminarily it can be inferred that the availability of the tidal energy system for power generation is in a range of 66.45-72.5%.

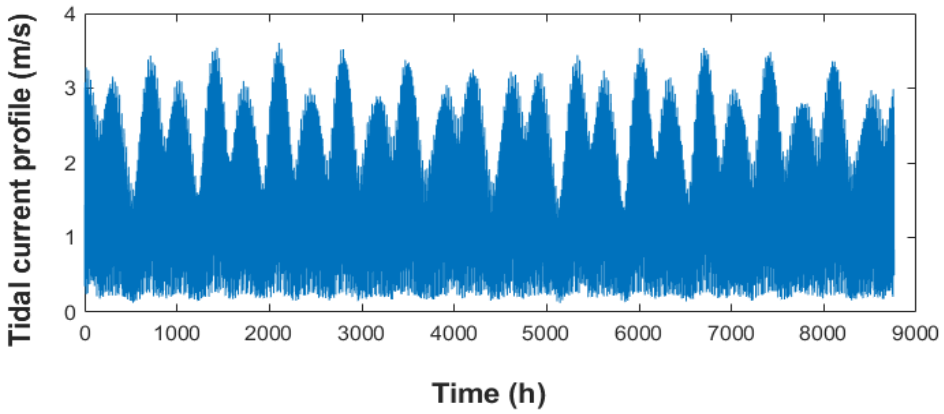

Figure II-19. Annual tidal current profile for the year 1998.

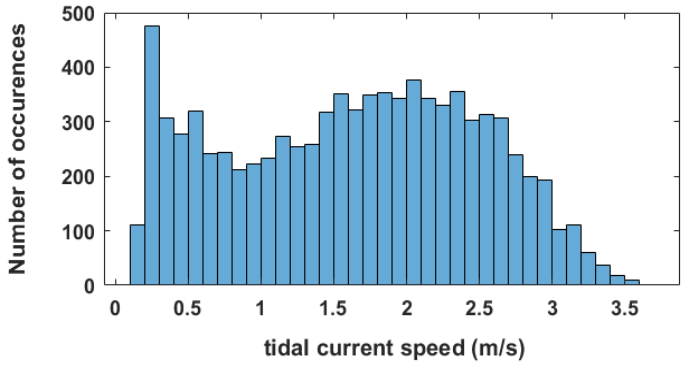

Figure II-20. Annual occurrences of specified tidal current speeds for the year 1998.

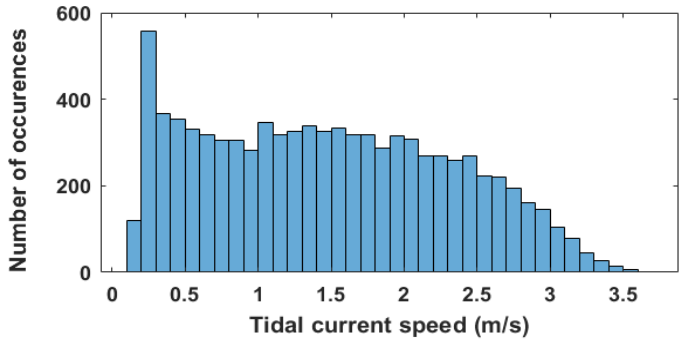

Figure II-21. Annual occurrences of specified tidal current speeds for the year 2001.

On further analysis from the Figure II-18, monthly tidal profile for March 1998 and December 2001 are analysed and given in the Figures II-22 and III-23. A large variation in terms of the tidal current availability is observed in this case. (please note the change in y-axis scale).

A preliminary calculation of the annual mean capacity for the 10-year data for each year from 1996-2005 for the TSES. The losses are also included for this purpose. The capacity is calculated based on the formula:

$$Capacity\ factor = \left(\frac{Power\ at\ the\ transformer\ end}{Rated\ power\ of\ the\ tidal\ system}\right)100 \quad \text{(II-18)}$$

The annual mean capacity factors for the 10 years are given in Figure II-24. The value ranges from 27.32-33.17%. The value for the year 2001 seems like an outlier on further analysis based on monthly capacity factor calculations. It is seen that, cf. Figure II-25, the mean capacity factor available for two months for the year 2001, i.e., for the month of November and December is too low at about 5.95% and 4.87%, respectively compared to other values which seems to be in the range of 30.61-34.94%. This is presumably a miss in the available data set, as typically tidal stream energy has shown to have consistent monthly flows [3].

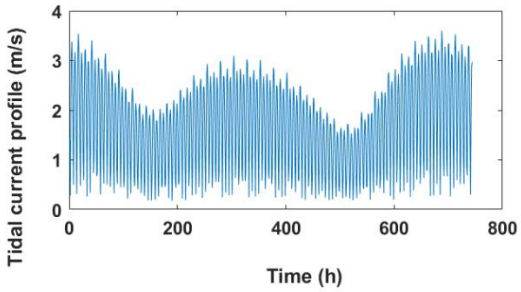

Figure II-22. Monthly tidal current profile for March, 1998.

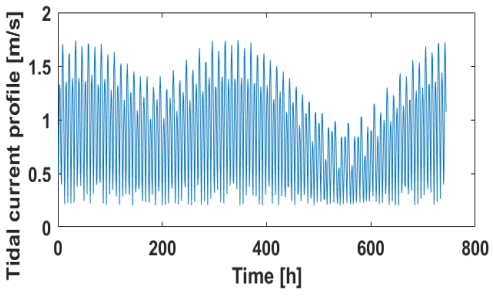

Figure II-23. Monthly tidal current profile for December, 2001.

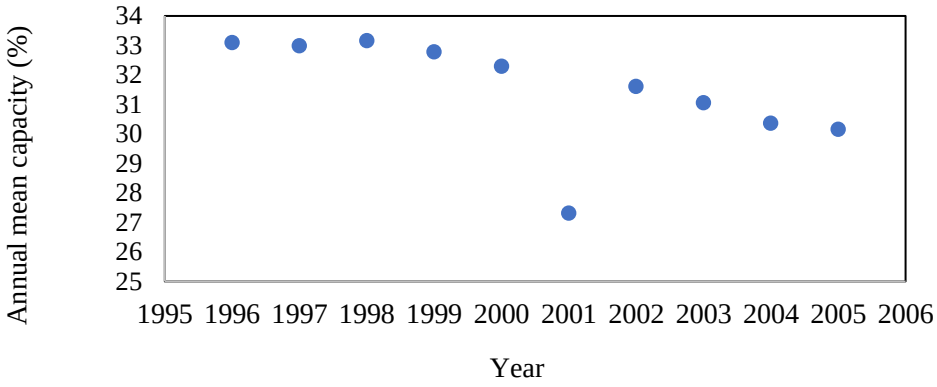

Figure II-24. Annual mean capacity factor of tidal energy plant for ten years.

Subsequently, the occurrence of daily tidal current conditions is considered. Considering the ten years data, 3652 daily profiles are estimated. By using the frequency of repetition clustering algorithm [70], the most frequency occurring daily tidal profiles dataset were extracted and was made available. It is estimated that 231 daily profiles have less than 1% of occurrence and hence, they are excluded. The occurrence of remaining profiles are considered, as they have significant occurrent percentages. This reduces the data set to 27 daily profile conditions associated with a frequency of occurrence percentage. As the exclusion of 231 profiles is due to a low occurrence and not to a zero-speed condition, 27 reference profiles are considered as most representative of the 100% conditions.

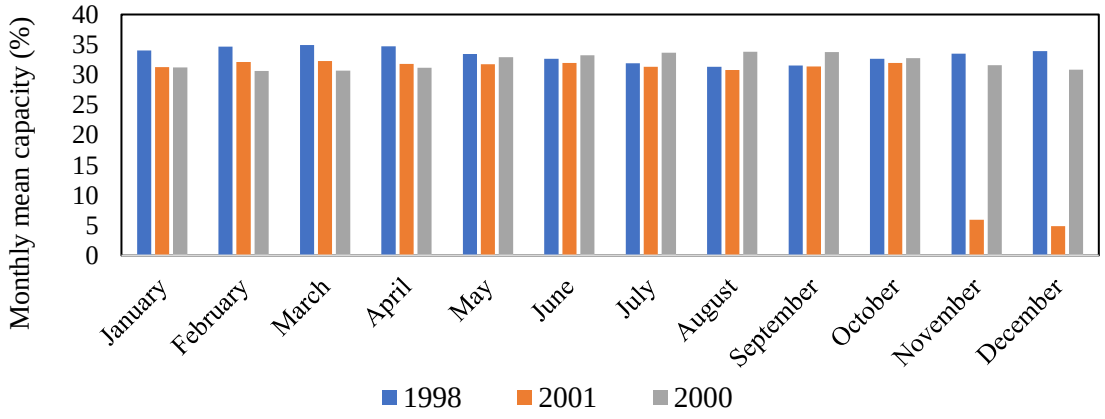

Figure II-25. Monthly mean capacity factor of tidal power generation.

The resultant 27 tidal profiles are given in Figure II-26. The corresponding frequency of occurrence of tidal profiles is given in Figure II-27. Compared to the frequency of occurrence, the corresponding occurrence of these tidal profiles annually, in terms of the numbers of days is given in Figure II-28. As the tidal energy is highly predictable, these large data sets are valuable in order to characterise the TSES availability and performance in an annual context. In addition, tidal stream energy is found to have no significant seasonal variation [75]. However, it is to be kept in mind that as per the estimate in [88], sea level rise caused due to global warming will have an effect on tidal energy sources. This aspect is to be included in the future modelling.

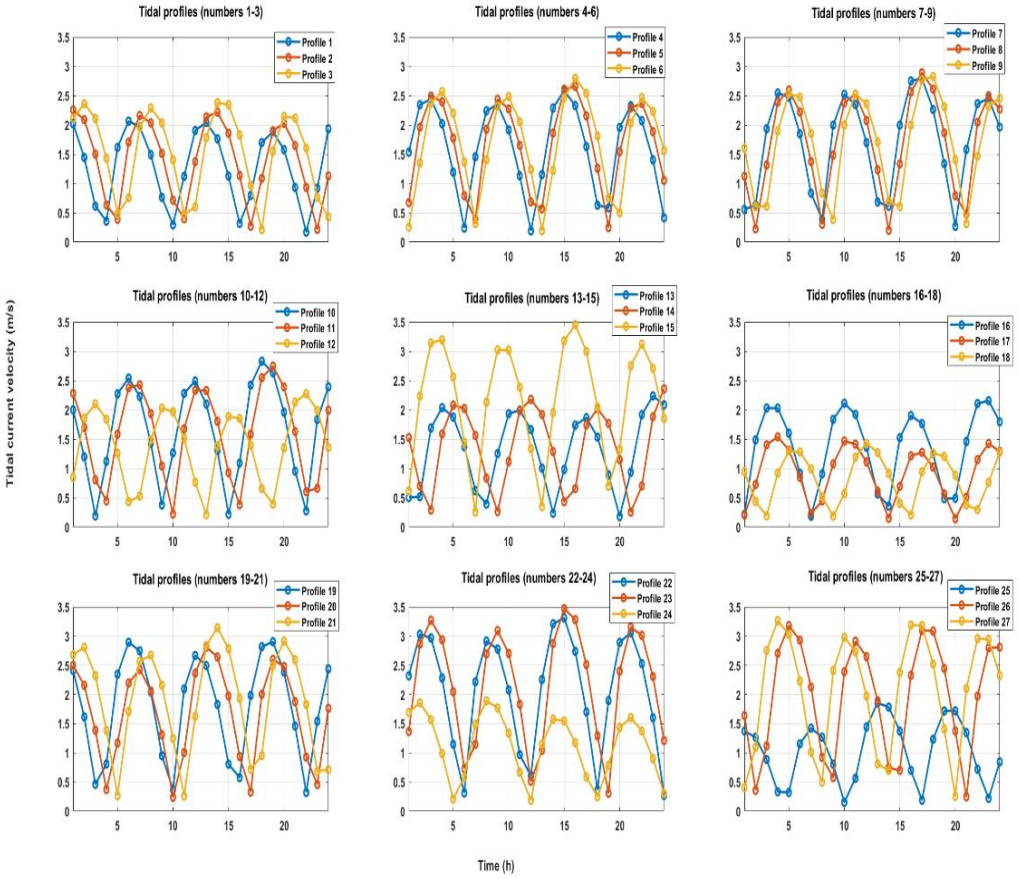

Figure II-26. The 27 tidal profiles characterise the most occurrent tidal current conditions in 10 years of measurements.

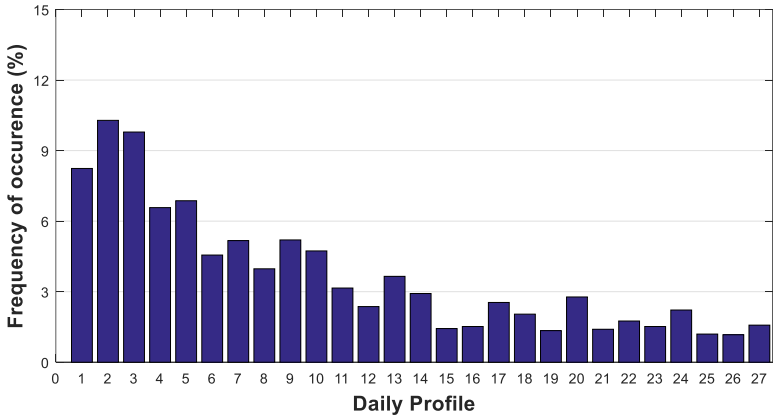

Figure II-27. Frequency of occurrence of selected 27 tidal profiles.

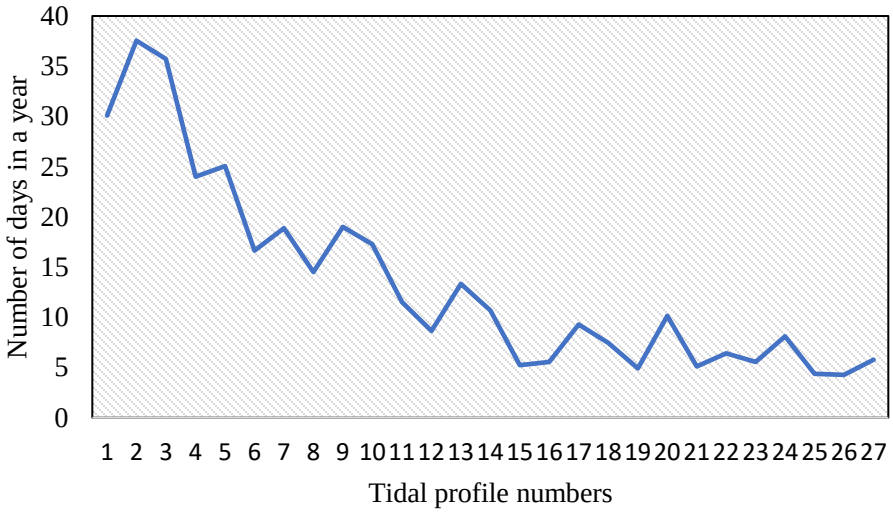

Figure II-28. Cumulative sum of the number of days of occurrence in a year of the given 27 tidal profiles.

2. Wind velocity profiles

The available ten years offshore wind velocity data at the site are used towards the data characterisation for this subsection. Offshore wind data are used in the study as they were readily available for the considered duration. The typical annual wind profile of the Orkney Islands is given in Figure II-29. It can be observed that the wind velocities are generally low in the summer seasons but it is quite high during the winter season. It is inferred that since Orkney is a set of islands, the offshore and onshore wind velocities do not differ largely. Consequently, the available offshore data set is used for the analysis. A common and single set of

wind velocity daily profile is then considered. Data are sampled at each hour in terms of the highest and average conditions and it is extrapolated using harmonic mean analysis cf. Figure II-30. Even though offshore wind data were used, it was observed that the available data matched with the onshore wind data [89]. It is observed that the lowest daily wind velocity samples are too low to generate enough power. The mean daily capacity of the given wind system in the highest and average tidal profiles are found to be 72.3% and 23.49%, respectively. Wind energy plant is considered as an external supplier in the analysis in Chapter IV. To characterise the hybrid energy system in an annual context, a common daily profile corresponding to the average wind velocity daily profile is considered as the reference profile.

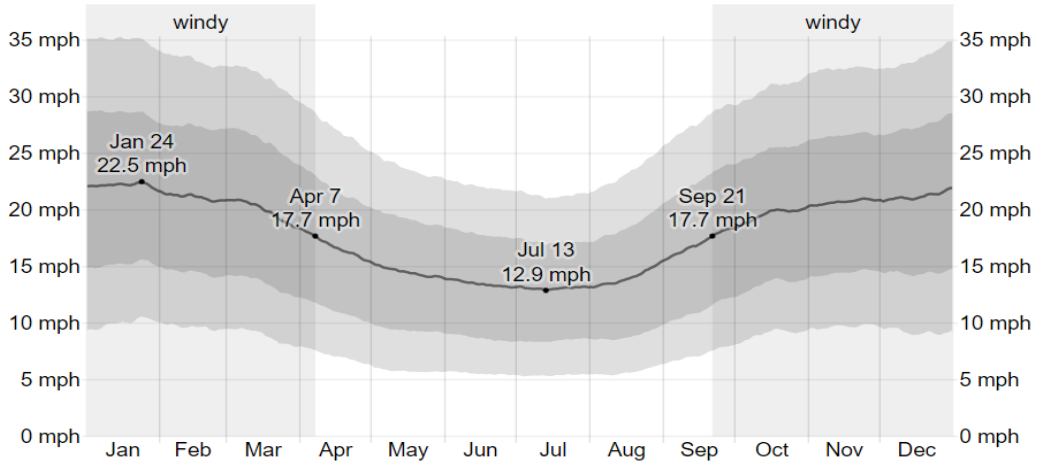

Figure II-29. Typical annual wind profile of the Orkney Islands.

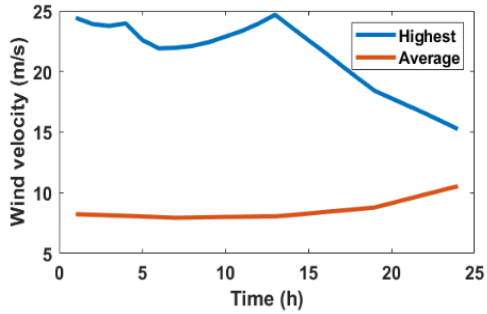

Figure II-30. Highest and average daily wind velocity profiles.

.

III. Conclusion

The specific models of the proposed system components such as floating tidal stream energy plant, onshore wind energy system and PEM electrolyser and are presented in this chapter. The associated power converter devices, power loss in the system, hydrogen production auxiliary units like the compressor, balance of plant and storage are briefly discussed. The PEM electrolyser model based on different operating modes and associated energy consumption is presented. The models were validated using suitable references. Tidal current data and wind velocity data set at the test site is analysed for a comprehensive analysis of the available RES sources in terms of its occurrence. It is inferred that the tidal energy is more reliable compared to wind energy, as the later accounts for much uncertainties. However, it is advisable to combine these two energy sources due to the cyclic nature of tidal current profile and also to ensure maximum utilisation of green energy. It is worth noting that even though the input data used especially for the tidal current profiles in the model is about 15-25 years old, the model is capable to work with newer data that can result in more updated accurate estimations.

Chapter III

Rule-based energy management approach

This chapter explores the working of different configurations of the system such as tidal stream energy system (TSES) alone configuration, TSES-grid connected configuration, TSES-hydrogen system configuration and TSES-grid/wind-hydrogen system configuration. The different aspects of annual performance of the tidal stream energy plant are investigated initially. Based on the frequently occurring daily tidal current profile data, i.e., the 27 tidal profiles presented in Chapter II, the annual tidal energy production, associated carbon emission savings and cost/benefits are analysed. The sensitivity of the tidal levelised cost of energy (LCOE) with respect to different system parameters are analysed to have a comprehensive understanding. The economic analysis, when the TSES is connected to the grid is further assessed.

Additionally, the operational synergies of the tidal stream energy plant integration with green hydrogen production are explored. Towards reaching this goal, the individual system models described in the previous chapter are used. A rule-based energy management strategy is formulated and the overall system performance of both the electrolyser units are analysed. Different system configurations such as tidal-hydrogen, tidal-wind/grid-hydrogen system are discussed here. The electrolyser operating modes during transitionary operation, when subjected to intermittent RES input are analysed.

Towards the later part, a preliminary assessment of hydrogen production cost in the case of a standalone tidal-hydrogen and tidal grid-hydrogen energy system configuration is analysed to particularly analyse the hydrogen production cost variation based on different daily tidal profiles and the target hydrogen production. The model can be used as a generic tool to estimate hydrogen production with the associated costs representing the core of the system optimisation process.

I. Analysis of annual tidal energy generation

The most occurrent 27 daily profiles are used for the analysis here, along with TSES model presented in Chapter II. As tidal stream generated power is cyclic in nature, the corresponding peak power of the 27 different profiles is analysed and it is illustrated in Figure III-1. It can be observed that the given site is highly energetic in nature, with above average to peak power available for considerable time durations with low power conditions reduced to least occurring daily tidal current profiles. Subsequently, the daily cumulative tidal stream energy generation is also analysed for the same data set as illustrated in Figure III-2.

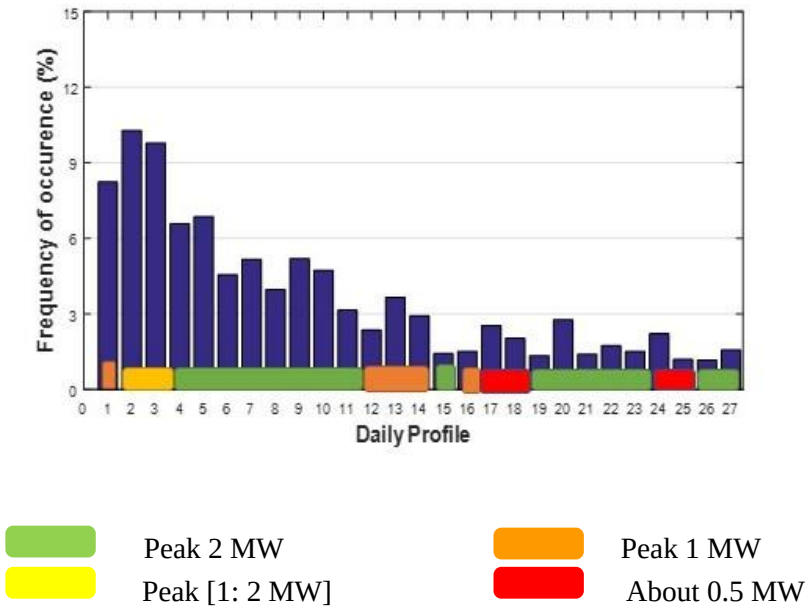

Figure III-1. Peak power occurrence of the selected 27 tidal profiles.

The cumulative tidal energy generation data also suggests that the average daily energy generation profiles of above 11MWh-24 MWh are quite frequently occurring with lower tidal energy generation profile among the least occurring daily profiles. The losses in the TSES under different stages are given in Figure III-3. It can be observed that the inevitable hydrodynamic losses constitute the major part with other losses related to power conversion and transmission aspects constituting about 15.6%.

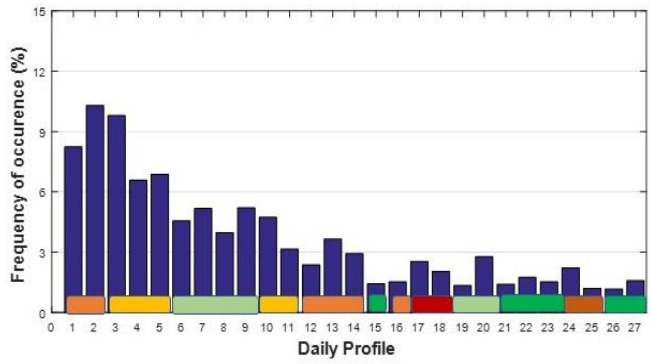

Colour codes	Tidal stream energy (MWh/day)
	0- 5
	6- 10
	11-15
	16-20
	21-24
	25-30

Figure III-2. Daily tidal energy production range for the different tidal profiles based on their frequency of occurrence.

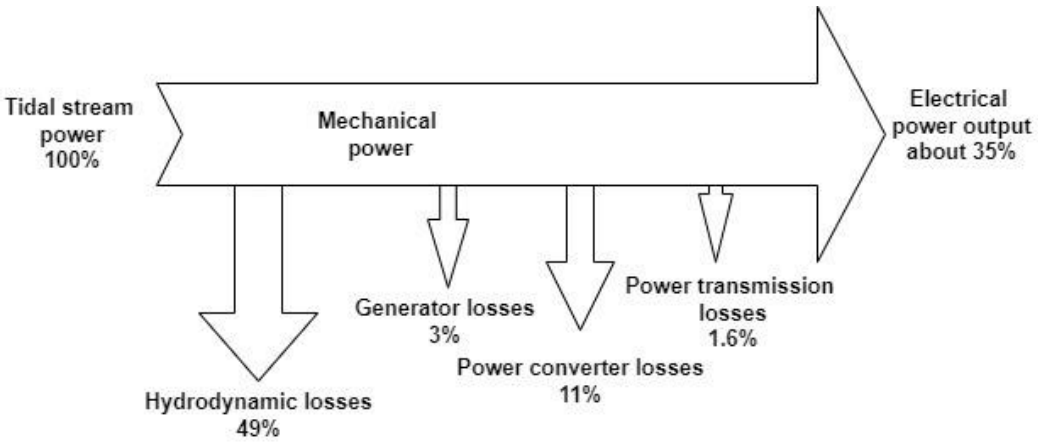

Figure III-3. Different losses in TSES.

The major losses in conversion stage are due to the three stages of conversion involved and it is also strictly dependent on the efficiency of the considered converters.

Further, the production hours and zero power production hours of the tidal energy plant in an annual context are presented in Figure III-4. It can be observed that the production hours are quite consistent at about 14-18 hours a day with the exception of low tidal current profiles for which it is at 8 hours day. Another interesting thing to note is the zero energy production hours at about 4-8 hours a day, which is also consistent for average to above average tidal current profiles. Again, this feature can be attributed to the cyclic nature of the tidal energy.

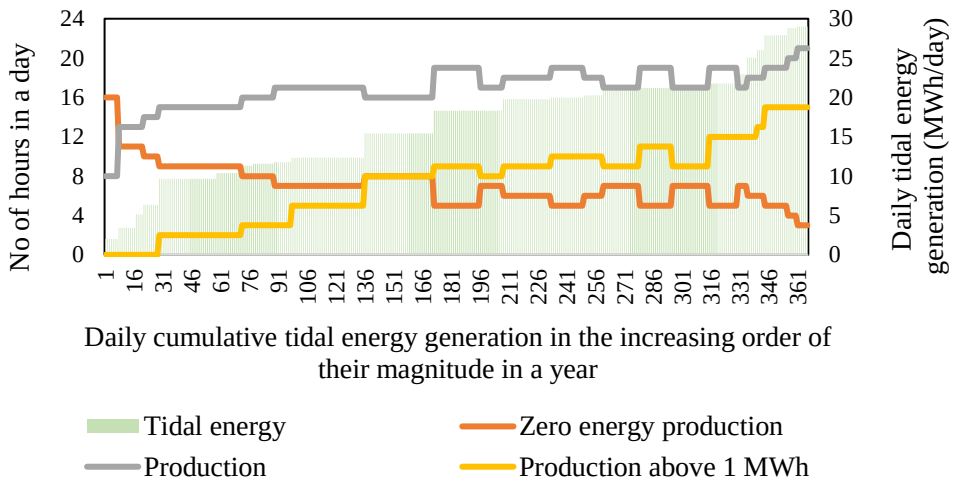

Figure III-4. Production hours, above 1MWh production occurrences and zero production hours of the tidal energy plant in an annual context.

Finally, different system parameters such as the annual tidal energy generation, the utilisation factor, and the capacity factor are analysed. Table III-I lists the different parameters specific to the annual performance of the given floating TSES. Annual tidal stream generation is initially estimated without considering any downtime due to maintenance. An advantage with tidal energy system is that the zero power conditions also called as slack period which generally lasts for 1-2 hours continuously and it can be utilised for regular maintenance checks. According to Coles et al. [3], highly energetic tidal sites have a disadvantage in terms of the duration of slack tide period as they may not be sufficient for the maintenance operation considering vessels needed for maintenance are to be rented per/day cost basis. However, this phenomenon is more pronounced for tidal farm and the maintenance cost can be weighed against the production period cost for a better decision [25].

The carbon emissions associated with the TSES at the current stage of learning rate is 18 gCO_{2e}/kWh [90]. A fairly medium carbon intensity of 209 gCO_{2e}/kWh for the UK electricity distribution system is selected for a fair assessment on carbon emission offsetting [91]. The value is also estimated with the standard coal production carbon emission estimation. Thus, considering a lifetime of 25 years for the tidal stream plant, tidal energy generation in its entire system life time would be of about 150 GWh and the corresponding CO_2 savings in comparison with the carbon intensity of UK grid would be 28745 tonnes. On further analysis on the peak power occurrence data, it is estimated that the tidal potential of the selected site is quite suitable for the tidal plant implementation with about 43% availability for tides in days with potential for peak power up to maximum limit. The capacity factor of the TSES, the ratio of annual energy generation to the energy generation at the maximum capacity is estimated to be 34%, which is typical of other tidal stream energy devices available in literature considering the loss and downtimes in the system [25]. Capacity factor

excluding the zero energy generation hours is also estimated to be 48.7%. This is included to highlight the system efficiency excluding the obvious cyclic nature of tidal stream energy, i.e., the inevitable zero power production hours. As mentioned before, it is worth noting that that due to the predictable nature of tidal stream, the difference in capacity factor would be only ±10% throughout the system lifetime from a geographical perspective [3]. A reliability, availability and maintainability (RAM) analysis performed by Diagon et al. [26], on a floating multi-rotor tidal turbine has estimated a base case availability factor of 80.09% for the TSES in its overall lifetime of 20 years. Further, the paper describes that a major failure that requires the TSES to be towed to the shore for repair, would need offshore supply vessel (OSV) and for 'minor failure', the failures that could be repaired on-board requires the use of a crew transport vessel (CTV). The corresponding frequencies of use of OSV and CTV use in a year is found to be 1.87 and 1.43 times [26].

Table III-1. Annual tidal stream energy system parameters.

Annual system performance parameters	Values
Tidal energy production (GWh/year)	6.02
Carbon emission savings considering carbon intensity of the UK grid (tonnesCO_2/year)	1149.82
Carbon emission savings considering the carbon intensity of coal production (tonnesCO_2/year)	1940
Production hours	6175.1
Zero power production hours	2589.69
Utilisation factor	70.49
Utilisation factor of above 1 MW production in the production period	43.11
Capacity factor (%)	34.37
Capacity factor (%) excluding zero power production hours	48.77

1. TSES LCOE cost analysis

The tidal stream energy generation is calculated using the levelised cost of energy (LCOE) method.

The LCOE is given in equation (III-1),

$$\mathrm{LCOE} = \sum_{T=0}^{N} (\mathrm{CapEx} + \mathrm{OpEx}_{t)}/(1+r)^t \,/\mathrm{AEP}_t/(1+r)^t/(1+r)^t \qquad \text{(III-1)}$$

where, *T* is the year under consideration, *N* is the system life time, CapEx corresponds to the capital expenditure and OpEx corresponds to the operating expenditures, AEP is the annual energy production and *r* is the discount rate.

An indicative cost estimates of a standalone floating tidal stream energy plant is taken from the literature [3][25] and it is shown in Table III-2. The LCOE is assessed with a discount factor assumed as 12%, which is typical of offshore renewable technologies [19] and O& M growth rate of 3%/year. According to Myhr et al. [92], the floating offshore technologies can have a reduced discount rate of 10%.

The LCOE evaluation tool by Corporate Finance Institute (CFI) [93] is used to obtain the levelised costs. The floating tidal stream LCOE is calculated for the values mentioned in Table III-2; a corresponding value of 0.25 €/kWh is obtained.

Table III-2. Indicative parameters for LCOE estimation [74].

Indicative parameters selected for LCOE estimation	**Values**
CapEx (M€/MW)	4.89
OpEx (M€/MW/year)	0.05
Annual electricity input (GWh)	6.02
System Lifetime	25
Discount rate (%)	12
O&M growth rate (%)	3

Further, a sensitivity analysis is done on understanding the relationship between LCOE and other individual parameters in the equation (III-1). Figure III-5 shows the variation of LCOE with respect to the change in individual parameters like life time, discount rate, O&M growth rate, annual electricity production, capital expenditure and operating expenditure, respectively. The values in Table III-2 are used for the estimation of LCOE in the figures, unless otherwise specified in individual graphs. Overall, it can be observed that slight variations in the discount rate and capital expenditure have major impacts on the LCOE. The other deciding factors that have significance on the LCOE are annual electricity production and system lifetime, while, the O& M growth rate and costs are quite negligible. This analysis is useful on understanding the deciding dynamics of LCOE estimation. The tidal stream LCOEs in the literature is estimated in a wide

range of 0.115 €/kWh-0.476 €/kWh [19]. Reference [94] estimated a tidal LCOE evolution in the range of 0.079-0.159 €/ kWh based on the cost evolution models used for offshore wind energy technologies, whereas the forecasted LCOE of early production stage tidal technology in the US is estimated to be 0.107-0.23 €/kWh considering appropriate currency conversion rates [95].

Based on the results available from the projects under demonstration or in the pre-commercial phase; with the increase of technology-specific learning rates, a high-cost reduction is estimated for the TSES [96]. The tidal stream energy LCOE target of the strategic energy technology implementation plans (SET-Plans) for offshore wind and ocean energy in the UK is 0.15 €/kWh and 0.1 €/kWh for the year 2025 and 2030 respectively [19]. It must be noted that LCOE is typically specified over the entire lifetime of the system. It is important to define the cost boundaries, while estimating the LCOEs and also while comparing with other system LCOEs. Further, certain factors like the reliability, social & environmental costs or the power quality of a system are not quantified in the LCOE. Hence, it is important to understand that LCOE cannot be used as an all-in-one cost factor for deciding on a particular RES, especially when an integrated system is to be designed. Either ways, LCOEs provide a preliminary assessment on the possible range of cost at which generated electricity is to be sold to generate income to the system or to avoid net loss in a real economic sense.

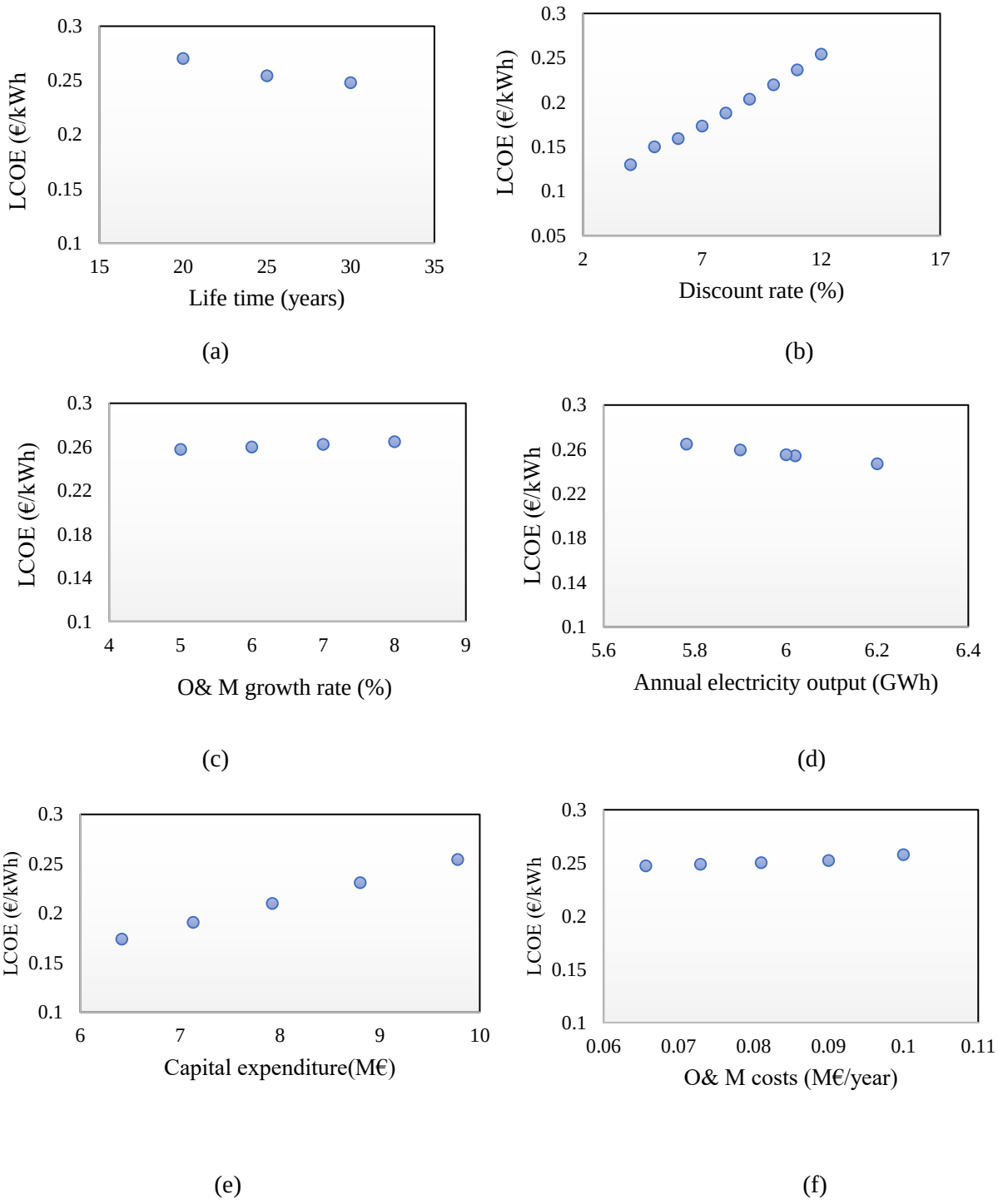

Figure III-5. Sensitivity analysis of LCOE values with respect to (a). Life time, (b). Discount rate, (c). O&M growth rate, (d). Annual electricity output, (e). Capital Expenditure, (f). O&M costs.

II. Tidal energy export to the grid- Economic analysis

As introduced in Chapter I, a contract for difference (CfD) support scheme is considered for the economic analysis of the tidal plant operation [3]. According to this scheme, when the CfD strike price is higher than the market electricity price, the contract supplier has to pay the tidal plant operator the difference amount. Accordingly, the tidal plant operator has to pay back to the contract supplier the difference amount in case, when the strike price is lower than the electricity price. An electricity price of 0.251 €/kWh is selected as the strike price for tidal energy powered electricity for the CfD scheme in this case. This value represented the set strike price for the tidal stream energy system in the year 2011/12 [3][96], which is the updated value in literature for the tidal stream energy strike price. The day ahead hourly auction prices for the electricity export to the grid in the UK is selected as the reference prices for electricity export [97]. The carbon credits for each unit of tidal energy would be about 0.0045 €/kWh, calculated from the current carbon emissions selling price in the UK (23.8 €/tonne of CO_2) [98]. Consequently, the carbon credits related to the tidal energy exported to the grid is calculated. The hourly grid electricity export prices and the strike price defined for tidal energy export is given in Figure III-6.

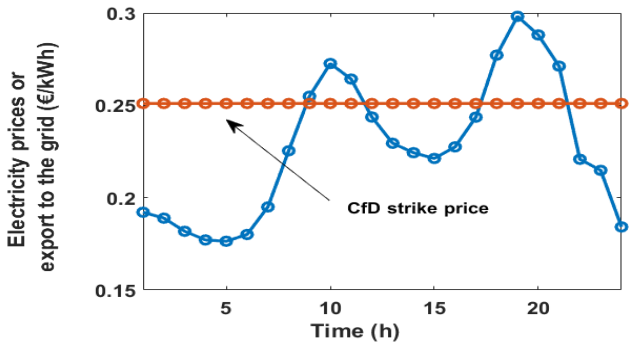

Figure III-6. Grid electricity prices for export and tidal energy strike price [74].

Based on the selected data, the corresponding tidal energy generation costs, the revenue from tidal energy export to grid, the carbon credits revenue from tidal energy export, and the payment to the intermediate company based on the CfD strike price are evaluated annually.

The annual profit is then evaluated as follows:

$$\text{Annual profit} = \text{Revenue} - \text{Cost} \tag{III-2}$$

with, cost evaluated as, $\text{Cost} = \text{CCF}_t + \text{OpEx}_t + \text{PTC}$ (III-3)

and revenue evaluated as, $\text{Revenue} = \text{GER} + \text{TCS}$ (III-4)

where, CCF is the annualised capital expenditure (€/year), OpEx is the operating expenditure of the tidal stream system (€/year), PTC is the payment by the tidal plant to the intermediate company (€/year), GER is the annual grid energy export revenue (€/year), TCS is the annual tidal energy export carbon savings (€/year).

The variation of annual profit with respect to different strike prices for the given system is analysed below. The range of 0.1-0.25 €/kWh is selected as the strike price considerations under the CfD scheme with the minimum value, based on the SET plan target for the offshore wind and ocean energy. Additionally, 27 daily tidal stream current profiles extracted using the frequency of occurrence method is applied to estimate the annual tidal energy production capability. For an easier comprehension, the tidal stream energy generation in MWh/day is plotted against the occurrence percentage data in Figure III-7.
The net profit percentage with respect to the annualised CapEx for the annual tidal power profile conditions of the selected tidal stream energy plant under different strike price values in CfD are given in Figure III-8.

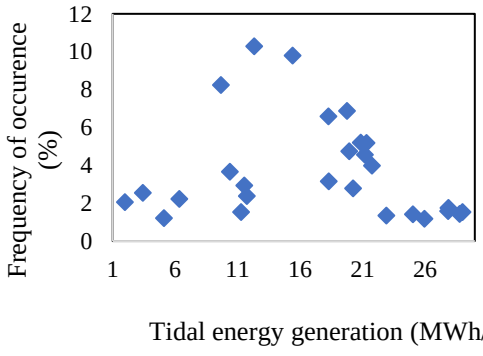

Figure. III-7. The variation of the available daily tidal energy generation from the floating tidal stream plant and their corresponding occurrence percentage [74].

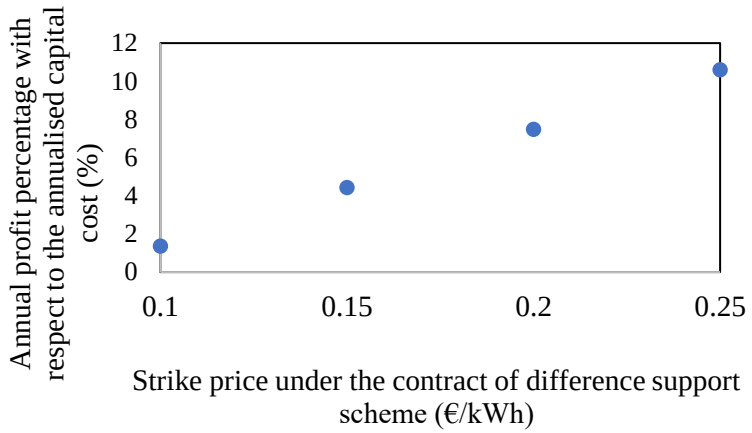

Figure III-8. Variation of annual profit (%) with respect to the strike prices under CfD.

It is observed that with increase in the strike price value, as it is evident the tidal energy export revenue is increased; at the same time the payment to the contract supplier for the difference price is reduced. It is worth noting that this aspect is strictly dependent on the selected hourly electricity reference prices. Without consideration of any discount values and other taxes on the system on an annual basis, the overall system profit in its lifetime for the strike price range of 0.1-0.25 €/kWh is about 0.34-2.65 times higher than the total capital cost.

III. Tidal –hydrogen energy system configuration

The integration of standalone TSES with two PEM electrolyser units both with a nominal rating of 500 kW with an electrolyser unit capable of working at 1 MW for three hours a day is evaluated in this subsection. In order to facilitate this, an energy management strategy based on rule-based approach (RBA) is devised.

Rule based approach ensures the ability of the system to give solution in limited calculation times. The rules are made logically based on the system requirements. This is also termed as a deterministic approach as the solutions remains the same for each run. Only real power dispatch is analysed in this analysis. Real or active power dispatching is analysed in this thesis as the focus is on green hydrogen production. Power quality is not a great concern as it is assumed to be included, based on the power converter topology considered in the individual components. The power dispatch to the electrolysers from the RES is modelled based on a rule-based power dispatching algorithm. It compares the available power with respect to the operation of the electrolyser units to estimate the daily green hydrogen production. In the RBA, it is made sure that only if the input tidal power to the individual electrolyser unit is within the electrolyser running operating mode limits; it is fed to the system. If the available power to the electrolyser unit is below its operating limits or

if there is excess power availability over the electrolyser capacity, it is injected into the grid accounting the transmission losses. The electrolyser set points based on the input power are decided and electrolyser unit 2 is given priority for power dispatch followed by electrolyser unit 1 and then to the grid. When the available tidal power to electrolyser is above 1 MW, electrolyser unit 2 is activated to perform up to 200% of its nominal capacity and the cycle continues until the three hours condition is fulfilled. The standby and operating mode transition energy consumptions of the electrolyser units are accounted for in the dispatch algorithm. Losses during the dispatch are accounted for by using the power converter efficiencies and tidal power transmission losses. The rule-based power dispatch strategy is illustrated in the flowchart in Figure III-9. The input parameters P_t, P_{emin}, P_{emax} and te represent the active tidal power, the minimum power of electrolyser for running status, maximum electrolyser power and power transmission efficiency to the grid respectively. The variable *loopcount* is used to count the instances, when the electrolyser unit 2 is allowed for operation at twice of its nominal capacity. The results of the flowchart represent the electrolyser unit 1 and 2 input active power and the resultant active power exported to the grid accounting the transmission losses.

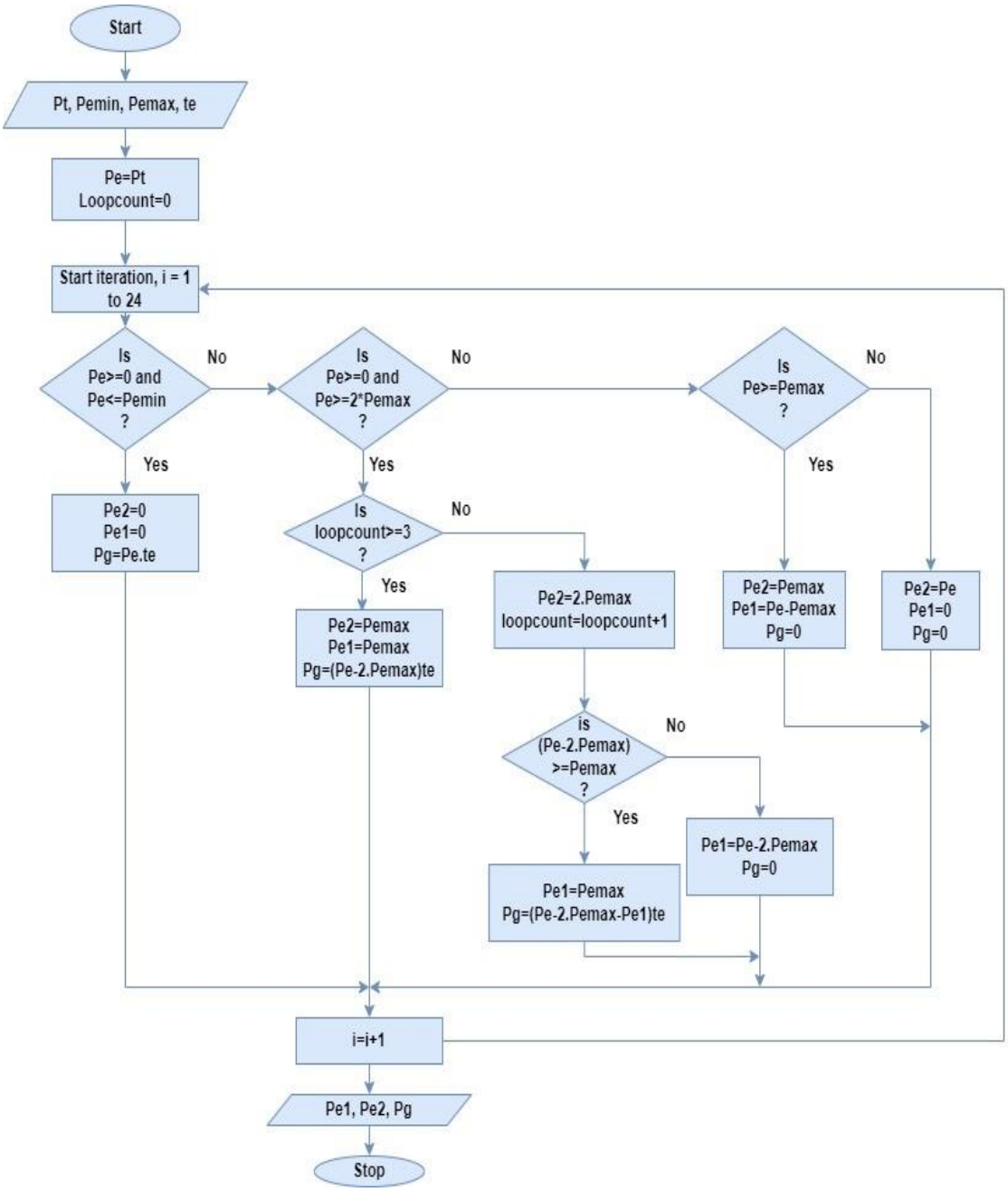

Figure III-9. Rule based tidal power dispatch to the electrolysers.

1. Annual performance analysis of the electrolysers

The annual performance parameters of both the electrolysers based on its power dispatch availability from the TSES is analysed in this subsection. The percentage composition of energy distribution to the electrolyser unit 2, electrolyser unit 1 and energy export to the grid, respectively according to the increasing order of magnitude of daily tidal energy generation is given in Figure III-10 in an annual context. It can be observed that under low tidal power profile conditions only electrolyser unit 2 is fed as it is given priority. However, at higher daily energy generation profiles both the electrolysers are fed in addition to energy export to the grid. It is evident that the magnitude of energy fed to both the electrolysers differs largely with electrolyser unit 1 being underutilised overall. The utilisation factor for both the electrolysers is quantified in the later part of the subsection.

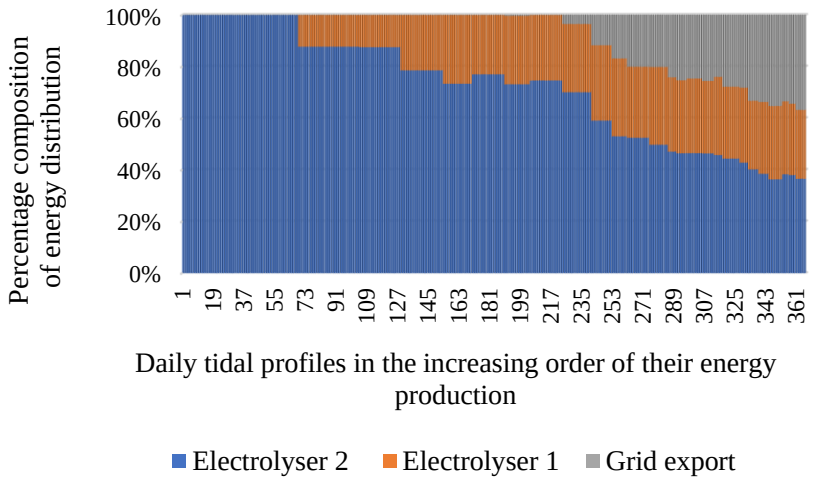

Figure III-10. The energy distribution to the electrolyser units and energy export to the grid.

The corresponding hydrogen production of both the electrolyser units according to the daily tidal energy generation in an annual context is given in the Figure III-11. It can be observed that the hydrogen production of electrolyser unit 2 is quite consistent except for the low energy generation profiles, with hydrogen produced in the range of 100-150kg/day. The hydrogen production of the electrolyser unit 1 is quite low in the range of about 34-100 kg/day, again with the exception of very low energy profiles.

Further, both electrolyser units are analysed based on their different operating modes and associated energy consumption for operating mode transitions. Figure III-12 illustrates the number of hours of stop, standby and running operating mode in a year for electrolyser unit 2 under the given input tidal energy conditions.

Evidently, the production hours increase with increase in energy availability. The stop operating mode hours are quite negligible for this electrolyser unit operation. An interesting factor is the almost stable standby operating mode occurrence at about 4-8 hours, except for very high energy availability conditions in a day throughout the year under the given tidal energy conditions. It is mainly due to the cyclic nature of tidal energy with inevitably zero power production occurrences. This in turn increases the associated energy consumption during transients and standby operating modes conditions as highlighted in Figure III-12. A similar analysis is illustrated for electrolyser unit 1 as given in Figure III-13.

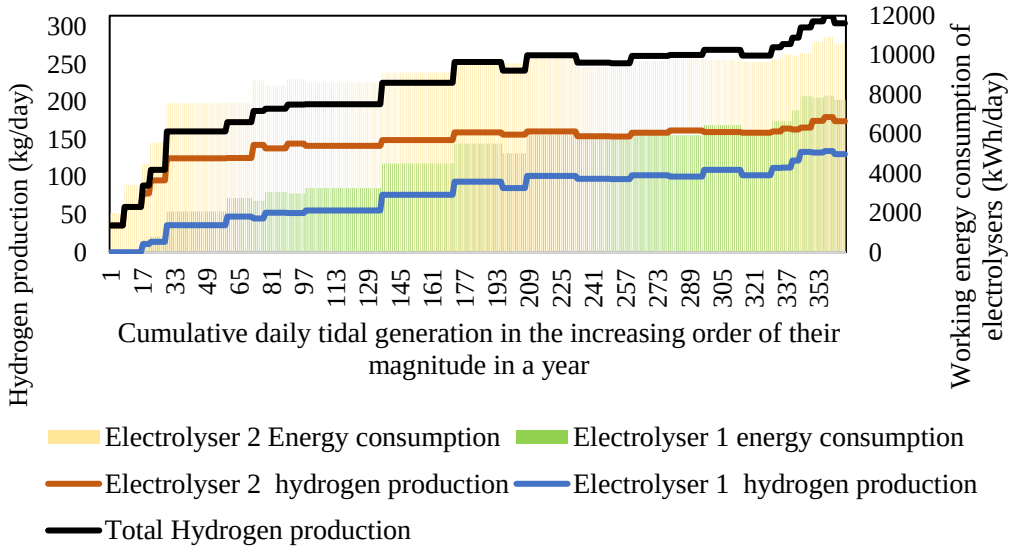

Figure III-11. Daily energy consumption and corresponding hydrogen production of both the electrolyser units in an annual context.

A major difference in the electrolyser unit 1 operating mode variation compared to the electrolyser unit 2, is the increased number of stop operating modes and decreased number of production operating modes due to the decreased power dispatch to the electrolyser unit 1. A relatively similar profile is observed for both the electrolyser units for the standby operating mode occurrences. Overall, the electrolyser unit 2 has lower energy consumption associated with operating mode transitions due to the increased energy availability to it avoiding multiple transitions. It is worth noting that the electrolyser transition cost is directly proportional to energy consumption during transitions.

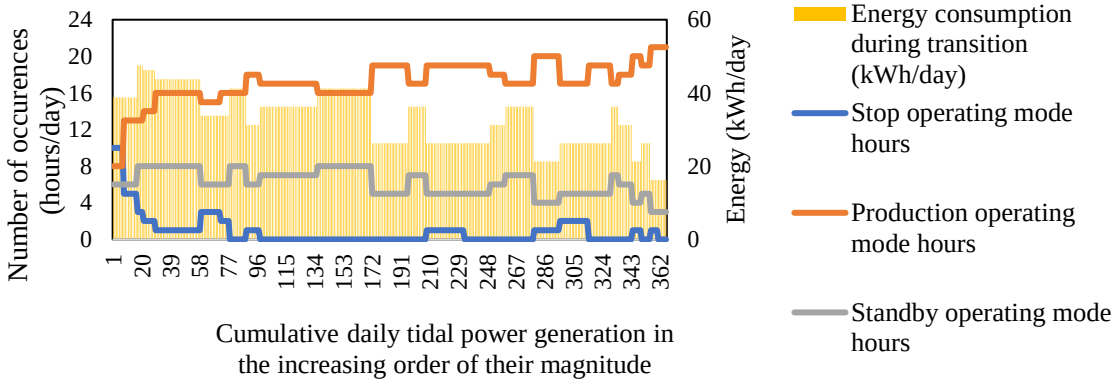

Figure III-12. Number of occurrences of different operating modes in electrolyser unit 2 and the associated energy consumptions during operating mode transitions.

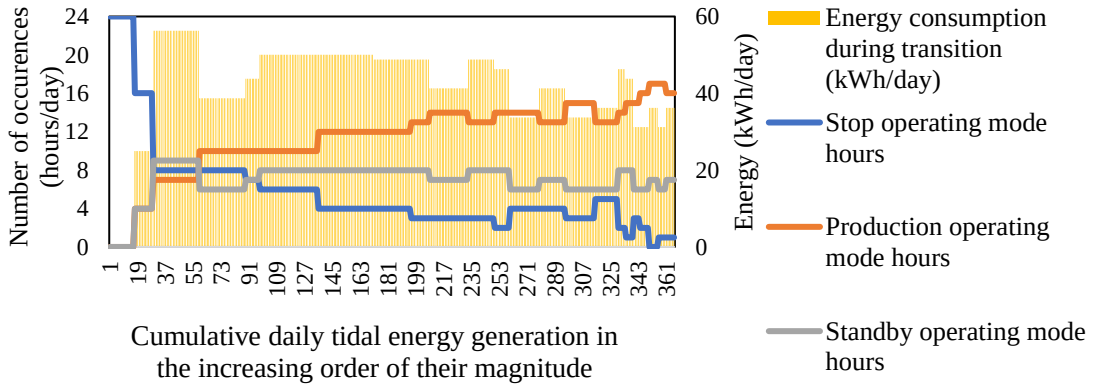

Figure III-13. Number of occurrences of different operating modes in electrolyser unit 1 and the associated energy consumptions during operating mode transitions.

The comparison of operation of both the electrolyser units based on the frequency of cold start, that is the transition from stop to running/production operating mode and warm start, which is the transition from standby operating mode to production mode are analysed and given in Figure III-14.

The difference in their operation is clearly evident here, with electrolyser unit 2 having majorly more warm start occurrences, while electrolyser unit 1 has more cold start occurrences in its annual operation under the given conditions. According to Matute et al. [99], the effect of cold starts on the stack life time of the electrolysers in terms of its degradation is not yet clear in literature.

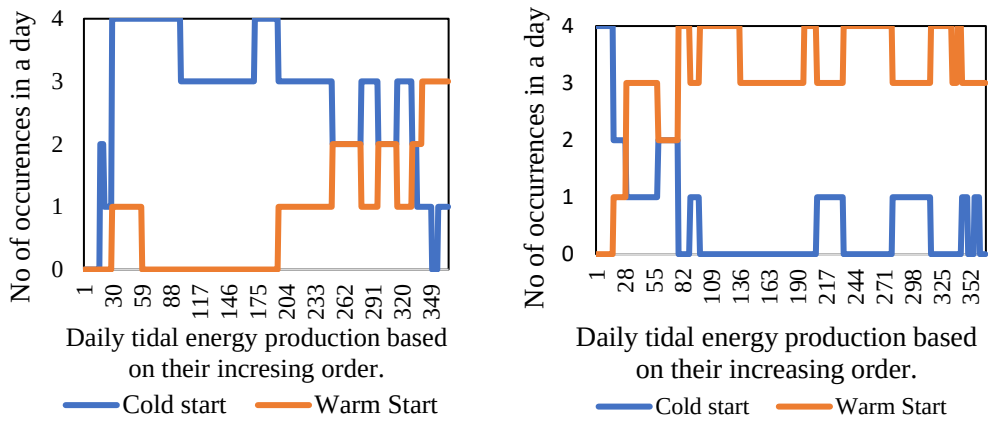

(a) (b)

Figure III-14. (a). Cold and warm start occurences of electrolyser unit 2. (b). electrolyser unit 1 in an annual context.

However, typically manufacturers advise to limit the number of cold starts to 5000 times in its system lifetime. Consequently, stack degradation is avoided by avoiding multiple transitions [99].

The annual system performance of the electrolyser units 1 and 2 like the hydrogen production, utilisation factor, carbon emission savings potential by green hydrogen production and other main indicators under the RBA are given in Table III-3. Overall, about 81 tonnes of green hydrogen can be produced over a year. Out of the available tidal energy, about 53.32% is utilised in electrolyser unit 2, 27.57% utilisation in electrolyser unit 1 and about 18.95% is used for export to the grid respectively. The potential carbon emission reductions related to the green hydrogen production is valorised with respect to the carbon intensity of the grey hydrogen production through steam methane reforming (SMR). The carbon intensity of grey hydrogen from SMR is estimated to be 8.9 $kgCO_2/kg$ of hydrogen [51][100]. In comparison with this value, the green hydrogen from tidal energy provides a carbon emission saving of 5.5 $kgCO_2/kg$ of hydrogen considering the average specific energy requirement of the hydrogen production.

The operating hours of the electrolyser units in Table III-3, refer to the sum of the production hours and standby operating mode hours. The zero production hours, as the name suggests refer to the stop and standby operating mode hours. An annual utilisation percentage factor of 47.32% of electrolyser unit 1 operation is utilised in production operating mode, with 28.65% in standby mode utilisation and 24.05% for stop mode operations. The corresponding values for electrolyser unit 2 are 71.5%, 25.77% and 3.77%, respectively. Thus, a relative increase of 51.31% utilisation of electrolyser unit 2 is observed, when compared to electrolyser unit 1 is observed. For the given PEM electrolyser, it takes a minimum of 15 minutes for the electrolyser to perform cold start with associated energy consumption too. This causes an approximate additional 248 hours cumulatively in a year where electrolyser unit 1 is down due to the cold start occurrences. The corresponding estimate for electrolyser unit 2 is 60 hours annually. The highest specific energy consumption range for electrolyser unit 1 is about 78.75 kWh/kg due to the lower energy availability to the same as it is expected due to the characteristic feature of PEM electrolysis. The electrolysers load factor defined as the ratio between the actual load with respect to the maximum possible loading capability is also analysed in addition to the utilisation factor for the respective electrolysers. As mentioned earlier, the study particularly on the degradation aspects of the electrolyser units were not under the scope of the given analysis, however, the effect of PEM electrolyser degradation, especially when coupled to a periodically cyclic RES like tidal stream energy compared to other RES systems would be interesting. It could be added as an extension of the analysis undertaken here.

Table III-3. Annual performance of electrolyser unit 1 and 2 when connected to the tidal stream energy system under RBA.

Annual system parameters	**Electrolyser unit 1**	**Electrolyser unit 2**		**Total**
Green hydrogen production (tonnes/year)	28.283	52.79		81.07
CO_2 emission savings by green H_2 production (tonnes CO_2e/year)	155.56	290.35		445.91
Energy consumption (GWh/year)	1.66	3.21		4.87
Energy consumption during operating mode transitions (MWh/year)	15.12	12.06		27.18
Load factor (%)	37.89	65.05		
Load factor (%) (considering 98% availability)	38.67	66.37		
Operating hours	6653.2	8521		15174
Zero production hours	4616	2588		7204
Production hours	4144	6263		10407
Stand-by operating mode hours	2509	2258		4767
Stop operating mode hours	2107	330		2437
Cold start occurrences	992	240		1232
Warm start occurrences	313	1131		1444
Utilisation factor (%) (excluding standby operating hours)	47.31	71.5		
Utilisation factor (%) (including standby operating hours)	75.95	97.27		
Full load operating hours	At 500 kW	At 500 kW	At 1000kW	
	1791	3221	847	5859
Full load hours utilisation factor (%)	20.44	36.77	9.6	
Specific energy consumption range (kWh/kg)	55.7-78.75	55.7-65.86		
Efficiency (HHV) (%)	50.03-70.74	59.8-70.74		

IV. Tidal-wind/grid- hydrogen system configuration

To avoid the underutilisation of electrolyser units, when connected to standalone TSES and also to avoid multiple transition of the operating modes caused by the inherently cyclic nature of tidal stream energy, it is proposed to integrate the TSES with other energy sources. In the given system configuration, wind energy system is proposed to be connected to the tidal-hydrogen system, allowing grid exchanges if required. However, power import from the grid is limited especially, if the grid is carbon intensive to aid the production of green hydrogen. This configuration helps to avoid the zero power production hours, ensures continuous operation due to the multiple RES source with magnitudes of power available above low power conditions required for the electrolyser units. Most importantly, they avoid the multiple operating mode transitions in the electrolysers ensuring reduced energy consumption during transitions, thereby reduction in transition operating cost and reduced degradation of the system in the long run.

For these two approaches are presented: firstly, the tidal energy is dispatched to the electrolyser units based on the rule base strategy given in Figure III-9. Later, the new energy source either wind/grid energy is dispatched to each electrolyser units. This step by step approach is useful in order to identify the source of energy fed to the electrolyser. It is estimated that the green hydrogen from wind energy provides a saving of 6.775 kgCO_2/kg of hydrogen which is 23.18% higher than the tidal powered green hydrogen carbon saving. Secondly, following the flowchart in Figure III-9, two or more power profiles are combined together for power dispatch. Following the first approach, again the power is dispatched to the electrolyser unit 2 initially ensuring peak power operations for the specified hours followed by the electrolyser unit 1. The strategy for power dispatch to electrolyser units, when another RES is connected is given in flowchart in Figure III-15 and III-16. Figure III-15 represents the power dispatch to the electrolyser unit 2 and then Figure III-16 represents the power dispatch to electrolyser unit 1. Wind power dispatch is considered for illustration here, however, any energy sources preferably RES would suit for the operation. The peak power operations of electrolyser unit 2 under the tidal energy dispatch is checked using the variable ‘count’. The input variables are P_{e2} and P_{w2}, that represents the power in the electrolyser unit 2 and the available wind power, respectively. The output variables are P_{e2total}, the total power fed to the electrolyser unit 2 from both wind and tidal sources, $P_{\mathrm{wr}}$is the remaining wind power available for electrolyser unit 1, P_{we2} is the wind power fed to the electrolyser unit 2 and P_{we2r} is the required power by the electrolyser unit 2. Similarly, for the Figure III-16, P_{e1} is the electrolyser unit 1 power fed from the tidal plant is the input variable along with P_{wr}. The result is P_{e1total}, that is total power in electrolyser unit 1, P_{wrr}, the remaining wind power available for export if present, P_{we1}, the wind power fed to electrolyser unit 2, and P_{we1r} is the required power by the electrolyser unit 1, respectively.

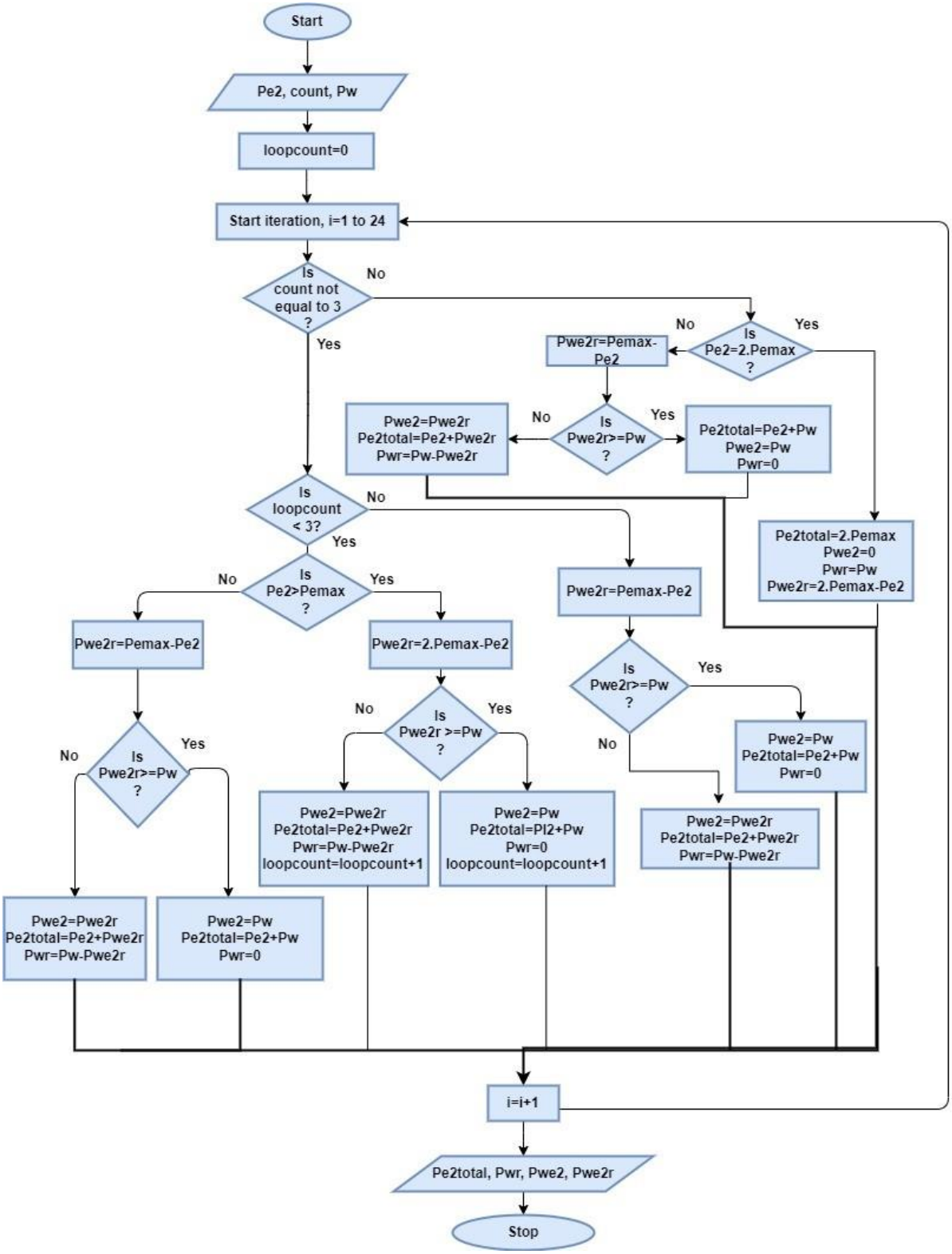

Figure III-15. Rule-based wind power dispatch to the electrolyser unit 2.

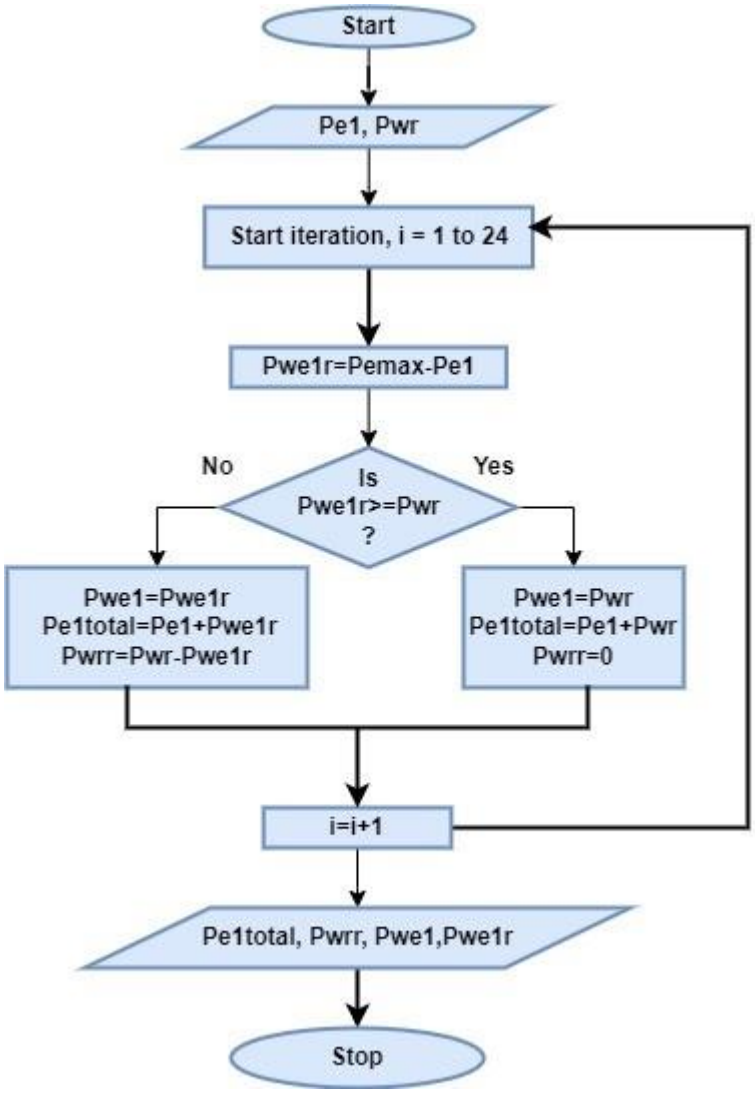

Figure III-16. Rule based wind power dispatch to electrolyser unit 1.

A comparative analysis with the rule-based approach in Figure III-9 and Figure III-15,16 under average tidal daily power profile and average wind daily power profiles given in Figure II-18 and II-30 was undertaken. It is possible to state that with the later approach the energy fed to the electrolyser unit 1 is increased by about 12.65% and the energy export to grid is decreased by about twice as that of former RBA. On further comparison with tidal-hydrogen alone configuration, it can be observed that about 7 hours of zero power availability period for electrolyser unit 2 and 15 hours of zero power availability period for electrolyser unit 1 in tidal-hydrogen configuration is reduced to absolutely no zero-power availability for electrolyser unit 2 and 9 hours of zero power availability to electrolyser unit 1. However, due to the specified rule of power dispatch priority to the electrolyser unit 2, makes electrolyser unit 1 underutilised in most of the cases.

V. Preliminary assessment of hydrogen production cost

A preliminary assessment of hydrogen production cost in case of a standalone tidal and tidal grid configuration is analysed initially to particularly analyse the hydrogen production cost variation based on different daily tidal profiles and the target hydrogen production.

The tidal current annual data of the year 2005 are treated here to obtain three reference daily profiles representing the highest, average, and the lowest cases, respectively. The corresponding hydrogen production is evaluated for both standalone tidal and tidal-grid-connected configurations. Here, the hydrogen production cost variation based on different daily tidal profiles and the target hydrogen production are particularly assessed.

The general system configuration is presented in Figure III-17 [75]. The simplified version of the proposed system developed under the framework of ITEG project [1], consists of a floating TSES with double rotor each electrically rated at 1 MW, a constrained local grid, a custom 500kW rated PEM electrolyser by ITM and another 500 kW PEM electrolyser by ELOGEN for onsite hydrogen production. It is to be noted that the capability of electrolyser unit 2 to operate at twice of its nominal capacity is not included here. An undersea transmission line is used to connect the offshore TSES to the electrolyser units situated onshore. A 4 MW of export limit and a 500 kW of import power limit is defined for the local electrical grid. Time steps of one hour for a 24-hour duration is considered for modelling.

The formulated algorithm for power dispatch is illustrated in Figure III-18 [75]. Tidal power is dedicated for hydrogen production and any excess if available is exported to the grid at a fixed price based on local electricity tariff. The power can be imported from the grid in case the available tidal power is insufficient for hydrogen production. The export electricity price and import electricity cost are considered to be the same in this analysis. The resultant electricity cost in the UK corresponding to a similar customer i.e., a small category non-domestic customers adding the climate change levy is about 0.146 €/kWh [101]. Thus, this value is considered as the fixed cost for both export to and import from the grid. It is worth noting that the gird import and export limit is considered in the power dispatch algorithm. When power import for the grid is considered, the resultant configuration is termed as *tidal-grid connected configuration* and the case with no power import is termed as *standalone tidal configuration*. As specified earlier, here too the tidal power dispatch to electrolyser unit 2 is given priority. In case if the available power exceeds the capability of the electrolyser unit 2, then it is fed to the electrolyser unit 1. TSES power converter losses and transmission losses are accounted for in the calculation of resultant tidal power. A transformer efficiency of 98% is considered for the analysis. The power loss is evaluated for a 600 m cable length with the associated resistance of 0.52 Ω/m. As mentioned in the Chapter I, the power dispatching strategy of the system

configuration is extracted from the rule-based approach proposed as per the project EMS. It is worth noting that the detailed power consumption of the auxiliaries is not included in this analysis.

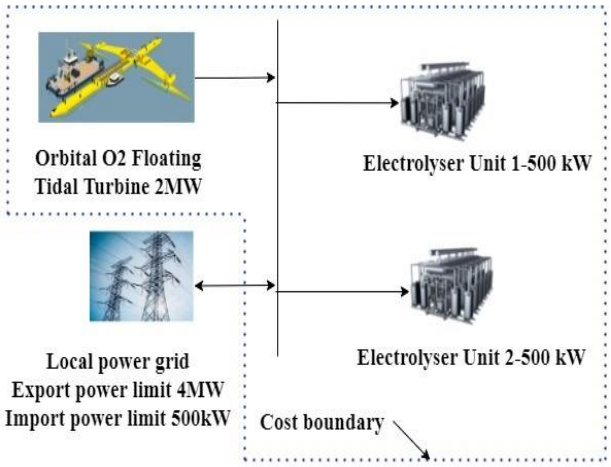

Figure III-17. General system configuration [75].

The cost boundary of the system analysis is presented in Figure III-17. It is considered that the tidal plant and both the electrolyser units are owned by the system operator with the exception for the grid connection as it is considered to be external. The life time of the system is assumed as the same as that of the chosen value in LCOE evaluation. The cost function to evaluate the system operating profit (SOP) is given in (III-5) [75].

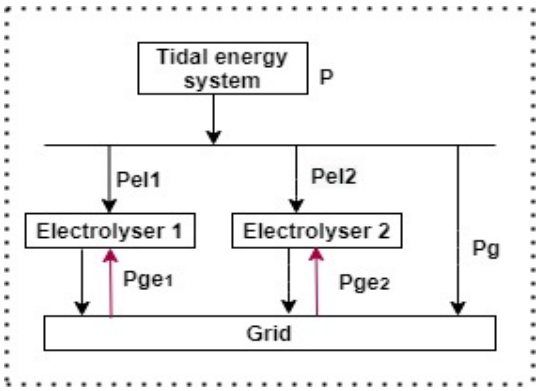

Figure III-18. Representation of power dispatching algorithm. The red arrow power flows are included when tidal-grid connected configuration is considered, otherwise it is omitted [75].

$$\mathrm{SOP} = (-\mathrm{GTEC} + \mathrm{HSR} \pm \mathrm{GEC}) \quad \text{(III-5)}$$

where, GTEC is the Generated Tidal Energy Cost in €, HSR is the Hydrogen Selling Revenue in €, GEC is the Grid Energy Cost/revenue based on import or export respectively in €. The sign of GEC is negative for import and it is positive for export energy flows. The individual cost components formulations are given below [75]:

$$\mathrm{GTEC} = c_{\mathrm{t}} \sum_{i=1}^{24} E_{t,i} \quad \text{(III-6)}$$

$$\mathrm{HSR} = \mathrm{HP} \sum_{i=1}^{24} H_{p,i} \quad \text{(III-7)}$$

$$\mathrm{GEC_{ex}} = c_{ex} \sum_{i=i}^{24} \left(E_{g,ex,i}\mathrm{te}\right) \quad \text{(III-8)}$$

$$\mathrm{GEC_{im}} = c_{im} \sum_{i=i}^{24} \left(E_{g,im,i}/\mathrm{te}\right) \quad \text{(III-9)}$$

where i is the number of hours in a day, E_t is the tidal energy produced during one hour of operations in kWh/h (power conversion and transmission losses are included in this value) and c_t is the tidal energy cost based on the selected LCOE in €/kWh. HP is the hydrogen production cost in €/kg, H_{p} is the hydrogen produced in kg/h, E_g is the energy exported/imported from the grid in kWh/h, te is the grid power transmission efficiency, $c_{\mathrm{ex}}, c_{\mathrm{im}}$ are the grid export/import electricity costs in €/kWh, respectively.

The available annual tidal current profiles are first analysed to estimate the daily hydrogen production capability under different conditions. The data are then classified in daily velocity profiles, and sampled by using the harmonic mean method. The tidal turbine model presented in Chapter II is used to obtain the daily available power profiles, the integration of which gives the daily energy production conditions. The results are classified to obtain the highest, lowest, and average hydrogen production potential of the system and the associated costs and revenue.

The lowest tidal daily profile is too low to generate enough energy for hydrogen production in accordance with the electrolyser units power constraints. The highest capabilities class involves the tidal velocity profiles able to rise the tidal turbines to full operations. The average energy capability is then evaluated for the remaining tidal velocity profiles.

Subsequently, the reference daily power profiles are used to evaluate the daily hydrogen production capabilities. For this purpose, the dispatching rules of Figure III-18 are used. It is to be noted that from this step, only the average and highest profiles are considered.

The TSES LCOE target value of 0.15 €/ kWh, considering an average capacity factor of 37% is used for this analysis [96]. The target tidal LCOE is used as the standard per unit tidal energy cost in this analysis because it is practical and is set based on the daily capacity factor, which is calculated as the ratio of daily

available energy to daily nominal energy. In particular, the highest profiles yield a plant capacity factor of about 65%, while the average profiles yield a value of about 39%. Then, two different scenarios considered. The first scenario is estimated using a constant tidal energy cost value of 0.15 €/kWh for all input profile conditions, based on the cost reduction potential applied in the SET-Plan LCOE target proposed in [96]. The second is obtained by combining the variation in tidal energy cost with the daily weighted capacity factor. Based on the literature estimates [94][96] and the resultant capacity factors, the tidal energy cost values for the highest and average daily profiles for the second scenario [75] are 0.11 €/kWh and 0.15 €/kWh, respectively.

The evaluated hydrogen production capabilities are given in Figure III-19 [75]. A capability of about 230 kgH_2/day and 300 kg H_2/day can be attained in the stand-alone tidal configuration in the case of the average and highest daily profiles respectively. The corresponding values including power import is estimated as 340 kgH_2 and 370 kgH_2, respectively. Further, a sensitivity analysis is performed to study the hydrogen cost variation under the considered configurations. Towards this, the daily target for hydrogen production is varied from 150 to 300 kg/day with a step of 50 kg/day. This range is based on the estimates of hydrogen production capabilities in both standalone tidal configuration and tidal-grid connected configuration. It is worth noting that the standalone tidal configuration directly solves the 150 kg/day and 200 kg/day cases.

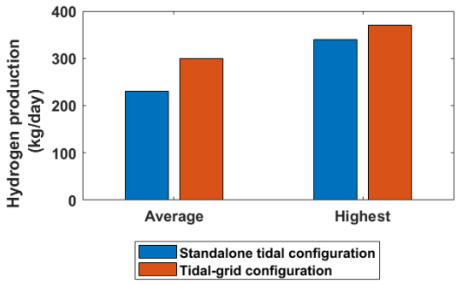

Figure III-19. Daily hydrogen production capabilities at different daily profiles.

The power import from the grid is solely considered in this case to ensure that the electrolysers start/stop, stand-by, and eventually transients in high-dynamic tidal power variations. In the event of surplus tidal power availability, power export to the grid is permitted due to grid constraints to achieve the planned production and optimise the system operations. However, achieving hydrogen production rates of 250 kg/day and 300 kg/day requires imported grid electricity. It was also shown that as hydrogen production increases, the cost gap between the highest and average circumstances narrows. This is mainly because once the hydrogen production target exceeds 200 kg/day, the contribution of the grid is not negligible. In fact,

contributions of the grid have a positive impact on the cost of hydrogen produced, primarily due to the low electricity costs of the grid.

Particularly, it was observed that the hydrogen production costs variate from about 10 to 13 €/kg in the case of average and highest profiles, respectively at 150 kg/day of hydrogen production, to about 9 to 11 €/kg in the case of 300 kg/day of hydrogen production. It is worth noting that, the considered LCOE value is chosen in accordance to the literature [75]. However, the value of 0.15 €/kg is calibrated for a plant capacity factor of 37%, that is consistent with average conditions but completely different for the highest profiles. Therefore, an accurate scenario will be obtained considering a variable LCOE [75], based on daily conditions capacity factor. Considering that in the case of the highest conditions, the capacity factor rise to about 65%, the corresponding LCOE was evaluated at 0.11 €/kWh.

With this idea in mind and to avoid costs overestimation, the new costs are evaluated for the hydrogen production considering at first instance a linear variable LCOE included in a range of between 0.11 €/kWh and 0.15 €/kWh for highest and average conditions, respectively. As expected, no changes were observed in the average conditions, confirming a cost reduction from about 11 €/kg to 9 €/kg in the case of hydrogen production from 150 kg/day to 300 kg/day, respectively. On the contrary, in the case of highest conditions, the lower LCOE value resulted in minor costs. Particularly, a hydrogen production cost varying from about 5 €/kg to 7 €/kg can be stated for 150 kg/day and 300 kg/day hydrogen production targets, respectively. The fact that in this case, the cost trend is increasing with hydrogen production is mainly because of the reduction of the tidal energy export to the grid. These results are in accordance with Matute et al. [99], that estimate the hydrogen production cost from relatively low-cost RES like solar and wind technologies in a range of 3.7 and 10.5 €/kg. The authors also observed a highly dependence of hydrogen cost on the operating hours of electrolysers. All these considerations are particularly interesting for the next chapter, where the system optimisation is considered.

VI. Conclusion

Concluding, it can be observed that different system configurations are analysed in this chapter. The annual tidal energy generation aspects are initially examined in detail with the associated system costs and revenue analysis. The respective losses in the TSES are estimated. The production hours, peak power production hours and zero production hours are analysed in an annual context. The TSES specific LCOE sensitivity analysis was performed with six different parameters. Further, profitability of the TSES when it is grid connected with capability to sell electricity to grid was analysed under different strike prices. It is estimated that the considered system is profitable for strike prices fixed in the range of 0.1-0.25 €/kWh under the given conditions. The tidal stream energy integration for green hydrogen production is analysed based on a rule-

based energy management strategy. The electrolyser units operating mode transitions and associated system parameters were estimated. Mainly, it is noticed that electrolyser unit 1 is subjected to cold start occurrences more than thrice compared to electrolyser unit 2. This corresponds to a cumulative cold start occurrences period of 10.3 days annually for electrolyser unit 1 and 2.5 days for electrolyser unit 2. Further, an increased load factor of 71.68% is observed for electrolyser unit 2 compared to electrolyser unit 1. The rule-based approach is further formulated for tidal-wind/grid-hydrogen system configuration and the corresponding results are presented for a reference daily average profile condition. In the RBA, only if the low power conditions can be satisfied the input power is dispatched to the electrolyser, even though it is acceptable from a technical perspective, this approach includes multiple operating mode transitions especially for electrolyser unit 1 even under a hybrid system configuration with multi-energy sources. The main advantage of RBA is that, it can ensure operation of the system without requiring an optimisation function or tools, thus reducing computational complexity. However, as observed for tidal-wind/grid-hydrogen configuration the designing complexity increases as the number of variables increase. As pointed out in Chapter II, it is important that the electrolysers work under a minimum power conditions in order to ensure safe electrolysis operation. Therefore, it is important to design an optimal energy management for the system based on different system constraints.

As for the analysis on hydrogen production cost to assess the cost variation based on different tidal daily profiles and target hydrogen production, a comparative-sensitivity analysis with different daily power profiles and tidal energy cost scenarios is performed.

The tidal energy cost values used in the fixed and variable scenarios are referred from the literature estimates. These values are particularly calibrated depending on the indicative system capacity factor evaluated at the average and highest daily operating conditions. This preliminary analysis highlights that the hydrogen cost is reduced by increasing the hydrogen daily production subjected to the capability of the system and constraints. This behaviour is mainly due to the grid integration in system operation. As expected, a certain gap in hydrogen production cost can be observed, when the average and highest conditions are considered. This gap is also reduced by increasing the daily hydrogen production. Finally, the best results are obtained considering the variable tidal energy cost scenario. This resulted mainly in the reduction of the overestimation of the tidal energy cost in the case of the high capacity factor operations. Hydrogen production from tidal energy can be made competitive in the long run considering the increased cost reduction potential of ocean energy technologies, especially in places with abundant tidal energy sources, with increase in the economies of scale, carbon credits economies, and the possible integration with the electrical grid or other RES to increase the operating hours of the electrolyser units. Hydrogen breakeven price point and thereby, the system operating revenue can be further improved with a suited system optimisation and management strategy.

The presented results are the object of a preliminary study based on an indicative tidal LCOE target value adapted to the given system under different scenarios. The given analysis is focused on the daily system operation and operating costs/revenues. A comprehensive cost analysis including the PEM electrolyser system costs, hydrogen compressor costs, storage costs, and other associated costs is to be done to effectively assess the system economics. In continuation of this work, further analysis is performed in Chapter IV to study the performance growth in the case of the TSES integration with other RES and grid-connected configurations for power balance and system optimisation. This, the proposed cost/revenue analysis of the hydrogen production by two different electrolyser units based on the energy management strategy of RBA and optimisation approach is described in detail in the following chapter.

Chapter IV

Optimal techno-enviro-economic analysis

The optimal techno-enviro-economic aspects of hydrogen production using polymer electrolyte membrane electrolysers (PEM) powered by a hybrid grid-connected tidal-wind energy system are presented in this chapter. Towards this end, the individual components models presented in Chapter II are used. A floating tidal energy system and onshore wind energy system with an external grid connection are considered for hydrogen production using PEM electrolysers. The framework of the proposed analysis is given in the Figure IV-1. The energy management strategies and the associated system economics for hydrogen production are initially analysed based on a rule-based approach (RBA) as presented in Chapter III. EMS optimisation is then implemented to analyse the technical and economical characteristics of the integrated system. Initially, a cost function is formulated for the RBA to evaluate the overall system profit. The objective function to maximise the operating profit under optimal system operation is then formulated, considering the variable energy costs, capital and maintenance expenditure, and real system constraints. The study aims to ensure optimal electrolyser operation with a goal to maximise hydrogen production and maximises the daily operating profit ensuring priority to green hydrogen production from tidal energy as far as possible. The optimisation of an electrolyser capable of working up to twice of its rated capacity for a limited duration is also included. Carbon credits and the associated economic benefits are also discussed [74]. A comprehensive cost analysis of the system is presented by comparing two different optimisation approaches based on fixed- variable cost and levelised cost factors, respectively. The use of single objective – constrained mixed integer genetic algorithm optimisation is presented.

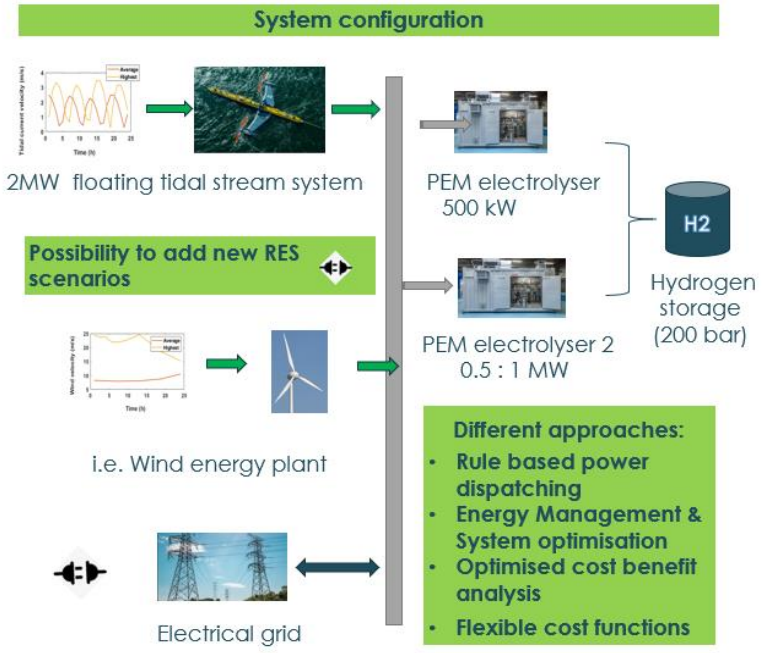

Figure IV-1. Framework of the proposed analysis.

Daily system operation based on average power profile conditions, annual system cost benefit analysis and the overall system performance in its lifetime are analysed in a subsequent manner. The chapter proceeds as follows: the system description is initially presented. The cost function formulation for the rule-based approach and optimisation approaches are then detailed. Further, the GA algorithm implementation aspects are introduced. Later, the different input data considerations for the hybrid system are presented in addition to the ones already described in the previous chapters. Results and discussion are then presented followed by conclusion.

I. System configuration and EMS approaches

A detailed version of the Figure III-17 in Chapter III is used for the analysis in this chapter. In addition to the components presented there, an onshore wind energy plant, and auxiliary units for hydrogen production like compressor, storage and balance of plant units are considered. The system comprises of a horizontal axis floating tidal stream energy converter rated at 2 MW and two PEM electrolyser units rated at 500kW units. Both units are located onshore for hydrogen production. This integrated system is owned by the plant operator. Additionally, an onshore wind energy system and grid connection with import/ export capabilities are considered in the configuration from external operators. The resultant hybrid system configuration is shown in Figure IV-2 [74]. Similar to the electrolyser unit 2 presented in the RBA analysis in Chapter III, the capability of operating at twice of the nominal rating is considered with peak power operations limited to a maximum of three hours a day. The 30-bar compressed hydrogen gas at the outlet of the electrolyser units is fed to a compressor. In the compressor, the hydrogen gas is compressed to 200 bar. The TSES is connected via a subsea transmission cable, called the umbilical cable to the electrolyser units situated onshore. The power converter devices used for interconnected are presented in the Figure IV-2.

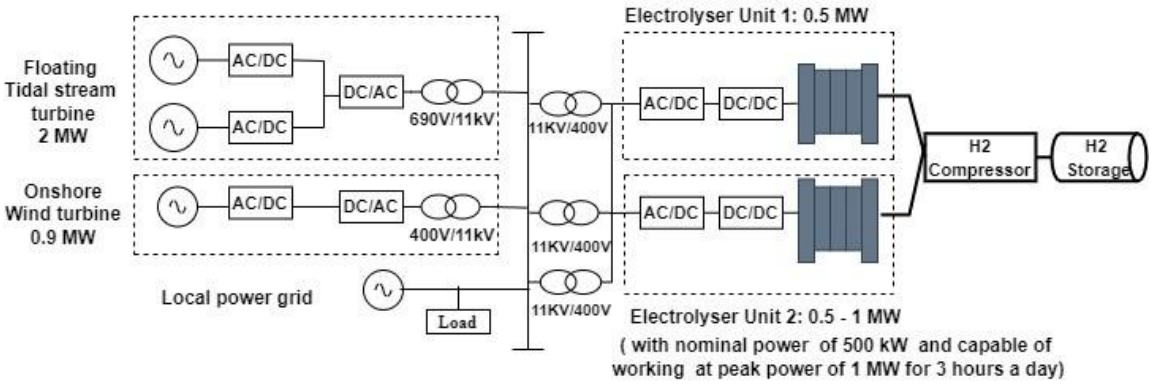

Figure IV-2. System configuration [74].

Following the analysis in Chapter III, the tidal energy is exported to the grid based on the day-ahead hourly electricity prices and the strike price under CfD scheme. The source of the import electricity from the grid is assumed to be carbon intensive. The EMS and system optimisation in this analysis are performed on pre-determined capacity of system components as per the project specifications. However, for an optimal operation, the consideration of optimal sizing is an important aspect. Interested readers can refer to the study by Lazar et al.[102], on the optimal sizing of marine current hydrogen based micro grid system.
Initially, the EMS strategy is divided into two steps. Step 1 includes the RBA described in Chapter III. As mentioned, it follows the available tidal power with respect to the operation of the electrolyser units, to estimate the green hydrogen production. Electricity import from the grid is not considered in this case, however tidal energy export to the grid is allowed. Next, a cost benefit analysis is carried out in terms of daily operational profit. The cost function formulation for the same is presented in the next section. Power dispatch from the wind and grid is not considered in this step as they are external providers.

Step 2 involves the system optimisation approach. The optimisation procedure is implemented in this step, with the objective to obtain the maximum daily profit conditions while ensuring optimal utilisation of electrolysers for maximising the hydrogen production respecting all the system constraints. Power import from the wind energy system (WES) and grid is permitted in this case to optimise the system operation, while maintaining the respective system constraints. Tidal powered hydrogen is given priority here. Further, power import from the grid is limited in order to ensure strictly 'green' hydrogen production. In the end, the obtained results are saved and compared with the RBA. The optimal power dispatch to the electrolyser units, optimal wind power dispatch, grid export/ import power flows are extracted for the cost benefit analysis. An integer decision variable implementation is presented to track the peak power operation of electrolyser unit 2.

The formulation of cost functions for the RBA and the optimised approach are described in the following. It is assumed that the subsea electrical infrastructure already exists in the system including the required transmission and distribution network. A whole system lifetime of 25 years is considered in this case.

An overview of the main input considerations, the variable parameters and the fixed parameters of the system are given in Table IV-1. In addition to the tidal and wind data profiles, various costs and prices are considered as input to the system. The system costs are estimated considering the daily fixed recovery costs on the capital expenditure (CapEx), while the maintenance expenditure, are added to the operating cost (OpEx) of the system components. The system components include tidal energy plant, two electrolyser units, hydrogen compression, storage and balance of plant units. Import electricity from the grid, wind energy import cost, and water consumption cost for hydrogen production are considered as variable operating costs. In addition, the electrolyser transition costs are included in the RBA approach as the

operating mode transitions of the electrolysers account for a cost due to its energy consumption. Further, specific energy consumption cost of the compressor is also included in the configuration. In order to quantify the cost and benefits of tidal energy export to the grid, a CfD scheme is used in this analysis.

The revenue factors considered are the hydrogen selling revenue and the revenue gained from tidal energy export to the grid. The carbon emission savings of green hydrogen production form the tidal and wind energy are evaluated in comparison with the conventional SMR process for grey hydrogen production. The carbon credits are then evaluated based on the carbon credit value in the UK. Similarly, the carbon credits of the tidal energy exported to the grid is also assessed as mentioned in Chapter III. As per the emission trading scheme of the UK government, a carbon emissions selling price up to 23.8 €/tonne of CO_2 can be gained [98]. This value is used as the reference in this analysis. Hence, the system revenue is evaluated considering carbon credits from green hydrogen production and tidal energy export to the grid, hydrogen selling revenue and the revenue from tidal energy export to the grid based on CfD scheme.

Table IV- 1. Overview of the system input considerations, the variable and fixed parameter considerations.

Input Data
Hourly tidal current data Hourly wind speed data Fixed wind electricity price Hourly market reference price for grid electricity export Fixed price for grid electricity import Carbon saving benefits of tidal energy exported to grid Carbon saving benefit of green hydrogen from tidal and wind plant Strike price of tidal stream energy under contract for difference scheme (CfD) Transmission efficiency Electrolyser water consumption cost Compressor specific energy consumption
Variable parameters
Tidal energy consumption by the electrolysers Wind energy consumption by the electrolysers Tidal electricity export to grid --> Grid energy export revenue Payment from owner based on hourly strike price and market reference price Grid electricity import --> Grid electricity import cost Variable to track peak power switching of electrolyser unit 2
Fixed parameters
Sizing of the components Capital costs Maintenance cost Lifetime of the plant

As mentioned earlier, two approaches are considered in order to evaluate cost and benefits optimisation of the system. They are as follows:

i) The fixed cost factor (FC) method.

ii) The levelised cost (LC) factor method.

The fixed cost factor method includes the CapEx and OpEx of the system components. The levelised costs method includes the levelised cost of the system components, particularly the levelised cost of energy (LCOE) for the floating tidal stream energy system and the levelised cost of hydrogen (LCOH) for the associated hydrogen production and storage related units such as electrolysers, compressor, storage and balance of plant units.

Step 1 – Rule based approach

The cost function for estimating the daily system variable operating profit is initially formulated considering the above aspects. The daily system variable operating profit is referred as DSOP (€/day) and is calculated as presented in equation (IV-1) [74]:

$$\mathrm{DSOP}_{\mathrm{variable}} = \sum_{i=1}^{24}\sum_{n=1}^{2}\left(-\mathrm{EWC}_{i,n} - \mathrm{ETC}_{i,n} - \mathrm{PTC}_{i} + \mathrm{TCS}_{i} + \mathrm{HSR}_{i,n} + \mathrm{HCS}_{i,n} + \mathrm{GER}_{i}\right) \quad \text{(IV-1)}$$

where, *i* is the time counter in hours, *n* is the number of electrolysers, EWC is the electrolyser water consumption cost (€/h), ETC is the electrolyser transition costs (€/h), PTC is the payment from tidal generator to the intermediate company based on contract for difference scheme (€/h), TCS is the tidal energy carbon savings (€/h), HSR is the hydrogen selling revenue (€/h), HCS is the hydrogen carbon savings revenue (€/h), and GER is the grid energy export revenue (€/h).

The individual cost and revenue components formulation are detailed below:

$$\mathrm{EWC} = \mathrm{WC}\, H_p \quad \text{(IV-2)}$$

$$\mathrm{ETC} = \begin{cases} \mathrm{tcf_{stb}} \text{ for transition } 2 \rightarrow 2 \\ \mathrm{tcf_{start,stop}} \text{ for transition } 0 \rightarrow 1, 2 \rightarrow 0 \\ 0, \text{otherwise} \end{cases} \quad \text{(IV-3)}$$

where, $\mathrm{tcf_{stb}} = E_{\mathrm{stb}} c_{\mathrm{t},w}$ (IV-4)

$\mathrm{tcf_{start,stop}} = E_{\mathrm{start,stop}} c_{t,w}$ (IV-5)

$$\mathrm{PTC} = \begin{cases} (c_{\mathrm{ex}} - \mathrm{sp_{CfD}})E_g \mathrm{te} \text{ for } \mathrm{sp_{CfD}} < c_{\mathrm{ex}} \\ 0, \text{ otherwise} \end{cases} \quad \text{(IV-6)}$$

$$\mathrm{TCS} = E_g \mathrm{cs}_t \quad \text{(IV-7)}$$

$$\mathrm{HSR} = \mathrm{HSP}\, H_p \quad \text{(IV-8)}$$

$$\mathrm{HCS} = \%H_{p_s} H_p \mathrm{HCP}_s \quad \text{(IV-9)}$$

$$\mathrm{GER} = \begin{cases} c_{\mathrm{ex}} E_g \mathrm{te} \text{ for } \mathrm{sp_{CfD}} < c_{\mathrm{ex}} \\ \mathrm{sp_{CfD}} E_g \mathrm{te} \text{ otherwise} \end{cases} \quad \text{(IV-10)}$$

where, WC is the water consumption (€/kg), H_p is the hydrogen production (kg/h), tcf is the transition cost factor (€/h), stb is the standby mode, start, stop is the start and stop operating mode. The modes 0, 1 and 2 in equation (IV-3) represents stop, running and standby operating modes, respectively c.f. Figure II-10 in Chapter II. E_{stb} is the electricity consumption of standby (kWh), $c_{t,w}$ is the electricty cost (€/kWh), $E_{\mathrm{start,stop}}$ is the electricity consumption of start and stop operating modes transition considering the time delay (kWh), c_{ex} is the day ahead grid electricity price for export (€/kWh), $\mathrm{sp_{CfD}}$ is the fixed strike price for contract for difference scheme (€/kWh), E_g is the tidal energy exported to grid (kWh), te is the power transmission efficiency, cs_t is the carbon credits of tidal energy (€/kWh), HSP is the hydrogen selling price (€/kg), $\%H_{p_s}$ is the percentage factor of hydrogen production by different source, the computation of which is given in equation below:

$$\%H_{p_{s,n}} = (E_{s,n}/E_n)H_{p_n} \quad \text{(IV-11)}$$

where, E_s (kWh) is the electrolyser electricity consumption by source, while E_n (kWh) is the total electricity consumption of the electrolyser, $\mathrm{HCP_s}$ is the hydrogen carbon saving price by source (€/kg).

a) Profit evaluation with fixed cost factor method.

The cumulative daily system operating profit, SOP (€/day) can thus be evaluated using the equation (IV-12) [74]:

$$\mathrm{SOP} = \mathrm{DSOP_{variable}}\text{-}\mathrm{CCF}_{t,\mathrm{e}_n,C,H_2S,\mathrm{BoP}}\text{-}\mathrm{MCF}_{t,\mathrm{e}_n,C,H_2S,\mathrm{BoP}} \quad \text{(IV-12)}$$

where, CCF is the fixed CapEx factor (€/day), MCF is the fixed maintenance cost factor (€/day) of the tidal energy plant (t), electrolysers (e_n), compressor (C), hydrogen storage equipment ($\mathrm{H_2S}$),) and remaining balance of the plant (BoP) units like power supply unit of electrolysers, piping, heat exchangers etc.

$$\mathrm{CCF} = \mathrm{CapEx}/(365 \times \mathrm{Lifetime}) \quad \text{(IV-13)}$$

$$\mathrm{MCF} = \mathrm{Maintenance\ Cost}/(365) \quad \text{(IV-14)}$$

b) Profit evaluation with levelised cost factor method.

In this approach, the CapEx and maintenance costs are replaced by the levelised costs for the tidal energy plant (TEC), electrolyser units (EC), compression and storage (CSC) and BoP (BPC). SOP evaluation in (IV-12) is then modified as follows [74]:

$$\mathrm{SOP} = \sum_{i=1}^{24} \sum_{n=1}^{2} \left(\mathrm{DSOP}_{\mathrm{variable}} - \mathrm{TEC}_i - \mathrm{EC}_{i,n} - \mathrm{CSC}_i - \mathrm{BPC}_i\right) \quad \text{(IV-15)}$$

where,

$$\mathrm{TEC} = \mathrm{LCOE}_t \times E_t \quad \text{(IV-16)}$$

$$\mathrm{EC} = \mathrm{LCOH} \times H_p \quad \text{(IV-17)}$$

$$\mathrm{CC} = \mathrm{LCOMP} \times H_p \quad \text{(IV-18)}$$

$$\mathrm{HSC} = \mathrm{LH2S} \times H_p \quad \text{(IV-19)}$$

$$\mathrm{BPC} = \mathrm{LBOP} \times H_p \quad \text{(IV-20)}$$

where, LCOE_t is the levelised cost of energy of the tidal stream plant (€/kWh), E_t is tidal energy generation (kWh), LCOH is the levelised cost of hydrogen for electrolyser units (€/kg), H_p is the hydrogen production (kg/h), LCOMP is the compression cost factor (€/kg), LH2S is the hydrogen storage cost factor (€/kg), and LBOP is the balance of plant cost factor (€/kg).

Step 2 – Optimisation

The optimisation step is formulated as a mixed integer nonlinear problem. The optimisation cost function for evaluating the daily system variable operating profit is given by equation (IV-21) [74]:

$$\max f(X) = \sum_{i=1}^{24} \sum_{n=1}^{2} \left(-\mathrm{WEC}_i - \mathrm{EWC_{i,n}} - \mathrm{PTC}_i - \mathrm{GIC}_{i,n} + \mathrm{TCS}_i + \mathrm{HSR}_{i,n} + \mathrm{HCS}_{i,n} + \mathrm{GER}_i\right) \quad \text{(IV-21)}$$

Where, $f(X) = \mathrm{DSOP}_{\mathrm{variable}}$ and X is the decision variable.

It is worth noting that the cost components listed in (IV-2), (IV-6)- (IV-10) holds the same in the optimisation step too. In addition to it, as wind and grid import are considered in the optimisation steps, two

other cost components for wind energy consumption cost, WEC (€/h) and grid electricity imports cost, GIC (€/h) are introduced in (IV-22) and (IV-23).

$$\mathrm{WEC} = E_w c_w \tag{IV-22}$$

$$\mathrm{GIC} = c_{\mathrm{im}} E_{\mathrm{im}} \mathrm{te} \tag{IV-23}$$

where, E_w is the wind energy (kWh), c_w is the wind electricity cost (€/kWh), c_{im} is the grid electricity import cost (€/kWh), E_{im} (kWh) is the electricity import from the grid.

The inequality and equality constraints for the optimisation approach are formulated as follows:

Inequality constraints

$$0 \leq X_{\mathrm{te1}} + X_{\mathrm{te2}} \leq P_{\mathrm{t1}} \tag{IV-24}$$

$$\text{with, } P_{\mathrm{t1}} = \begin{cases} P_t \text{ for } P_t \leq 2P_{\mathrm{emax}} \\ 2P_{\mathrm{emax}} \text{ for all other cases} \end{cases} \tag{IV-25}$$

$$0 \leq X_{\mathrm{te2}} \leq P_{\mathrm{emax}} \tag{IV-26}$$

$$0 \leq X_{\mathrm{we1}} + X_{\mathrm{we2}} \leq P_w \tag{IV-27}$$

$$0 \leq X_{\mathrm{g1}} + X_{\mathrm{g1}} \leq P_{\mathrm{gimmax}} \tag{IV-28}$$

$$P_{\mathrm{emin}} \leq P_{\mathrm{e1}} \leq P_{\mathrm{emax}} \tag{IV-29}$$

$$P_{\mathrm{emin}} \leq P_{\mathrm{e2}} \leq (2(P_{\mathrm{emax}}/X_{\mathrm{count}})) \tag{IV-30}$$

$$\text{with, } X_{\mathrm{count}} = \begin{cases} 1 \text{ for } 200\% \text{ of rated capacity} \\ 2 \text{ for all other cases} \end{cases} \tag{IV-31}$$

$$\sum_{i=1}^{24} X_{\mathrm{count,i}} \geq \text{maximum summation of occurences} \tag{IV-32}$$

Equality constraints

$$P_g = P_t - (X_{\mathrm{te1}} + X_{\mathrm{te2}}) \tag{IV-33}$$

$$P_{\mathrm{e2}} = X_{\mathrm{te2}} + X_{\mathrm{we2}} + X_{\mathrm{g2}} \tag{IV-34}$$

$$P_{\mathrm{e1}} = X_{\mathrm{te1}} + X_{\mathrm{we1}} + X_{\mathrm{g1}} \tag{IV-35}$$

where, $X_{\mathrm{te1}}, X_{\mathrm{tel2}}$ characterise the hourly tidal power dispatch to electrolyser unit 1 and 2, respectively. $X_{\mathrm{we1}}, X_{\mathrm{we2}}$ are wind power dispatch to electrolyser 1 and 2, respectively. $X_{\mathrm{g1}}, X_{\mathrm{g2}}$ are the grid power import to electrolyser 1 and 2, respectively, X_{count} is the integer decision variable to track electrolyser unit 2 peak power operation limitations, $P_{\mathrm{emin}}, P_{\mathrm{emax}}$ are the minimum and maximum power condition requirement of

electrolysers, P_t, P_w, P_g represents tidal, wind and grid export powers, respectively. Finally, the parameter P_{gimmax} is the maximum allowable limit of grid import power.

The inequality constraints (IV-30), ensure that the operating modes of the electrolyser units are always in running mode ensuring safe electrolysis operation and reduced unit degradation rate. Equations (IV-30) - (IV-32) monitors and enables the capability of electrolyser unit 2 to work at twice of its rated power for a maximum of three hours per day. It is realised as follows: an integer decision variable is used in this case where the integer 1 is assigned for X_{count} for operation up to 1 MW, while the integer 2 is assigned for operation up to 500 kW. Further (IV-32) ensures that the maximum summation of occurrences in X_{count} array to be greater or equal to the maximum occurrence value to limit peak power working for a maximum of three hours. Similar to step 1, the overall system profit is then evaluated both with the FC and LC approaches.

II. Genetic algorithm implementation strategy

A probabilistic evolutionary genetic algorithm (GA), is selected as optimisation method as it is the most popular, robust to use, and it is proved to be efficient for the control strategies design [103]. This tool is particularly used to solve the nonlinear mixed integer problems. The algorithm is formulated as a mixed integer program as the integer decision variables are used to monitor the capability of the peak power operation of electrolyser unit 2.

A brief description of GA is given below for understanding the overall functionality of the algorithm.

This nature inspired probabilistic algorithm was introduced by John Holland in the early 1970s and developed by D.E. Goldberg [56]. It is a derivative free meta-heuristic tool for global search [104]. This method can deal with multivariable, non-smooth, non-continuous, non-differentiable, and non-linear constrained optimisation problem [104]. As for other similar evolutionary algorithm, the basic mechanisms in GA is population generation, selection and crossover [56]. The main advantages of GA highlighted in the literature is that GAs search for a population of parallel points and not with a single point. It requires only the objective function and the corresponding fitness levels that influence the directions of the search. It uses probabilistic transition rules and not deterministic ones as is in the case of RBA [2]. Hybrid genetic algorithm have demonstrated significant success in difficult real word application areas [3].

The general working of GA is as follows: GA creates random initial values called population unless otherwise particularly specified. A feasible population is also automatically generated, when linear and integer constraints are given. The fitness of each member of the population called the chromosome is then

evaluated. Based on the fitness, they are rearranged. Members with the best fitness values are generally chosen as parents to create a child by a 'crossover' process. Members with the best fitness levels are called elite and they are usually directly passed to the next population. Children, i.e., the next population are produced from 'parents' either by mutation or cross over in a population. Thus, a set of new population is created. Mutation occurs when changes are applied to a single parent. The execution of the algorithm stops when a stopping criterion is reached. The stopping criteria could be number of prescribed generations, monitoring of constraint tolerance value etc. More details of GA methods are available in papers [5][62][105]. The probability of finding the optimal solution increases with the definition of a feasible initial population. Based on the above aspects, optimisation program based on genetic algorithm is implemented. The flowchart of the GA implemented for the corresponding problem is presented in Figure IV-3. The GA is implemented in the MATLAB R2019a. A total of 168 decision variables are considered for the optimisation program, as shown in Table IV-2.

Table IV-2. Decision variables considered for the optimisation program.

Decision variable parameters	Number of decision variables
Tidal power disptach to electrolyser 1	24
Tidal power dispatch to electrolyser 2	24
Wind power dispatch to electrolyser 1	24
Wind power dispatch to electrolyser 2	24
Grid power dispatch to electrolyser 1	24
Grid power dispatch to electrolyser 2	24
Integer variable to track electrolyser 2 operating at twice its nominal capacity	24

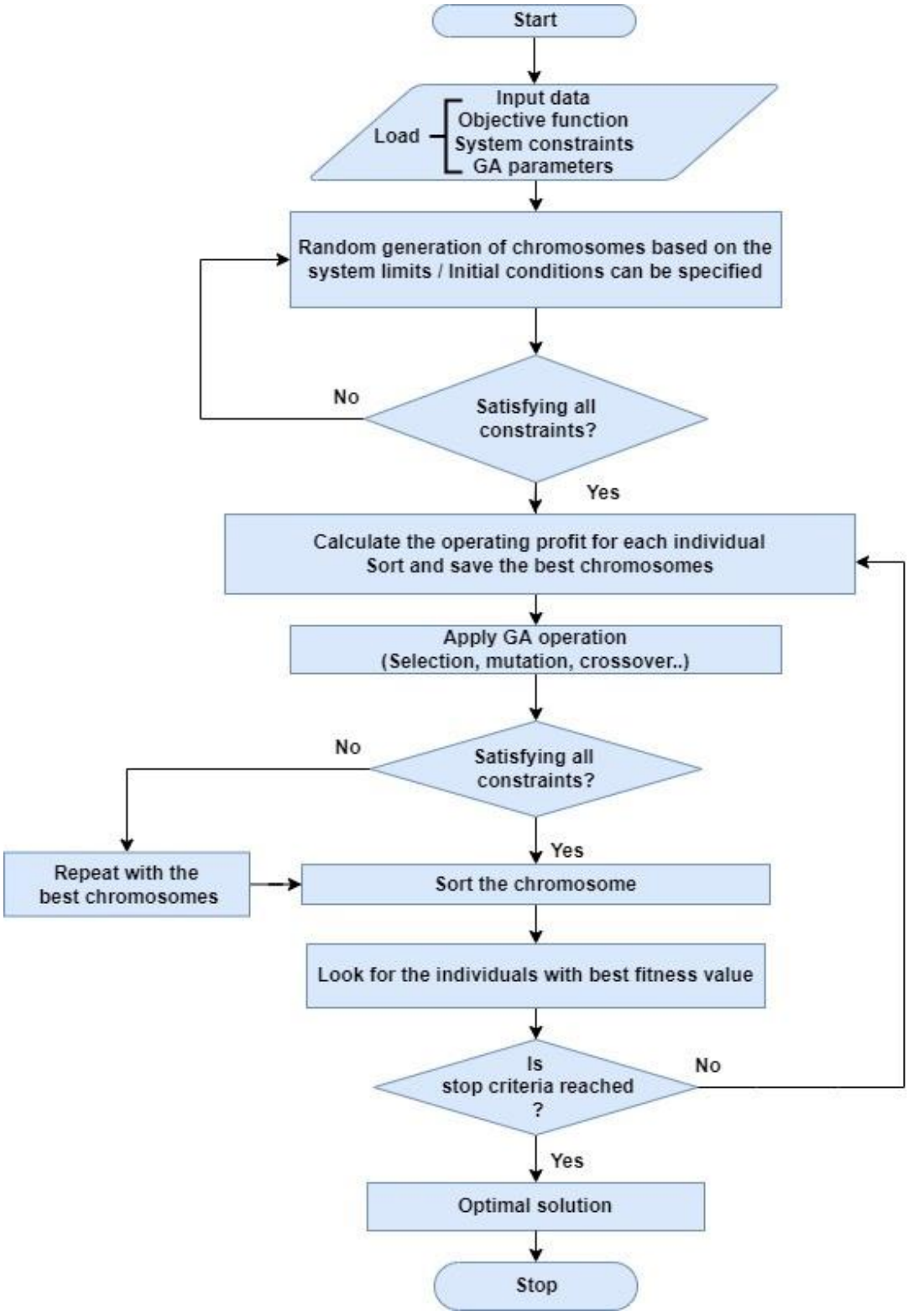

Figure IV-3. Flowchart of the genetic algorithm.

III. Input data considerations

The input data considered for the optimisation are presented here. Initially, according to the harmonic mean approach detailed in Chapter II, a single set of average daily tidal current and wind current profiles are used to analyse the integrated system performance under average daily operating conditions. Subsequently, 27 different daily tidal current profiles data-set, composed by the most recurrent daily tidal current profiles in Chapter II are used to analyse the annual performance of the system. This approach enables reducing the computational time for the algorithm and considers system evaluation in an annual context. In fact, the real operating conditions are more aligned [74] in this approach than in the harmonic mean approach. The power converter efficiencies and transmission losses are accounted for as mentioned in Chapter II. The input data consideration in the fixed costs approach includes the CapEx and OpEx of the system components like floating tidal stream energy plant, electrolyser units, compressor unit, storage units and balance of plant unit. In the levelised cost approach, the levelised cost evaluations of the same system components are used. Particularly, the LCOE of the floating tidal stream plant evaluated from the given CapEx and OpEx in Table III-2 in Chapter III are used. For the hydrogen production units, the corresponding CapEx and OpEx are used for levelised cost evaluation in addition to other parameter as detailed below.

The estimates of the CapEx and OpEx data of the system component available in literature are summed in Table IV-3 [74]. Best case scenario referring to the low-cost estimate and worst-case scenario for the high cost estimate are added to have a comprehensive grasp on the costs. The high cost estimate is typically referred to the standalone systems in the current market scenario; while, the low-cost estimates represent the system costs in scaled up scenarios like economies of scale or improved learning rate scenarios. For example, the high cost estimate of the tidal stream plant is an indicative cost for a standalone system at an early stage of development. The low-cost estimate of the tidal stream energy plant is at an improved learning rate with an indicative scale up to 500 MW. In the case of PEM electrolyser units, the highest and lowest cost estimates available in literature are used [108]. However, it is to be noted that cost is very subjective and the deviation is greater in different regions of the world, even when exchange rates are applied based on other external factors involved like local conditions.

Similar cost data are used for both the electrolyser units as both have the same power rating. The ideal gas equation based formula in [106], is used to estimate the CapEx of the compressor. The maximum possible hydrogen flow rate involving both the electrolyser units is evaluated to be around 452 kgH_2/day. Considering this aspect, the power rating of the compressor considering a single stage of compression from 30 bar to 200 bar is estimated to be 20.41kW. The value is increased to 21.48 kW, considering a motor efficiency of 95%. The capital expenditure on the compressor based on the estimated power rating is then

evaluated using the equation developed by Nextant and National Research Council (NRC) in the US, respectively [106]. The outcome from the Nextant relation is given as the highest estimate and the outcome from the NRC is used as the lowest estimate. In addition, a 1.57 kWh/kg of specific energy requirement for compressor OpEx is estimated as in Chapter II [86]. It is assumed that the compressor is always connected to the grid in the proposed analysis. Further, care is taken to include the compressor energy consumption to the total OpEx of the compressor in addition to its fixed maintenance expenditure. It is considered that the hydrogen is stored on a daily basis and it is dispensed the next day. Considering the maximum hydrogen production of the electrolyser units for a day, the CapEx of the storage is estimated for a pressurised storage tank at 200 bar. The cost data for the same are obtained from B. D James et al. [107] which is used as the high cost estimate.

Table IV-3. Different cost estimates of the system components [74].

		High cost estimates	Low cost estimates
Floating tidal stream energy plant (twin rotor)	CapEx (M€/MW)	4.89[75]	1.758 [108]
	OpEx (M€/MW/year)	0.05 [3]	0.035 [108]
Electrolyser units	CapEx (€/kW)	1830 [106]	340 [106]
	OpEx (€/kW/year)	40 [106]	10 [106]
Hydrogen compressor at 200 bar	CapEx (€/kW-compressor power rating)	6887[106]	2545 [106]
	OpEx (€/kW/year)	344 [109]	127 [109]
High pressure hydrogen storage tank	CapEx (€/kgH_2-day)	800 [2][107]	380 [107].
Balance of plant	CapEx (€/kW-electrolysis)	45 [106]	8.4 [107]

The cost of the storage tank at an indicative scaling of capacity up to 500000 systems/year is used as the low cost estimate [107]. The BoP components such as the piping, heat exchanges cost estimates in high and low cost are taken from [106]. For a fair comparison, the ratio of high and low-cost estimate of the electrolyser units is also used to evaluate the BoP units high and low-cost estimates. This is selected in particular to represent the possibility of decrease in the cost for the BoP units as highlighted by James et al. [107].

Further, the standard formula to evaluate the LCOE [110], is implemented to calculate the levelised costs. In analogy with the analysis in Chapter III, the LCOE tool by CFI [93] is used to obtain the levelised costs. For the tidal LCOE estimation, an O&M growth rate of 4% and a discount rate of 10% per year, are considered. The corresponding values of floating tidal stream energy LCOE estimation for a life time of 25 years under the highest and lowest-cost estimates are presented in Table IV-4 [74].

In a similar way, the LCOH values of the electrolyser units are evaluated based on the CapEx and OpEx values in Table IV-3 [74]. It is to be kept in mind that as the electrolyser unit 2 has higher capability to produce hydrogen compared to the electrolyser unit 1 because of its ability for peak power switching; this factor affects the final LCOH estimation. As a first step, the LCOH cost factors are estimated considering an availability factor of 0.98 under full load operations throughout. Similar to the tidal LCOE estimation, an O&M growth rate of 4% and discount rates of 8%, which is typical of such systems are used for the LCOH cost factor estimation. Throughout the study, the overall system components lifetime is assumed as 25 years including the electrolyser units, compression, storage and balance of plant units. The typical stack lifetime of a PEM electrolyser is assumed as about 60,000 hours [48]. The stack replacement cost is also considered in the evaluation of the overall electrolyser units CapEx considerations. The International Council of Clean Transport (ICCT) estimates the stack replacement cost of an PEM electrolyser is assumed as the 50% of the initial CapEx [106]. Thus, the stack of the electrolyser units is replaced after about every seven years, assuming continuous operation of the electrolyser units. The LCOH of the electrolyser units are then estimated considering the above aspects. In the same way, the levelised cost of the compressor unit, the storage unit and the BoP are estimated considering the related CapEx and OpEx, including the energy consumption for 25 years system life time; with O& M growth rate of 4 % and discount rate of 8%. The final estimated levelised cost factors are logged in the Table IV-4 [74].

As per International Renewable Energy Agency, with an average capacity factor of 0.4, the wind electricity cost is estimated as 0.052 €/kWh, which is the weighted average LCOE estimate [111]. The wind energy cost is considered to be paid to an external provider, which can be facilitated through a typical power purchase agreement (PPA) for contract duration of 25 years.

The LCOH quantities from the renewable and low carbon electricity across the globe is evaluated in the wide range of about 2-20 €/kg [36][52]. The typical electrolytic hydrogen production cost with low carbon

electricity at an approximate cost of 0.09 €/kWh is about 6 €/kg in Europe [9][36][112]. The electrolytic hydrogen production cost with complete proportion of wind energy in the given context is approximately 3.5 €/kg [74]. The similar estimate with tidal energy considering the SET target LCOE value of 0.15 €/kWh, is about 12 €/kg. Additionally, 11.34 €/kg was the green hydrogen median price in the Europe based on the year 2020 estimates [106]. Considering the above aspects, 12€/kg is chosen as the base hydrogen selling price for the analysis of the given system configuration. This value is selected to be not far from the European average price. In addition, as mentioned earlier, it is to be kept in mind that in the given system configuration, tidal energy is considered as the priority energy source. Wind energy and grid electricity is used only in the EMS for improved electrolyser performance and for power balancing aspects. The tidal energy strike price for export is chosen as 0.251 €/kWh, as this value represents the updated value in literature for tidal stream energy system [3] and also according to the report by EU commission [96]. The hourly electricity prices in the UK on a day ahead basis is fixed as the reference price point for electricity export to the grid as represented in Figure III-6 in Chapter III [97].

Table IV-4. Levelised costs estimation based on Table IV-3 values [74].

	High cost estimates	Low cost estimates
Floating tidal stream energy plant, LCOE (€/kWh)	0.22	0.09
Electrolyser 1 unit, LCOH cost factor (€ kg)	2.95	0.57
Electrolyser 2 unit, LCOH cost factor (€/kg)	2.68	0.52
Compressor cost factor (€/kg)	0.59	0.49
Short term hydrogen storage (€/kg)	0.24	0.12
Balance of plant cost factor (€/kg)	0.03	negligible

As the grid is carbon intensive, to justify the production of renewable (green) hydrogen by not compromising the safety of electrolyser operation, the minimum power requirement of both the electrolyser units, which is 10% of their nominal capacity is specified as the maximum limit for the grid import power [74]. A preliminary simulation considering these aspects estimated a yearly grid import electricity consumption of

approximately 876 MWh at its maximum limit. The resultant electricity cost in the UK for the grid import of about 0.146 €/kWh as mentioned in Chapter III is considered corresponding to a similar customer including the climate change levy [101].
The water consumption cost for electrolytic hydrogen production which is usually considered a minor cost in literature is fixed at 0.017 €/kgH_2. This value corresponds to the use of desalinated sea water for hydrogen production that is typically the highest cost estimate scenario [39].

As mentioned earlier, the carbon intensity of SMR processed grey hydrogen and typical grid electricity are selected as the reference points to quantify the carbon credits. The UK grid carbon intensity of 209 gCO_{2e}/kWh, which is a medium estimate is specified [91]. The carbon intensive case of the UK grid with 45% of complete renewable in its energy mix amounting to a 63% of low carbon energy sources is used [74]. In contrast, the Orkney Islands have 100% renewable based electricity with about 86% renewable energy in its overall energy mix. The case of the UK is selected to present the carbon credits revenue streams and implications of the system based on the estimates.

Carbon credits evaluation on the tidal energy export to the grid is already estimated in Chapter III. Similarly, the CO_2 saving potential of wind energy consumption is calculated from the reference grid value. As specified earlier, the UK grid electricity carbon intensity is taken as the reference case. As per the Intergovernmental Panel on Climate Change (IPCC) report, the average CO_2 emissions associated with the wind energy production is about 11 gCO_{2e}/kWh [113]. Consequently, the amount of CO_2 emissions savings per unit of wind electricity consumption would be 198 gCO_{2e}/kWh. The CO_2 emission reduction related to tidal and wind powered green hydrogen production is also quantified by referring to the reference carbon intensity of the conventional SMR processed grey hydrogen i.e., 8.9 kgCO_2/kgH_2 [51][100]. Thus, the electrolytic green hydrogen production from tidal and wind energy provides a CO_2 emission saving of 5.5 and 6.775 kgCO_2/kgH_2, respectively considering a specific energy consumption for hydrogen production of 55 kWh/kg with respect to carbon intensity of grey hydrogen. Carbon credits for green hydrogen production from tidal energy source and wind energy source resulted in 0.1309 €/kgCO_2 and 0.161 €/kgCO_2, respectively. The selling price of hydrogen, CfD strike price for tidal energy export to the grid, and the import electricity cost from the grid is considered to be fixed under all scenarios as they are based on contracts.

IV. Results and discussion

Initially, the system performance under the average daily tidal current profile condition is analysed. Subsequently, the system performance in annual profile conditions is analysed, which is followed by overall system lifetime performance analysis.

The system operation under the average daily profile conditions is analysed in the following. Here, the EMS approach with the RBA is analysed first followed by the two optimisation approaches. It can be observed that the recurrent start/stop and stand-by operating modes of the electrolyser units observed in RBA are avoided in the optimisation step. In the RBA, as it follows the power dispatch based on tidal power follow-up strategy with priorities for electrolyser unit 2 compared to electrolyser unit 1, the electrolysers are subjected to recurrent operating mode transitions particularly due to the cyclic nature of tidal power with flood and ebb tides [74]. The resultant operating modes in the electrolyser unit 1 in RBA and in the optimisation approach are presented in Figure IV-4 [74]. In the case of RBA, negligible power is exported to the grid as illustrated by the results in chapter III. However, in the optimisation approach, by importing power from the wind energy plant and if necessary with the aid of grid export/ import, the power flows are balanced. This in turn smoothens the operating mode of electrolysers and recurrent start, stop and stand-by operating modes are avoided.

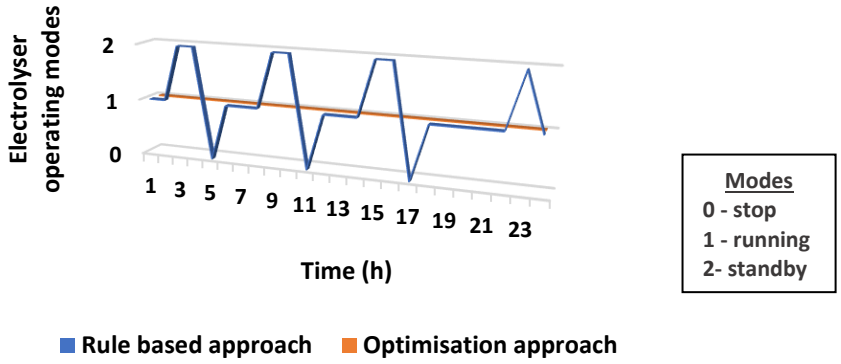

Figure. IV-4. Transitionary operation of electrolyser unit 1 in RBA and optimisation approach in reference average daily profiles [74].

To illustrate this working principle, the working power profiles of the electrolyser units, the wind power dispatch, and the grid export/import power dispatch under the RBA , FC and LC optimisation approaches are represented in Figure IV-5a-b-c [74]. Additionally, the variable to track the peak power operations of

the electrolyser unit 2 is included in the figures. A detailed look at the power profiles of the FC and LC optimisation methods highlight that both the approaches converge to similar result patterns. In addition, it is observable that the wind energy consumption improves the utilisation of electrolysers especially for the electrolyser unit 1 (represented by the green line). Simultaneously, the peak power operation of the electrolyser unit 2 at 1MW is limited in the optimisation approach to ensure maximum profit scenario considering the tidal energy export to the grid, at the same time to balance the operation of both the electrolyser units.

Referring to Figure III-7 in Chapter III, it can be observed that the majority of the occurrences fall within the daily tidal power generation of about 11-21 MWh. The average profile condition analysed before was for a cumulative tidal stream energy generation of about 9.95 MWh/day. Hence, it is necessary to evaluate the tidal power profile in an annual context to learn the overall system behaviour in realistic conditions under the most occurring daily profiles. As the wind energy system is an external provider, a common and single set of reference daily wind current profile in average profile conditions is used to simulate the annual performance of the integrated energy system. Similarly, the hourly prices for the electricity export to the grid are also considered to be the same throughout the year.

Subsequently, the annual system performance, especially the optimal power profiles of the electrolyser units, the grid export/import energy flows, wind energy dispatch, are represented in Figure IV-6 a-b-c [74] for RBA, FC and LC optimisation approaches, respectively. Furthermore, total number of peak powers switching hours of electrolyser unit 2 are also added. In analogy to the daily system operation in average profile conditions, the electrolyser unit 1 operation (represented by the yellow line) is balanced. Considerable difference in the number of hours of operation of peak power switching of electrolyser unit 2 is observed in the RBA and the optimisation approaches (represented by green lines) as in the optimisation approach peak power switching is applied for the maximised profit case including the consideration of grid export revenue, where as in RBA power follow-up strategy is employed, which causes imbalance in the operation of the electrolyser units.

It is possible to state that, although quite different strategies (green line) are chosen for peak power switching in both the optimisation approaches, a well distributed power dispatching is applied to both the electrolyser units. This behaviour, in addition to the highest hydrogen production are the main outcomes of the optimisation.

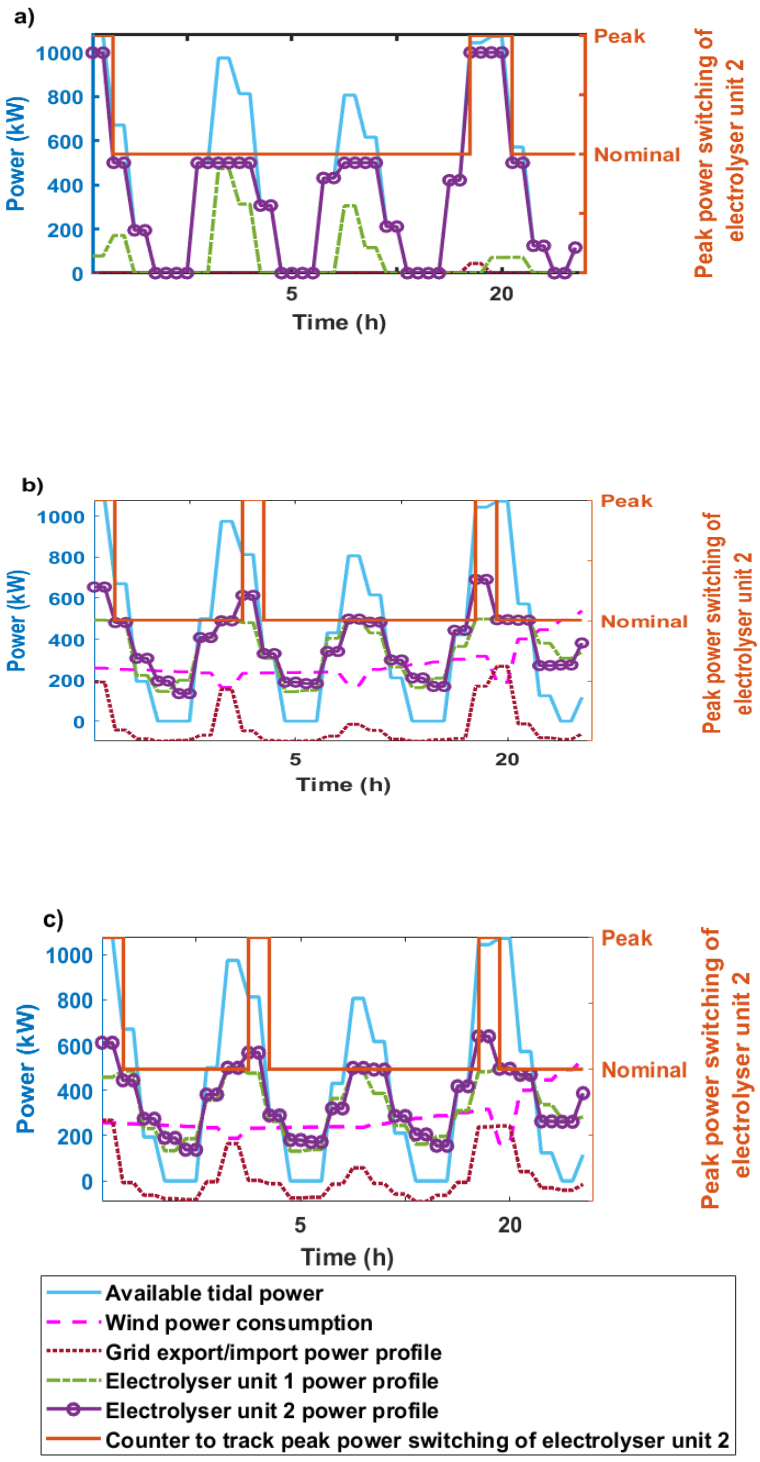

Figure IV-5. Optimal profiles of the PEM electrolyser units, wind power dispatch and optimal grid electricity import/export power dispatch. (a) Rule based approach, (b) FC optimisation method, (c) LC optimisation approach [74].

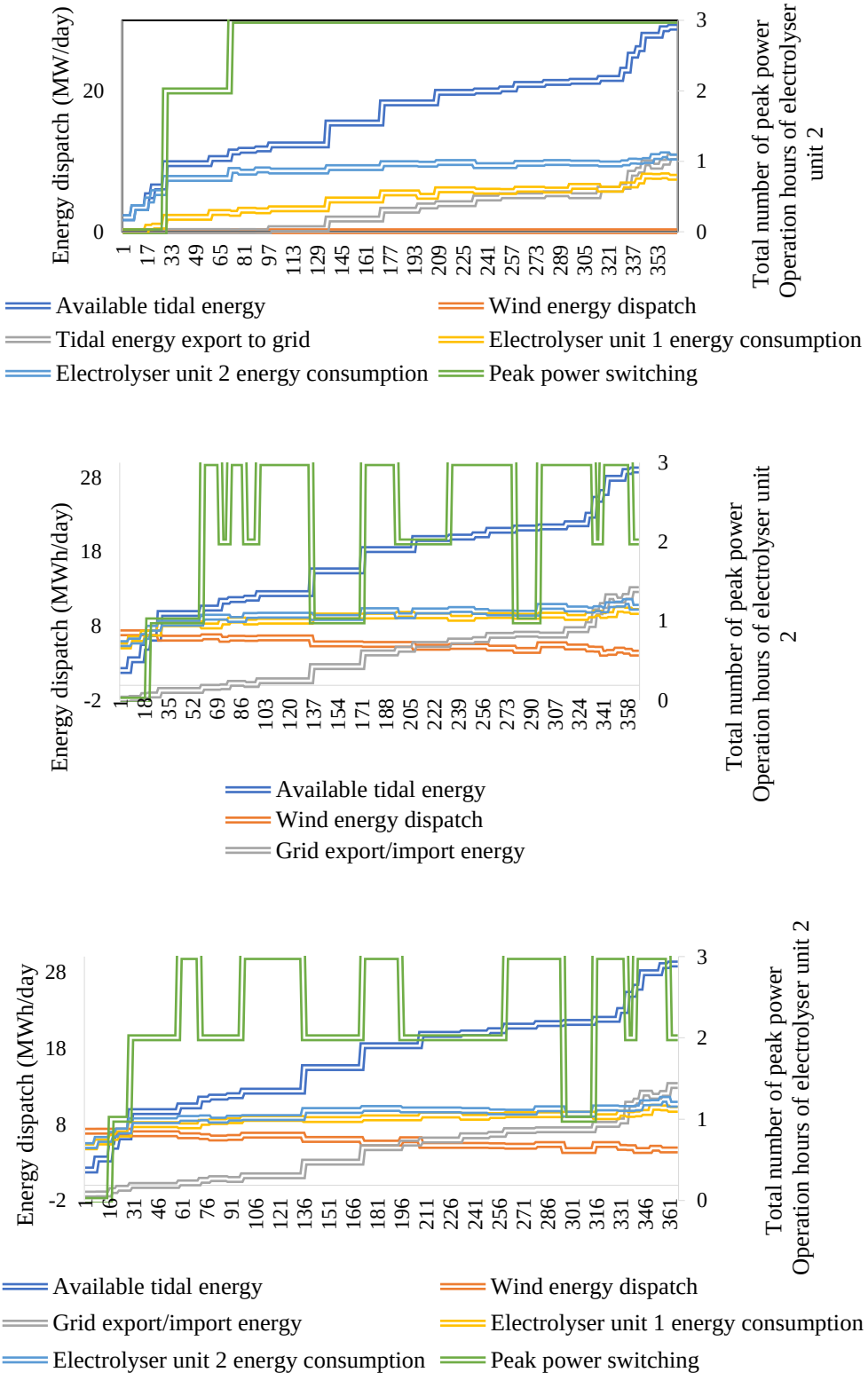

Figure IV-6. Optimal power profiles of the electrolyser units, wind energy dispatch and grid electricity import/ export power flows in annual context: (a). Rule based approach, (b). FC optimisation method, (c). LC optimisation.

The correlation between the hydrogen production resulting from the different energy sources, the corresponding tidal energy export to the grid in comparison with the associated tidal energy generation for the chosen 27 daily tidal profile conditions under both the optimisation based EMS approaches is illustrated in Figure IV-7 [74]. It can be observed that, with the increase in available tidal energy the corresponding hydrogen production from the wind and grid energy is reduced. This is desirable due to the decreased hydrogen production from external sources and increased hydrogen production from tidal energy. Again, similar to the average profile condition operation, the converging pattern of both the FC and LC optimisation approaches appear to be the same. Figure IV-8 compares the overall optimisation approach results with that of the RBA, in terms of overall daily hydrogen production and the corresponding tidal energy export to the grid under the same 27 different input tidal power profile conditions [74]. This has been extracted considering the sum of hydrogen production from tidal, wind, and grid energy, respectively as given in Figure IV-7. It can be observed that the green hydrogen production in the RBA is about 35 - 305 kg/day based on the quantity of tidal energy generation. In the optimisation approaches, these values are translated to about a hydrogen production of 190-360 kg/day.

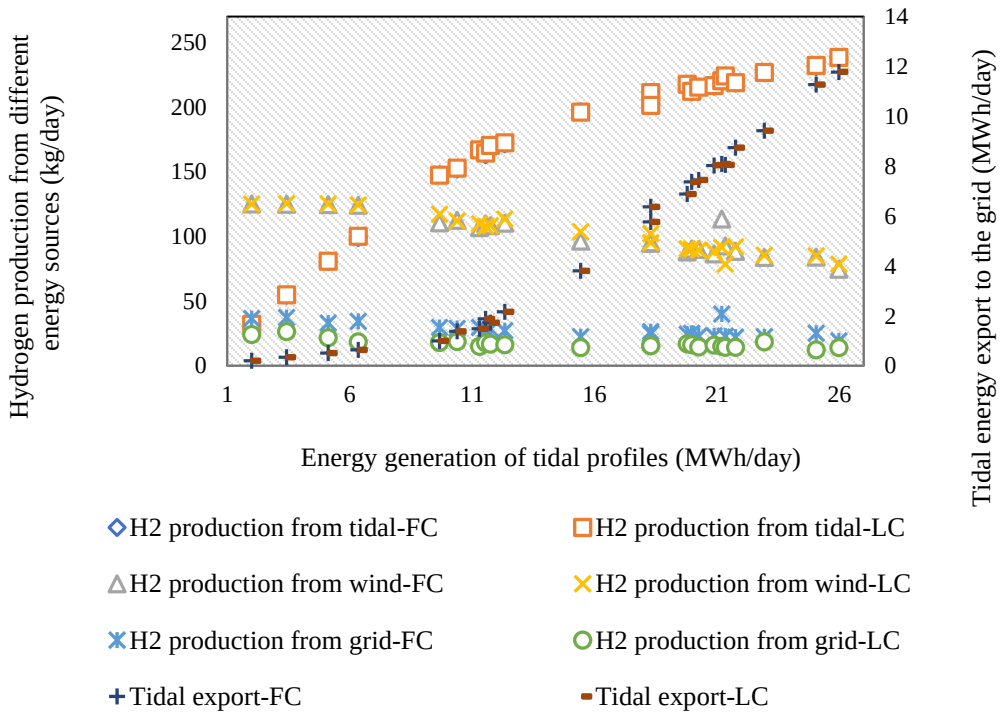

Figure IV-7. The variation of optimal hydrogen production from different RES and grid, the resultant optimal tidal energy export to the grid with respect to the available tidal energy generation [74].

Besides, in the optimisation approaches relatively higher contributions in the tidal energy export to the grid is observed. The cause of which is majorly due to the objective to maximise profit, particularly the CfD policies and the electricity costs.

The overall key performance indicator parameters like the percentage of tidal energy production share for hydrogen production ,grid export, the total hydrogen production, the share of hydrogen production from different energy sources, the CO_2 emission savings from green hydrogen production, grid export, the utilisation and the load factors of electrolysers corresponding to annual hydrogen production, under the RBA and optimisation approaches are summarised in Table IV-5 [74]. The utilisation factor specified here signifies the hours, the electrolyser units are in operation, whereas the load factor signifies the loading that the electrolyser units are subjected to compared to its overall capacity. It is observable that a 2.67% of increase in hydrogen production is seen under the LC optimisation approach in comparison with the FC optimisation approach. The relatively minor difference is related to the difference in cost estimations. On the other hand, a considerably higher difference of approximately 37% of increase is considered for green hydrogen production in optimisation approach compared to the RBA results. In fact, the annual hydrogen production is improved from 81 tonnes to about 110 tonnes. Clearly, same patterns are observable in CO_2 emission savings. It is evident that the energy export to the grid is more beneficial for overall CO_2 emission savings.

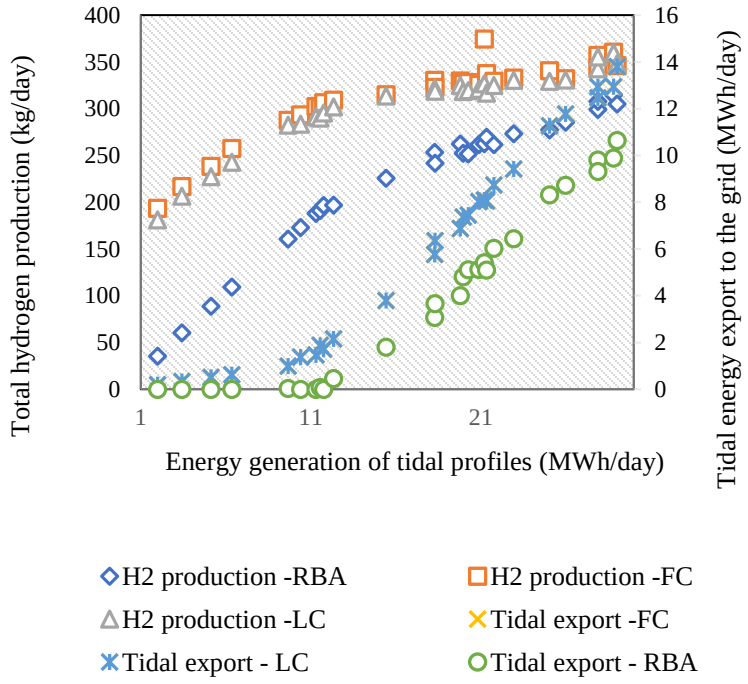

Figure IV-8. The relation between of total hydrogen production, tidal energy export to the grid under both RBA and the optimisation approaches [74].

Similarly, it is evaluated that 29.9-31.5% of the available tidal stream energy is exported to the grid annually in the optimisation approaches. Besides the evident flexibility related to the tidal energy strike price and the market grid electricity export, these quantities are to be anticipated because of the cyclic nature of tidal stream energy. The flood tidal current conditions generate energy higher than the capability of both the electrolysers causing the power to be sold to the grid irrespective of the prices. The overall grid import of the electricity for green hydrogen share is approximately 5 and 8%, for both FC and LC optimisation approaches, respectively. The corresponding percentage factor of electrolyser unit utilisation of both the electrolysers under the RBA and optimisation approaches is proposed in Table IV-5. In general, it can be concluded that the optimisation approaches are more environmentally friendly due to the reduced use of import electricity from the grid and increased CO_2 emission savings.

Table IV-5. Performance indicators of the system in an annual context under both the RBA and optimisation approaches [74].

	FC optimisation	LC optimisation	RBA
Annual energy generation from tidal plant (GWh/year)	6.02	6.02	6.02
Tidal energy for hydrogen production (%)	64.3	67.7	80.89
Tidal energy for grid export (%)	29.9	31.5	18.95
Hydrogen production (tonnes/ year)	108.7	111.6	81
Tidal energy export to the grid (GWh/year)	1.8	1.9	1.14
Hydrogen production share from different energy sources (%)			
Hydrogen production by tidal energy	60	62	100
Hydrogen production by wind energy	32	33	0
Hydrogen production by grid energy	8	5	0
Carbon emission savings ($MTCO_2e$ /year)			
CO_2 savings from green hydrogen production	581.4	615.4	445.91
CO_2 savings from tidal energy export	342.2	367.9	220.74
Total CO_2 savings	923.6	983.36	667
Load factor of the electrolyser units (%)			
Electrolyser unit 1	70.6	71.9	37.9
Electrolyser unit 2	66.6	68.7	65
Utilisation factor of the electrolyser units (%)			
Electrolyser unit 1	98	98	47.31*
Electrolyser unit 2	98	98	71.5*
Daily hydrogen production range (kg/day)			
Hydrogen production	193-360	181-360	36-305

*Utilisation factor excluding the standby operating hours.

Following the previous examination, the performance of the system during its lifetime is analysed for a comprehensive understanding.

A key aspect to remember in FC estimation is the inclusion of the electrolyser stack replacement costs, while considering the CapEx estimation of the system. Moreover, in accordance with the results of the comparative analysis, the FC and LC optimisation approaches has showed that the resultant costs in the LC optimisation approach are overestimated in comparison to the corresponding FC optimisation cost estimation.

The resulting percentages consisting of the different cost of the components of the system for both the FC and LC optimisation approaches are represented in the Figure IV-9a and 9b, respectively [74]. Similar behaviour with respect to the cost distribution can be observed. It is estimated that the floating tidal energy plant constitutes the major share in the costs, comprising approximately 53%. Clearly, an evident reason is the dimension of the tidal stream plant which is of 2 MW, whereas the other system components in the likes of the electrolyser units are rated at about 500 kW each. Wind energy consumption for hydrogen production, costs associated with the electrolyser units, import electricity from the grid electricity import and the associated costs of the compressor constitute the other major cost components in the decreasing order of its share. The hydrogen storage cost, the electrolyser water consumption cost, payment by the operator to the contract supplier (referred as the intermediate company) based on the tidal energy CfD scheme and the balance of plant costs are relatively lower constituting approximately a cumulative 5% of the total costs.

Similarly, the system revenue components percentage share is estimated in an annual context and it is represented in Figure IV-10 [74]. As anticipated, the revenue from the green hydrogen sale and the tidal stream energy export revenue constitute the higher share comprising almost equal values under both the approaches. Further, the carbon offsetting credits from the green hydrogen production and tidal energy export comprises approximately about 0.5 and about 1%, under both FC and LC approaches, respectively. This is because of the relatively low carbon price in Europe currently. In fact, this particular revenue stream is expected to increase in magnitude in the coming years, thanks to the increased aspiration to achieve net zero emission targets.

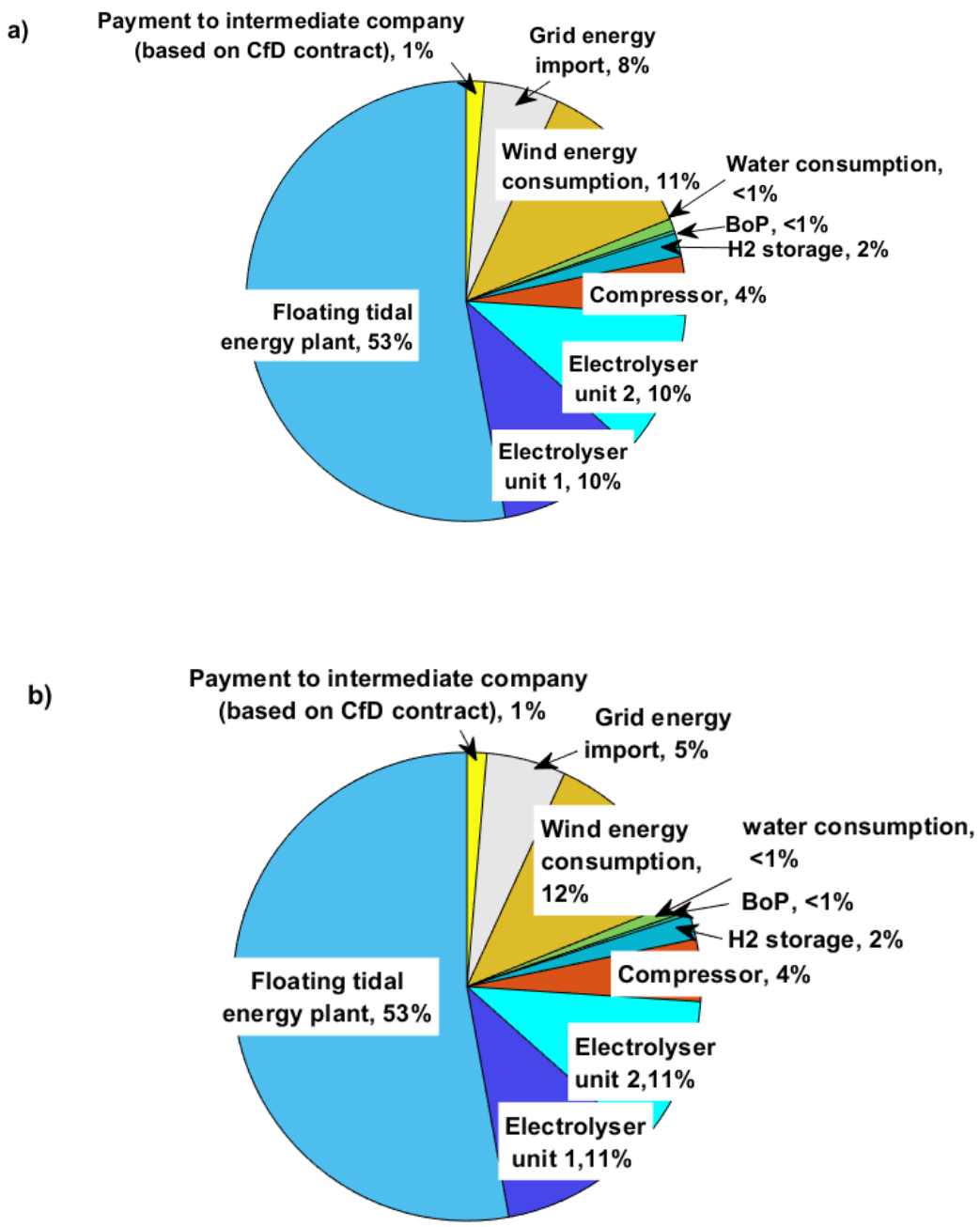

Figure IV-9. Cost breakdown (a) FC optimisation approach, (b) LC optimisation approach [74].

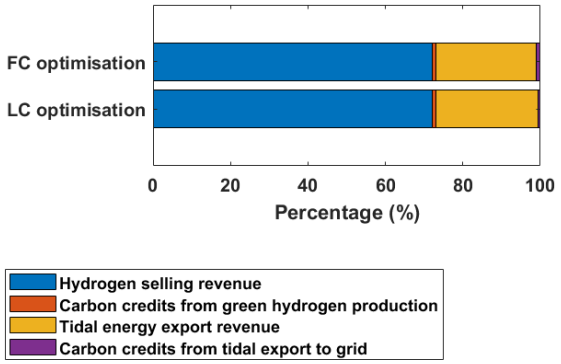

Figure IV-10. Percentage estimation of system revenues [74].

Lastly, the profit obtained in the case of the hybrid grid connected tidal-wind- hydrogen system in EMS base on optimisation approach and the tidal -hydrogen system under the EMS based on RBA is compared. A 41.5% of profit increase is observed through the optimisation approach in hybrid system compared to the RBA system configuration. Besides, the transition costs associated with the operating mode transitions in the electrolyser in RBA which constitute approximately 0.82% of the total costs are completely avoided in the optimisation approach, with the exception of limited start/stop conditions, if necessary. Further, this corresponds to an annual energy saving of 27.2 MWh which is the energy losses due to transition and standby operations in RBA.

It can be observed that the FC optimisation approach is fairly straightforward for estimation of costs. Nonetheless, suitable costs like stack replacement costs, and other risk factors are to be included for accurate estimation. Besides, it is important to evaluate the discounted cash flows to obtain a realistic estimation of operating profit especially at the end of the system lifetime. On the other hand, even though better results are obtained in the case of the LC approach by a low margin, it is important to possess a higher beforehand system operations knowledge to accurately evaluate the levelised cost factors.

To check the accuracy of the results obtained and to verify the performance of the algorithm under different parameters, multiple runs of the GA optimisation program are performed. In fact, one of the drawbacks of GA is that the global optima of the solutions cannot be ensured in the process [61], however near optimal solutions of complicated multi objective mixed integer optimisation problems are obtained. The resulting objective function values and the corresponding parameters are given in Figure IV-11. In general, it is observed that the results improve, when the number of generations are increased which in turn causes an increase in execution time. In contrast, the increase in number of populations does not necessarily increase

the solution optimality. However, it is possible to state that the objective function values do not vary significantly. The test is performed on a machine with 4 GB installed RAM and an Intel(R) Core (TM) i3-5005U CPU @ 2.00GHz processor. It is to be noted that the execution time naturally improves with improved processor capacity. To improve the results obtained and to ensure global optimal solutions are obtained, the GA performance under various system parameters are analysed and chosen appropriately.

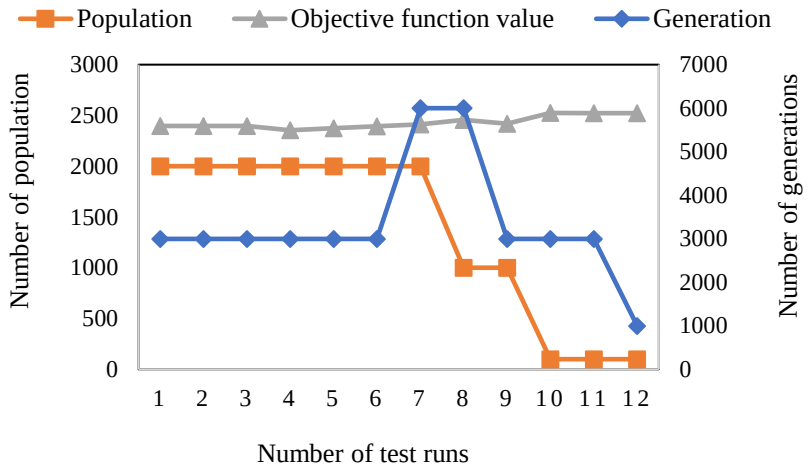

Figure IV-11. Trial runs of GA algorithm for robustness evaluation.

Further, as it is the inherent characteristic of stochastic programming, GA with random initial conditions has the tendency to converge to local optima especially when there is increasing complexity in the objective function. GA requires relatively fewer iterations to converge to a better solution, when improved heuristics based-initial conditions are applied [114]. Additionally, it is to be noted that effectiveness of an optimisation algorithm often lies on the model characteristics and so it is always advisable to select a suitable optimisation method and to try multiple trials and combinations before identifying a near optimal/global solution. For example, in one instance of the analysis interior point algorithm (IPM) was used. However, as IPM does not support mixed integer programming in MATLAB it was shelved later. But the initial tests run on IPM have shown that improved results are obtained which then when used in GA as the initial conditions improved the results significantly. Interested readers are directed to the article in the likes of [115] by Grefenstette for guidance for optimal selection of parameters.

The cost function formulated in this chapter is flexible. Costs can be easily modified based on different optimisation objectives. For instance, if the optimisation is to be carried under the conditions mentioned in the above section but with a daily target for hydrogen production, an equality constraint can be added as below in the equation (IV-36):

$$\sum_{i=1}^{24} \left(H_{\mathrm{p1},i} + H_{\mathrm{p2},i}\right) = H_t \tag{IV-36}$$

where, i is the time in hours, H_t is the target hydrogen demand in kg/day, $H_{\mathrm{p1},i}$ and $H_{\mathrm{p2,i}}$ is the hourly hydrogen production of electrolyser units 1 and 2. GA has restrictions on implementing nonlinear equality constraints, however this can be handled by including equality constraints with tolerance value or a separate general penalty function. Similarly, objectives to maximise electrolyser efficiency such as the reducing its specific energy consumption, minimise power dispatch from certain energy sources etc., could be realised using the given system models.

For future improvement, another solution could be the multi-objective optimisation consideration. In this case, the optimisation cost function is adapted as a multi-objective optimisation problem. As the objective of maximising system profit and priority for hydrogen production from tidal are two conflicting objectives; in this case, multi-objective algorithm could be used as parallel method to solve the problem. One of the advantages of multi objective optimisation is the opportunity to choose from multiple solutions based on preference of the user, rather than a single one obtained under single objective optimisation. Interested readers can refer [116], where the authors have compared the working of an offshore wind farm O&M optimisation having three different objectives using a multiple single objective optimisation approach, by assigning weighted sum for different objective function based on its priority and as multi-objective optimisation approach using genetic algorithm.

Authors in [27], concluded that including an additional energy vector like hydrogen production is desirable to improve the economic aspects of the overall system compared to the traditional tidal energy export to the grid alone revenue because of the currently higher HSPs. Ferguson. [2], studied a supply driven scenario powered by wind/tidal system for hydrogen production using curtailed and non- curtailed power. It is estimated that non-curtailed tidal power reduced the hydrogen production cost as the utilisation of the electrolyser was increased, whereas for the curtailed power even though electricity cost was low, the capital cost of the electrolysers influenced the hydrogen production cost as the load factor was too low. This justifies the approach taken in this analysis for dedicated hydrogen production irrespective of the electricity cost of the RES.

As there is scarcity of literature in the domain tidal energy to hydrogen production focussing on optimal electrolyser operation. The existing literature in power to gas (PtG) field, where the electrolysers were connected to conventional RES like wind/solar energy system were referred to validate the part related to optimal electrolyser operation. Mixed logic dynamic including both continuous and integer variables has been used in most of the literature assessing the optimal electrolyser operation as in the research article by

Abdelghany [99][117]. As different cost factors are used in other research articles, a direct validation of the results is not estimated. However, the trends of the results obtained are similar in the existing literature.

G. Matute et al. [99], presented a multi-state model for grid connected electrolyser is under dynamic conditions. The operating modes of production, stop, and standby is included in the study which is termed as 'multi state' modelling. Authors estimate that the system can be made profitable by switching off the electrolysers or by keeping it in standby mode when the electricity prices are high and can be run when there are low or negative prices of electricity. The energy consumption during hot standby, the number of cold starts allowed for the system etc is considered in the optimisation algorithm which is realised as a mixed integer non-linear programming (MINLP) model through general Algebraic Modelling System (GAMS). The study holds some similarities to the analysis done in this chapter such as the optimal hourly power dispatch of the electrolyser units. Subsequently, the annual performance of the system is analysed. However, in this analysis maintaining the system at standby is preferred at most cases, when there is low power or high electricity prices as this operating mode prevents excessive start/stop and thereby can limit the rate of degradation of the stack in its life time. The study aims to provide a case study to learn the techno-economic behaviour of the system. Degradation of the system is assumed to be constant by the authors during production operating mode. In the given study, it is observed that when the hydrogen demand is lower, there is higher savings as the electrolyser is run during low electricity prices and then it is move to stop operating mode. Optimal electrolyser utilisation in terms of its load factor is not given priority in this paper. An application of this paper for the given analysis in this chapter, would be to extend the analysis to include the electrolyser optimal operation in multi-state operating modes. Additional revenue streams for the system are recommended in this paper which is realised in the given analysis, where the CfD contract for the tidal stream energy is included. Further, multiple papers have already addressed multi state operation of electrolysers for AEL [118][119]. Hence, this addition would be to analyse the hybrid system operation in an overall context with much degrees of freedom for electrolyser operation at different operating modes. In addition to three operating modes two other modes called idle and safety operating mode which are representative of real electrolyser operating modes can be considered for a comprehensive analysis.

Another often followed approach is to compare the optimisation approach with different algorithms to check the algorithm performance such as execution time, global optimality of the results obtained. Literature estimates suggest that among the evolutionary algorithms, particle swarm algorithm (PSO) is better candidate over GA in terms of algorithm performance [102]. Additionally, distributed EMS strategy is a field that is gaining increased interest in recent years. This approach in contrast to the centralised EMS considered in this analysis, is beneficial specially to prevent cyber security failure as well as overall damage to the system in case of a single component failure, in addition to reducing the communication lines.

V. Conclusion

In this chapter, the hydrogen production, tidal energy export to the grid and associated cost-benefit analysis of an integrated system including a grid connected tidal-wind-system are evaluated under different power profile conditions. The EMS strategies both from RBA and optimised approaches are discussed. As observed in the analysis, about 81-111 tonnes of tidal powered hydrogen were estimated for both RBA and optimisation approach, respectively. Approximately 18.95-31.5% of the available tidal energy comprising 1.14-1.9 GWh/year is sent to the grid annually under both RBA and optimisation approach mainly due to cyclic nature of tidal energy in addition to the export price optimisation flexibility. High tide periods generate high energy which is sometimes forced to be exported to the grid as the electrolyser capacity is full. Above 1 MW of production of tidal power is observed for about 0-15 hours a day depending on the tidal current profile. Further, low tidal power operations which typically last for about 3-16 hours a day forces the electricity import from external energy suppliers like grid electricity. Previous results showed that the electrolysers are loaded from 38 to 72% of its capacity under the RBA and optimisation approach, respectively.

Additionally, the costs and benefits analysis of the system is implemented using two optimisation approaches, based on fixed-variables costs and levelised cost factor methods, respectively. Further, optimal electrolyser units power profiles, optimal wind power dispatch and grid power export/import dispatch profiles corresponding to the consideration of different input parameters are obtained using a mixed integer nonlinear program based genetic algorithm optimisation. The annualised profits in the optimisation approach were estimated to be 41.5% higher compared to RBA. Further, from an environmental view, the best optimisation results were approximately 47% higher than the RBA results in terms of carbon emission reductions. The electrolyser recurrent transitions in the RBA are eliminated with the optimisation approach. Further, there is an energy saving of 27.5 MWh annually under the optimisation approach compared to RBA, which is caused during multiple operating mode transitions in the former. Thus, associated energy consumption is avoided and more importantly the degradation rate of the electrolysers are reduced which was otherwise caused due to recurrent operating mode transitions. Most importantly, balanced loading of both the electrolyser units are observed in optimisation approach, where as in RBA electrolyser unit 1 is especially underutilised with an annual load factor of 38%. Besides, RES curtailment is avoided in the considered system configuration. An electrolyser unit capable of dynamically operation at peak power conditions for a prescribed duration was especially found to be useful for tidal stream energy profiles which has periodic flood and ebb tides. Priority is given for tidal powered hydrogen through appropriate system modelling and cost function. CO_2 emission savings and corresponding carbon offsetting credits are also

valorised. Besides, the possible over and under estimation in the levelised cost evaluation in comparison with FC evaluation is addressed. In general, it can be concluded that the optimisation approach improves the economic attractiveness of the system and all the system constraints are satisfied including optimal electrolyser operation unlike RBA. The model can be proposed as a generic model that can be utilised in several scenarios. It is especially useful to evaluate the hydrogen production capabilities in a hybrid system under different RES pathways. The flexibility of the cost function is highlighted. There is increased prediction for decrease in cost for both tidal stream energy technology and PEM electrolyser technology, mainly because of the improved learning rates and economic of scale. This paves a way for the applicability of the hybrid system configuration for green hydrogen production such as the one considered in this analysis to be increasingly reliable in the future.

Chapter V

Conclusions and perspectives

This thesis had undertaken to study the energy management and optimisation of a hybrid system involving floating tidal stream energy integration with green hydrogen production. Towards reaching these objectives, a methodical step wise approach was adopted. Initially, the research gap in this field in the existing literature was identified in Chapter I after performing a state-of-the-art literature review on tidal stream energy system (TSES), polymer electrolyte membrane (PEM) electrolysers and energy management strategies, respectively. The thesis objectives were then formulated. Further, the individual system components were modelled in Chapter II. Then, the annual system performance capabilities of the tidal stream energy plant were obtained in Chapter III, using the frequently occurring daily profiles estimation. In the same chapter, the PEM electrolyser units transitionary operating modes were analysed focusing on tidal plant alone configuration through a rule-based approach (RBA) energy management strategy. Further, the preliminary evaluation of the hydrogen production cost based on different daily hydrogen demand and tidal profile condition was assessed. Later, the optimisation approach was formulated in Chapter IV. The optimal techno-enviro economic operation of a hybrid grid connected tidal-wind-hydrogen energy system is then presented and system outcomes were compared against the RBA results. The economic viability of the hybrid system is checked. The main contributions and perspectives of this thesis are presented in this chapter. Lastly, suggestions for possible improvements are given for future works.

I. Key findings and main contributions

The annual key performance indicators for the given floating tidal stream energy plant is evaluated based on the real historic data at the Fall of Warness in the Orkney Islands. The model enables the assessment of performance attributes such as zero power production, peak power production, utilisation factor and capacity factor of the TSES. A capacity factor of 34%, with about 70% of utilisation factor for the floating tidal stream plant is obtained, yielding an annual energy of about 6 GWh. As the tidal energy is highly predictable and the pattern is universal with the exception of diurnal or semidiurnal natures, the model can aid in evaluating the TSES performance indicators at a given site.

Simulations of hydrogen production using two PEM electrolyser units connected to a floating tidal stream energy plant are performed in an annual context. The effect of tidal stream energy intermittency on the transitionary operation of both the electrolysers and the resultant green hydrogen production is investigated. To the best of author's knowledge, this is the first analysis, where the tidal stream energy impact on the transitionary operation of electrolyser units based on different operating modes is assessed. The loading of both the electrolyser units and the associated cold and warm start occurrences are analysed based on a rule-based approach strategy.

Hydrogen production cost variation based on daily tidal profile capabilities and hydrogen demand was analysed for tidal-hydrogen system configuration and tidal-grid-hydrogen configuration. In the preliminary analysis of hydrogen production cost, it was concluded that tidal energy utilisation for hydrogen production is economical under specific hydrogen target scenarios.

An optimisation approach is formulated as a single objective- mixed integer nonlinear problem (MINLP) and it is solved using a genetic algorithm. The objective was to analyse the technical, economic and environmental operation of a hybrid energy system including tidal-wind-grid-hydrogen configuration in particular to maximise system operating profit under various real system constraints and priorities. The overall system cost benefit analysis is performed under a reference average daily condition, annual context and for the proposed overall system lifetime. A comparative analysis based on fixed-variable cost and levelised cost factor approaches is analysed under the optimisation approach. It was determined that the fixed cost (FC) optimisation approach is relatively simple in terms of cost estimation. On the contrary, while the levelised cost (LC) approach yields slightly better results, it necessitates a greater prior knowledge of system operations to reasonably estimate the levelised cost factors. The system profitability can hence be increased by choosing an appropriate optimisation algorithm. Overall it can be concluded that the optimisation approach in a hybrid system, is the way to go forward to ensure an economically and environmentally viable system, subjected to various constraints.

The capability of electrolyser units to operate at twice of its nominal capacity for limited duration is simulated both under the rule-based approach and optimisation approach. Again, this represents another novelty of the thesis. This functionality resulted particularly advantageous, when coupled with tidal stream energy which is cyclic in nature, with predictable periods of high and low power generation.

Further, using a reliable predictive approach for tidal current estimation utilising advanced computational tools, the related hybrid system operation can be explored by using the given models. The hybrid model enables the evaluation of breakeven price for hydrogen production and the strike price under the CfD scheme. Finally, the proposed method can be used as a generic tool for electrolytic hydrogen production analysis under different contexts, with preferable application in high green energy potential sites with constrained grid facilities.

II. Suggestions for future work

Areas which would improve the work done in this thesis in terms of modelling and experimental validation are identified. Consequently, certain aspects that were out of scope of this thesis, but could be considered for a comprehensive optimal analysis of the system configuration is presented below.

Uncertainty and variability in the power generation of both floating tidal stream energy plant and wind energy plant is not accounted for in the modelling part in Chapter II. As the floating tidal stream energy system are placed closer to the sea surface, the effect of ambient turbulence is an important factor to be considered for model improvement. In the studied model, the TSES model availability is assumed to be 100%, with the possibilities to conduct maintenance work during slack tide periods. However, it is important to account the unavailability of the system components due to the long-time scheduled maintenance by assessing site specific practical operating constraints. Further environmental aspects like wave effects that could affect the floating tidal stream energy plant is to be looked into. Additionally, a detailed model for the subsea umbilical cable infrastructure and the related transmission loss is an important factor to consider. Overall, efforts have been made to provide relevant data, however, refining the data would give more accurate results.

Experimental validation of the rule- based and optimisation approaches would be an advantage for analysing the response time of the control algorithm in a hardware in loop (HIL) configuration, for assessing the validity of the results and suitability for real time application.

References

[1] "ITEG: Integrating Tidal energy into the European Grid." [Online]. Available: https://www.nweurope.eu/projects/project-search/iteg-integrating-tidal-energy-into-the-european-grid/ (accessed Oct. 08, 2021).

[2] J. L. B. Ferguson, "Technoeconomic modelling of renewable hydrogen supply chains on islands with constrained grids,"PhD thesis, University of Edinburgh,IDCORE and EMEC, 2021.

[3] D. Coles, A. Angeloudis, D. Greaves, G. Hastie, M. Lewis, L. Mackie, J. McNaughton et al., A review of the UK and British Channel Islands practical tidal stream energy resource, vol. 477, no. 2255. 2021.

[4] UNEP, Emissions Gap Report 21. 2021, [Online]. Available: https://www.unep.org/resources/emissions-gap-report-2021, last access: May 12, 2022.

[5] "An EU strategy to harness the potential of offshore renewable energy for a climate neutral future," 2020, [Online]. Available: https://eur-lex.europa.eu/legal-content/EN/TXT/?uri=COM%3A2020%3A741%3AFIN, last access: May 12, 2022.

[6] IRENA, Offshore renewables: An action agenda for deployment. 2021, https://www.irena.org/publications/2021/Jul/Offshore-Renewables-An-Action-Agenda-for-Deployment.

[7] M. Barakat, B. Tala-Ighil, H. Chaoui, H. Gualous, and D. Hissel, "Energy Management of a Hybrid Tidal Turbine-Hydrogen Micro-Grid: Losses Minimization Strategy," Fuel Cells, vol. 20, no. 3, pp. 342–350, 2020, doi: 10.1002/fuce.201900082.

[8] EU, "An EU Strategy to harness the potential of offshore renewable energy for a climate neutral future," p. 27, 2020.

[9] "Run on Less with Hydrogen Fuel Cells," Advanced Clean Tech News, 2019. [Online]. Available: https://rmi.org/run-on-less-with-hydrogen-fuel-cells/, last access: May 12, 2022.

[10] F. R. Islam and K. A. Mamun, "Possibilities and challenges of implementing renewable energy in the light of PESTLE & SWOT analyses for island countries," Green Energy Technol., vol. 0, no. 9783319501963, pp. 0–19, 2017, doi: 10.1007/978-3-319-50197-0_1.

[11] R. O'Hara Murray and A. Gallego, "A modelling study of the tidal stream resource of the Pentland

Firth, Scotland," Renew. Energy, vol. 102, pp. 326–340, Mar. 2017, doi: 10.1016/J.RENENE.2016.10.053.

[12] A. de Andres, A. MacGillivray, O. Roberts, R. Guanche, and H. Jeffrey, "Beyond LCOE: A study of ocean energy technology development and deployment attractiveness," Sustain. Energy Technol. Assessments, vol. 19, pp. 1–16, 2017, doi: 10.1016/j.seta.2016.11.001.

[13] IEA, "Net Zero by 2050: A Roadmap for the Global Energy Sector," Int. Energy Agency, p. 224, 2021, [Online]. Available: https://iea.blob.core.windows.net/assets/deebef5d-0c34-4539-9d0c-10b13d840027/NetZeroby2050-ARoadmapfortheGlobalEnergySector_CORR.pdf, last access: May 12, 2022.

[14] M. Nachtane, M. Tarfaoui, I. Goda, and M. Rouway, "A review on the technologies, design considerations and numerical models of tidal current turbines," Renew. Energy, vol. 157, pp. 1274–1288, 2020, doi: 10.1016/j.renene.2020.04.155.

[15] S. Walker and P. R. Thies, "A review of component and system reliability in tidal turbine deployments," Renew. Sustain. Energy Rev., vol. 151, no. November 2020, 2021, doi: 10.1016/j.rser.2021.111495.

[16] S. Walker, L. Cappietti, I. Simonetti, and A. Esposito, "Laboratory scale tests of a floating tidal turbine," Dev. Renew. Energies Offshore - Proc. 4th Int. Conf. Renew. Energies Offshore, RENEW 2020, pp. 582–590, 2021, doi: 10.1201/9781003134572-66.

[17] M. Lewis, J. McNaughton, C. Márquez-Dominguez, G. Todeschini, M. Togneri, I. Masters, M. Allmark, T. Stallard, S. Neill, A. Goward-Brown, P. Robins,"Power variability of tidal-stream energy and implications for electricity supply," Energy, vol. 183, pp. 1061–1074, Sep. 2019, doi: 10.1016/J.ENERGY.2019.06.181.

[18] M. Lewis, R.O. Murray, S. Fredriksson, J. Maskell, A.de Fockert, S.P. Neill, P. E. Robin, "A standardised tidal-stream power curve, optimised for the global resource," Renew. Energy, vol. 170, pp. 1308–1323, 2021, doi: 10.1016/j.renene.2021.02.032.

[19] Pennock, S.; Garcia-Teruel, A.; Noble, D.R.; Roberts, O.; de Andres, A.; Cochrane, C.; Jeffrey, H, "Deriving Current Cost Requirements from Future Targets: Case Studies for Emerging Offshore Renewable Energy Technologies," Energies, vol. 15, no. 5, 2022, doi: 10.3390/en15051732.

[20] S. P. Neill, K. A. Haas, J. Thiébot, and Z. Yang, "A review of tidal energy - Resource, feedbacks, and environmental interactions," J. Renew. Sustain. Energy, vol. 13, no. 6, 2021, doi:

10.1063/5.0069452.

[21] F. Wani and H. Polinder, “A Review of Tidal Current Turbine Technology: Present and Future,” EWTEC 2017. Proc. 12th Eur. Wave Tidal Energy Conf. 27th Aug - 1st Sept 2017, no. April, p. {1133\hyphen 1}--{1133\hyphen 7}, 2017, doi: 10.13140/RG.2.2.26857.44640.

[22] “Opportunity energy.” [Online]. Available: http://www.opportunityenergy.org/?p=316 (accessed May 09, 2022).

[23] Kenzie Lewis, “Tidal energy: the power thats making waves.” [Online]. Available: https://www.mcmasterenergyweek.com/the-power-line/2020/10/13/tidal-energy (accessed Apr. 14, 2022).

[24] S. Benelghali, M. Benbouzid, J. F. Charpentier. Marine Tidal Current Electric Power Generation Technology: State of the Art and Current Status. IEEE IEMDC’07, May 2007, Antalya, Turkey. pp.1407-1412. ffhal-00531255.

[25] D. S. Coles, L. Mackie, D. White, and J. Miles, “Cost Modelling and design optimisation of tidal stream turbines,” Proc. Eur. Wave Tidal Energy Conf., pp. 2139-1-2139–11, 2021.

[26] M. Le Diagon, Vincent P, Mayorga, Pedro. M, Sukendro, “Increased reliability of tidal turbines, thanks to a better knowledge of reslistic tidal conditions, use of RAM analysis, advanced monitoring, maintenance strategies and intelligent design components,” Proc. 14th Eur. Wave Tidal Energy Conf. 5-9th Sept 2021, Plymouth, UK, 2021.

[27] G. Rinaldi, B. Wray, R. Parkinson, and L. Johanning, “The operational assessment of a floating tidal farm with hydrogen production capabilities,” Proc. 14th Eur. Wave Tidal Energy Conf. 5-9th Sept 2021, Plymouth, UK, 2021, pp. 1–8.

[28] B. C. R. Ewan and R. W. K. Allen, “A figure of merit assessment of the routes to hydrogen,” Int. J. Hydrogen Energy, vol. 30, no. 8, pp. 809–819, Jul. 2005, doi: 10.1016/J.IJHYDENE.2005.02.003.

[29] F. Ueckerdt, L. Hirth, G. Luderer, and O. Edenhofer, “System LCOE: What are the costs of variable renewables?” Energy, vol. 63, pp. 61–75, Dec. 2013, doi: 10.1016/J.ENERGY.2013.10.072.

[30] A. S. Bahaj and L. E. Myers, “Fundamentals applicable to the utilisation of marine current turbines for energy production,” Renew. Energy, vol. 28, no. 14, pp. 2205–2211, Nov. 2003, doi: 10.1016/S0960-1481(03)00103-4.

[31] D. Coles, A. Angeloudis, Z. Goss, and J. Miles, “Tidal stream vs. Wind energy: The value of cyclic power when combined with short-term storage in hybrid systems,” Energies, vol. 14, no. 4, pp. 1–17, 2021, doi: 10.3390/en14041106.

[32] Starzmann, R., Kaufmann, N., Jeffcoate, P. “Effect of fouling on performance of an instream turbine.” Proc. 14th Eur. Wave Tidal Energy Conf. 5-9th Sept 2021, Plymouth, UK, pp. 2343-1-2343–7, 2021.

[33] G. Kakoulaki, I. Kougias, N. Taylor, F. Dolci, J. Moya, and A. Jäger-Waldau, “Green hydrogen in Europe – A regional assessment: Substituting existing production with electrolysis powered by renewables,” Energy Convers. Manag., vol. 228, no. July 2020, 2021, doi: 10.1016/j.enconman.2020.113649.

[34] J. J. Brey, “Use of hydrogen as a seasonal energy storage system to manage renewable power deployment in Spain by 2030,” Int. J. Hydrogen Energy, vol. 46, no. 33, pp. 17447–17457, 2021, doi: 10.1016/j.ijhydene.2020.04.089.

[35] IRENA, Green Hydrogen Cost Reduction. 2020, [Online]. Available: irena.org/publications/2020/Dec/Green-hydrogen-cost-reduction, last access: May 12, 2022.

[36] J. Proost, “State-of-the art CAPEX data for water electrolysers, and their impact on renewable hydrogen price settings,” Int. J. Hydrogen Energy, vol. 44, no. 9, pp. 4406–4413, Feb. 2019, doi: 10.1016/J.IJHYDENE.2018.07.164.

[37] M. Götz, J. Lefebvre, F. Mörs, A. McDaniel Koch, F. Graf, S. Bajohr, R. Reimert, T. Kolb, “Renewable Power-to-Gas: A technological and economic review,” Renew. Energy, vol. 85, pp. 1371–1390, Jan. 2016, doi: 10.1016/J.RENENE.2015.07.066.

[38] F. N. Khatib et al., “Material degradation of components in polymer electrolyte membrane (PEM)electrolytic cell and mitigation mechanisms: A review,” Renew. Sustain. Energy Rev., vol. 111, no. March, pp. 1–14, 2019, doi: 10.1016/j.rser.2019.05.007.

[39] IEA, “The Future of Hydrogen: Seizing today’s opportunities,” Propos. Doc. Japanese Pres. G20, no. June, p. 203, 2019, [Online]. Available: https://www.oecd.org/fr/publications/the-future-of-hydrogen-1e0514c4-en.htm

[40] B. Yodwong, D. Guilbert, M. Phattanasak, W. Kaewmanee, M. Hinaje, and G. Vitale, “Proton Exchange Membrane Electrolyzer Modeling for Power Electronics Control: A Short Review,” C — Journal of Carbon Research, vol. 6, no. 2, p. 29, May 2020, doi: 10.3390/c6020029.

[41] R. d'Amore-Domenech, Ó. Santiago, and T. J. Leo, "Multicriteria analysis of seawater electrolysis technologies for green hydrogen production at sea," Renew. Sustain. Energy Rev., vol. 133, p. 110166, Nov. 2020, doi: 10.1016/J.RSER.2020.110166.

[42] D. S. Falcão and A. M. F. R. Pinto, "A review on PEM electrolyzer modelling: Guidelines for beginners," J. Clean. Prod., vol. 261, 2020, doi: 10.1016/j.jclepro.2020.121184.

[43] B. Han, S. M. Steen, J. Mo, and F. Y. Zhang, "Electrochemical performance modeling of a proton exchange membrane electrolyzer cell for hydrogen energy," Int. J. Hydrogen Energy, vol. 40, no. 22, pp. 7006–7016, 2015, doi: 10.1016/j.ijhydene.2015.03.164.

[44] Ö. F. Selamet, F. Becerikli, M. D. Mat, and Y. Kaplan, "Development and testing of a highly efficient proton exchange membrane (PEM) electrolyzer stack," Int. J. Hydrogen Energy, vol. 36, no. 17, pp. 11480–11487, 2011, doi: 10.1016/j.ijhydene.2011.01.129.

[45] A. Kosonen et al., "Optimization strategies of PEM electrolyser as part of solar PV system," 2016 18th Eur. Conf. Power Electron. Appl. EPE 2016 ECCE Eur., no. September, 2016, doi: 10.1109/EPE.2016.7695649.

[46] A. Weiß, A. Siebel, M. Bernt, T.-H. Shen, V. Tileli, and H. A. Gasteiger, "Impact of Intermittent Operation on Lifetime and Performance of a PEM Water Electrolyzer," J. Electrochem. Soc., vol. 166, no. 8, pp. F487–F497, 2019, doi: 10.1149/2.0421908jes.

[47] M. Stern and A. L. Geaby, "Electrochemical Polarization," J. Electrochem. Soc., vol. 104, no. 1, p. 56, 1957, doi: 10.1149/1.2428496.

[48] A. E. Samani, A. D'Amicis, J. D. M. de Kooning, D. Bozalakov, P. Silva, and L. Vandevelde, "Grid balancing with a large-scale electrolyser providing primary reserve," IET Renew. Power Gener., vol. 14, no. 16, pp. 3070–3078, 2020, doi: 10.1049/iet-rpg.2020.0453.

[49] B. Yodwong, D. Guilbert, M. Phattanasak, W. Kaewmanee, M. Hinaje, and G. Vitale, "AC-DC Converters for Electrolyzer Applications: State of the Art and Future Challenges," Electronics, vol. 9, no. 6, p. 912, May 2020, doi: 10.3390/electronics9060912.

[50] G. Maggio, A. Nicita, and G. Squadrito, "How the hydrogen production from RES could change energy and fuel markets: A review of recent literature," Int. J. Hydrogen Energy, vol. 44, no. 23, pp. 11371–11384, 2019, doi: 10.1016/j.ijhydene.2019.03.121.

[51] S. Atilhan, S. Park, M. M. El-Halwagi, M. Atilhan, M. Moore, and R. B. Nielsen, "Green hydrogen as an alternative fuel for the shipping industry," Curr. Opin. Chem. Eng., vol. 31, p. 100668, 2021,

doi: 10.1016/j.coche.2020.100668.

[52] “Global average levelised cost of hydrogen production by energy source and technology, 2019 and 2050,” 2020. [Online]. Available: https://www.iea.org/data-and-statistics/charts/global-average-levelised-cost-of-hydrogen-production-by-energy-source-and-technology-2019-and-2050, last access: May 12, 2022.

[53] G. Glenk and S. Reichelstein, “Economics of converting renewable power to hydrogen,” Nat. Energy, vol. 4, no. 3, pp. 216–222, 2019, doi: 10.1038/s41560-019-0326-1.

[54] “Global green-hydrogen pipeline exceeds 250GW — here’s the 27 largest gigawatt-scale projects,” Energy transition, 2020, [Online]. Available: https://www.rechargenews.com/energy-transition/global-green-hydrogen-pipeline-exceeds-250gw-heres-the-27-largest-gigawatt-scale-projects/2-1-933755, last access: May 12, 2022.

[55] C. Deckmyn, J. Van de Vyver, T. L. Vandoorn, B. Meersman, J. Desmet, and L. Vandevelde, “Day-ahead unit commitment model for microgrids,” IET Gener. Transm. Distrib., vol. 11, no. 1, pp. 1–9, 2017, doi: 10.1049/iet-gtd.2016.0222.

[56] L. Meng, E. R. Sanseverino, A. Luna, T. Dragicevic, J. C. Vasquez, and J. M. Guerrero, “Microgrid supervisory controllers and energy management systems: A literature review,” Renew. Sustain. Energy Rev., vol. 60, pp. 1263–1273, 2016, doi: 10.1016/j.rser.2016.03.003.

[57] Y. Zahraoui, I. Alhamrouni, S. Mekhilef, M. R. B. Khan, M. Seyedmahmoudian, A. Stojcevski,B. Horan, “Energy management system in microgrids: A comprehensive review,” Sustain., vol. 13, no. 19, pp. 1–33, 2021, doi: 10.3390/su131910492.

[58] M. Hemmati, B. Mohammadi-Ivatloo, M. Abapour, and A. Anvari-Moghaddam, “Day-ahead profit-based reconfigurable microgrid scheduling considering uncertain renewable generation and load demand in the presence of energy storage,” J. Energy Storage, vol. 28, no. February, p. 101161, 202 0, doi: 10.1016/j.est.2019.101161.

[59] S. Esmaeili, A. Anvari-Moghaddam, and S. Jadid, “Optimal operational scheduling of reconfigurable multi-microgrids considering energy storage systems,” Energies, vol. 12, no. 9, 2019, doi: 10.3390/en12091766.

[60] M. S. Alam and S. A. Arefifar, “Energy Management in Power Distribution Systems: Review, Classification, Limitations and Challenges,” IEEE Access, vol. 7, pp. 92979–93001, 2019, doi: 10.1109/ACCESS.2019.2927303.

[61] I. Abdou and M. Tkiouat, “Unit commitment problem in electrical power system: A literature review,” Int. J. Electr. Comput. Eng., vol. 8, no. 3, pp. 1357–1372, 2018, doi: 10.11591/ijece.v8i3.pp1357-1372.

[62] S. R. Moasheri and M. Khazraei, “Optimal power flow based on modified genetic algorithm,” Asia-Pacific Power Energy Eng. Conf. APPEEC, no. June 2014, 2011, doi: 10.1109/APPEEC.2011.5747746.

[63] M. El-Hendawi, H. A.Gabbar, G. El-Saady, and E.-N. A. Ibrahim, “Optimal operation and battery management in a grid-connected microgrid,” J. Int. Counc. Electr. Eng., vol. 8, no. 1, pp. 195–206, 2018, doi: 10.1080/22348972.2018.1528662.

[64] A. Maleki, M. A. Rosen, and F. Pourfayaz, “Optimal operation of a grid-connected hybrid renewable energy system for residential applications,” Sustain., vol. 9, no. 8, 2017, doi: 10.3390/su9081314.

[65] O. S. Ibrahim, A. Singlitico, R. Proskovics, S. McDonagh, C. Desmond, and J. D. Murphy, “Dedicated large-scale floating offshore wind to hydrogen: Assessing design variables in proposed typologies,” Renew. Sustain. Energy Rev., vol. 160, no. February, p. 112310, 2022, doi: 10.1016/j.rser.2022.112310.

[66] M. R. Barakat, B. Tala-Ighil, H. Gualous, and D. Hissel, “Modeling of a hybrid marine current-hydrogen active power generation system,” Int. J. Hydrogen Energy, pp. 9621–9635, 2019, doi: 10.1016/j.ijhydene.2018.10.020.

[67] M. R. Barakat, B. Tala-Ighil, H. Gualous, and D. Hissel, “Energy Management of a Hybrid Tidal Turbine-Hydrogen Micro-Grid: Losses Minimization Strategy.”, Fuel Cell, 2020.

[68] A. Kartalidis, K. Atsonios, and N. Nikolopoulos, “Enhancing the self-resilience of high-renewable energy sources, interconnected islanding areas through innovative energy production, storage, and management technologies: Grid simulations and energy assessment,” Int. J. Energy Res., vol. 45, no. 9, pp. 13591–13615, 2021, doi: 10.1002/er.6691.

[69] J. L. B. Ferguson, A. Robinson, S. Crawford, and D. Mignard, “Impact of integration of wind and tidal power on hydrogen production costs (March 2021),” Proc. Eur. Wave Tidal Energy Conf., no. March, pp. 2028-1-2028–7, 2021.

[70] N. Lazaar, M. Barakat, M. Hafiane, J. Sabor, and H. Gualous, “Modeling and control of a hydrogen-based green data center,” Electr. Power Syst. Res., vol. 199, no. June, p. 107374, 2021,

doi: 10.1016/j.epsr.2021.107374.

[71] N. Lazaar, E. Fakhri, M. Barakat, H. Gualous, and J. Sabor, “Optimal sizing of marine current energy based hybrid microgrid,” Renew. Energy Power Qual. J., vol. 18, no. June, pp. 515–521, 2020, doi: 10.24084/repqj18.417.

[72] “Fast-tracking Offshore Renewable energy With Advanced Research to Deploy 2030MW of tidal energy before 2030,” European Commission, 2021, [Online]. Available: https://cordis.europa.eu/project/id/101037125, last access: May 12, 2022.

[73] “A scalable and sustainable proposal with hydrogen as fuel to meet IMO2050 targets,” RINA, 2022, [Online]. Available: https://www.rina.org/en/media/press/2021/11/25/ship-hydrogen-fuel, last access: May 12, 2022.

[74] A. Alex, R. Petrone, B. Tala-Ighil, D. Bozalakov, L. Vandevelde, and H. Gualous “Optimal techno-enviro-economic analysis of a hybrid grid connected tidal-wind- hydrogen energy system,” submitted to Int. J. Hydrogen Energy, 2022 (under review).

[75] A. Alex, R. Petrone, B. Tala-Ighil, H. Obeid, H. Gualous, and L. Vandevelde, “Electrolytic hydrogen production from tidal energy: A technical and economic perspective,” Proc. 14th Eur. Wave Tidal Energy Conf. 5-9th Sept 2021, Plymouth, UK, pp. 2343-1-2343–7, 2021.

[76] Orbital, “Orbital Marine Power (Orkney) plc. Orbital O2 2MW Tidal Turbine,” 2018 (available as part of ITEG project specification).

[77] R. Vennell, “Exceeding the Betz limit with tidal turbines,” Renew. Energy, vol. 55, pp. 277–285, 2013, doi: 10.1016/j.renene.2012.12.016.

[78] O. P. Mahela and A. G. Shaik, “Comprehensive overview of grid interfaced wind energy generation systems,” Renew. Sustain. Energy Rev., vol. 57, pp. 260–281, 2016, doi: 10.1016/j.rser.2015.12.048.

[79] A. Matine, C. Bonnard, A. Blavette, S. Bourguet, F. Rongère, et al. Optimal sizing of submarine cables from an electro-thermal perspective. European Wave and Tidal Conference (EWTEC), Aug 2017, Cork, Ireland. ⟨hal-01754060⟩

[80] M. Badshah, S. Badshah, M. Altaf, S. Jan, M. Amjad, and N. A. Anjum, “Research Progress in Tidal Energy Technology-A Review,” Technical journal, University of Engineering and technology (UET), Taxila, Pakisthan, vol. 22, no. 4, pp. 42–54, ISSN:1813-1786 (Print) 2313-7770 (Online), 2017.

[81] Enercon, “Enercon product overview.” [Online]. Available: https://www.enercon.de/fileadmin/Redakteur/Medien-Portal/broschueren/pdf/en/ENERCON_Produkt_en_06_2015.pdf (accessed Dec. 06, 2021).

[82] Ø. Ulleberg, “Modeling of advanced alkaline electrolyzers: a system simulation approach,” Int. J. Hydrogen Energy, vol. 28, no. 1, pp. 21–33, Jan. 2003, doi: 10.1016/S0360-3199(02)00033-2.

[83] C. Duncan, R. Roche, S. Jemei, and M.-C. Pera, “Techno-economical modelling of a power-to-gas system for plant configuration evaluation in a local context,” Appl. Energy, vol. 315, no. January, p. 118930, 2022, doi: 10.1016/j.apenergy.2022.118930.

[84] G. Sdanghi, “Hydrogen storage technologies : state-of-art and perspectives,” Presentation, Electrochemical systems for Microgrid Applications – Nancy, Summer School, July 05-08th 2021.

[85] A. Dadkhah, D. Bozalakov, J. D. M. De Kooning, and L. Vandevelde, “On the optimal planning of a hydrogen refuelling station participating in the electricity and balancing markets,” Int. J. Hydrogen Energy, vol. 46, no. 2, pp. 1488–1500, 2021, doi: 10.1016/j.ijhydene.2020.10.130.

[86] S. S. Makridis, “Hydrogen storage and compression,” Methane Hydrog. Energy Storage, no. June, pp. 1–28, 2016, doi: 10.1049/pbpo101e_ch1.

[87] George Mason University, “Wind: u and v Components.” [Online]. Available: http://colaweb.gmu.edu/dev/clim301/lectures/wind/wind-uv (accessed Dec. 06, 2021).

[88] D. Khojasteh, M. Lewis, S. Tavakoli, M. Farzadkhoo, S. Felder, G. Iglesias, W. Glamore, “Sea level rise will change estuarine tidal energy: A review,” Renew. Sustain. Energy Rev., vol. 156, no. September 2021, p. 111855, 2022, doi: 10.1016/j.rser.2021.111855.

[89] “Average Weather in Orkney, United Kingdom,” Weather Spark. https://weatherspark.com/y/40130/Average-Weather-in-Orkney-United-Kingdom-Year-Round (accessed Oct. 08, 2021).

[90] “How low can you go? Minimising our carbon footprint.” [Online]. Available: https://orbitalmarine.com/how-low-can-you-go-minimising-our-carbon-footprint/, last access: May 15,2022.

[91] “Carbon intensity of Great Britain,” Electricity Map. [Online]. Available: https://app.electricitymap.org/zone/GB, last access: May 15,2022.

[92] A. Myhr, C. Bjerkseter, A. Ågotnes, and T. A. Nygaard, “Levelised cost of energy for offshore

floating wind turbines in a lifecycle perspective," Renew. Energy, vol. 66, pp. 714–728, 2014, doi: 10.1016/j.renene.2014.01.017.

[93] CFI, "Levelized cost of energy template." [Online]. Available: https://marketplace.corporatefinanceinstitute.com/financial-model-templates/industry-specific-financial-models/levelized-cost-of-energy-lcoe-template/ (accessed Mar. 10, 2022).

[94] G. Allan, M. Gilmartin, P. McGregor, and K. Swales, "Levelised costs of Wave and Tidal energy in the UK: Cost competitiveness and the importance of 'banded' Renewables Obligation Certificates," Energy Policy, vol. 39, no. 1, pp. 23–39, Jan. 2011, doi: 10.1016/J.ENPOL.2010.08.029.

[95] U.S. Department of Energy, "Exploring Opportunities for Marine Renewable Energy in Maritime Markets," U.S. Dep. Energy, no. April, p. 170, 2019, [Online]. Available: https://www.ocean-energy-systems.org/about-oes/what-is-ocean-energy/, last access: May 12, 2022.

[96] European Commission, Ocean Energy Technology Development Report. 2019. [Online]. Available: https://op.europa.eu/en/publication-detail/-/publication/675542cd-0435-11ea-8c1f-01aa75ed71a1/language-en, last access: May 12, 2022.

[97] "N2EX Day Ahead Auction Prices," 2020, Nord Pool, 2022. [Online]. Available: https://www.nordpoolgroup.com/Market-data1/GB/Auction-prices/UK/Hourly/?view=table (accessed Feb. 11, 2022).

[98] "UK woodland Carbon code," Woodland carbon CO_2de. [Online]. Available: https://woodlandcarboncode.org.uk/landowners-apply/how-do-i-sell-my-carbon-units#pay (accessed Feb. 11, 2022).

[99] G. Matute, J. M. Yusta, J. Beyza, and L. C. Correas, "Multi-state techno-economic model for optimal dispatch of grid connected hydrogen electrolysis systems operating under dynamic conditions," Int. J. Hydrogen Energy, vol. 46, no. 2, pp. 1449–1460, 2021, doi: 10.1016/j.ijhydene.2020.10.019.

[100] G. Kakoulaki, I. Kougias, N. Taylor, F. Dolci, J. Moya, and A. Jäger-Waldau, "Green hydrogen in Europe – A regional assessment: Substituting existing production with electrolysis powered by renewables," Energy Convers. Manag., vol. 228, no. October 2020, 2021, doi: 10.1016/j.enconman.2020.113649.

[101] Department of Energy and Climate Change, "Quarterly energy prices - United Kingdom, Quarter 2

(April – June) 2020," vol. 2, no. June, p. 92, 2020, [Online]. Available: https://www.gov.uk/government/publications/quarterly-energy-prices-june-2013, last access: May 12, 2022.

[102] N. Lazaar, E. Fakhri, M. Barakat, H. Gualous, and J. Sabor, "Optimal sizing of marine current energy-based hybrid microgrid," Renew. Energy Power Qual. J., vol. 18, no. 18, pp. 515–521, 2020, doi: 10.24084/repqj18.417.

[103] A. J. Chipperfield and P. J. Fleming, "MATLAB Genetic algorithm toolbox," IEE Colloq., no. 14, 1995, doi: 10.1049/ic.

[104] L. O. P. Vasquez, C. A. C. Meneses, A. P. Martínez, J. L. Redondo, M. P. García, and J. D. Á. Hervás, "Optimal energy management within a microgrid: A comparative study," Energies, vol. 11, no. 8, 2018, doi: 10.3390/en11082167.

[105] Mathworks, "How the Genetic Algorithm Works." https://uk.mathworks.com/help/gads/how-the-genetic-algorithm-works. (accessed Apr. 12, 2022).

[106] ICCT, "Assessment of Hydrogen Production Costs from Electrolysis: United States and Europe," Int. Counc. Clean Transp., pp. 1–73, 2020, [Online]. Available: https://theicct.org/sites/default/files/publications/final_icct2020_assessment_of _hydrogen_production_costs v2.pdf, last access: May 12, 2022.

[107] B. D. James, C. Houchins, J. M. Huya-Kouadio, and D. A. Desantis, "Final Report: Hydrogen Storage System Cost Analysis Sponsorship and Acknowledgements," no. Nurul, N. Z., Yaakob, Z., Lim, K. L., Timmiati, S. N. (2016). The kinetics of lightweight solid-state hydrogen storage materials: A review. International Journal of Hydrogen Energy, 41(30), 13131–13151. https://doi.org/10.1016/j.ijhydene.2016.05.169 Ren, pp. 1–54, 2016.

[108] Energy Technologies Institure, "ESME v4.4," 2020. [Online]. Available: https://www.eti.co.uk/programmes/strategy/esme, last access: May 12, 2022.

[109] G. Sdanghi, G. Maranzana, A. Celzard, and V. Fierro, "Review of the current technologies and performances of hydrogen compression for stationary and automotive applications," Renew. Sustain. Energy Rev., vol. 102, no. November 2018, pp. 150–170, 2019, doi: 10.1016/j.rser.2018.11.028.

[110] F. Judge, "D2 . 8 Ocean Energy Technology Guidance Report Reports," no. January 2022, doi: 10.13140/RG.2.2.12146.22729.

[111] International Renewable Energy Agency, Renewable Power Generation Costs in 2019. 2020. [Online]. Available: https://www.irena.org/-/media/Files/IRENA/Agency/Publication/2020/Jun/IRENA_Power_Generation_Costs_2019.pdf, last access: May 12, 2022.

[112] "Mainstreaming Green hydrogen in Europe," Material Economics, 2020. [Online]. Available: https://materialeconomics.com/latest-updates/mainstreaming-green-hydrogen-in-europe#:~:text=Mainstreaming%20green%20hydrogen%20will%20mean,and%20securing%20strategic%2C%20open%20autonomy, last access: May 12, 2022.

[113] Intergovernmental Panel on Climate Change, Climate Change 2014 Mitigation of Climate Change. 2014. [Online]. Available: https://www.ipcc.ch/report/ar5/wg3/, last access: May 12, 2022.

[114] M. S. Saddique, A. R. Bhatti, S. S. Haroon, M. K. Sattar, S. Amin, I. A. Sajjad, S. Sadam ul Haq, A. B. Awan, N. Rasheed, "Solution to optimal reactive power dispatch in transmission system using meta-heuristic techniques—Status and technological review," Electr. Power Syst. Res., vol. 178, p. 106031, Jan. 2020, doi: 10.1016/J.EPSR.2019.106031.

[115] J. J. Grefenstette, "Optimization of Control Parameters for Genetic Algorithms," IEEE Trans. Syst. Man Cybern., vol. 16, no. 1, pp. 122–128, 1986, doi: 10.1109/TSMC.1986.289288.

[116] G. Rinaldi, A.C. Pillai, P.R. Thies"Multi-objective optimization of the operation and maintenance assets of an offshore wind farm using genetic algorithms," Wind Engineering, 44(4), pp. 390–409. doi: 10.1177/0309524X19849826.

[117] M. B. Abdelghany, M. F. Shehzad, D. Liuzza, V. Mariani, and L. Glielmo, "Optimal operations for hydrogen-based energy storage systems in wind farms via model predictive control," Int. J. Hydrogen Energy, vol. 46, no. 57, pp. 29297–29313, Aug. 2021, doi: 10.1016/J.IJHYDENE.2021.01.064.

[118] C. Varela, M. Mostafa, and E. Zondervan, "Modeling alkaline water electrolysis for power-to-x applications: A scheduling approach," Int. J. Hydrogen Energy, vol. 46, no. 14, pp. 9303–9313, 2021, doi: 10.1016/j.ijhydene.2020.12.111.

[119] Y. Zheng, S. You, H. W. Bindner, and M. Münster, "Optimal day-ahead dispatch of an alkaline electrolyser system concerning thermal–electric properties and state-transitional dynamics," Appl. Energy, vol. 307, p. 118091, 2022, doi: 10.1016/j.apenergy.2021.118091.

Acknowledgement

Ansu ALEX PhD Thesis, titled: "*Tidal stream energy integration with green hydrogen production: energy management and system optimisation*" is financially supported by the Interreg North-West Europe project 'Integrating Tidal energy into the European Grid (ITEG)' funded by the European Regional Development Fund - Grant number NWE 613.

"The ITEG project received 6,460,004.69 EURO of funding from the European Regional Development Fund through the Interreg North West Europe Programme"

https://vb.nweurope.eu/projects/project-search/iteg-integrating-tidal-energy-into-the-european-grid/